Year : 2016

Whole gene expression profiles and virulence traits of dermatophytes during infection

De Coi Niccolò

De Coi Niccolò, 2016, Whole gene expression profiles and virulence traits of dermatophytes during infection

Originally published at : Thesis, University of Lausanne

Posted at the University of Lausanne Open Archive http://serval.unil.ch
Document URN : urn:nbn:ch:serval-BIB_10980EA515FA0

UNIL | Université de Lausanne
Faculté de biologie et de médecine

Department of Dermatology

Whole gene expression profiles and virulence traits of dermatophytes during infection

Thèse de doctorat ès sciences de la vie (PhD)

présentée à la

Faculté de biologie et de médecine
de l'Université de Lausanne

Par

Niccolò De Coi

Master de l'Université de Lausanne

Jury

Prof. Vincent Barras, Président
Prof. Michel Monod, Directeur de thèse
Prof. Bertrand Favre, expert externe
Dr. Philippe Hauser, MER1, expert
Dr. Keith Harshman, expert

Lausanne 2016

Remerciements

Tout d'abord je souhaite remercier les institutions du Centre Hospitalier Universitaire du canton Vaud (CHUV) et de l'Université de Lausanne (UNIL) pour m'avoir permis de réaliser ma thèse en Science de la Vie et le Fond National Suisse (FNS) pour l'avoir financiée.

Un grand merci au directeur de thèse le **Prof. M. Monod** qui m'a dirigé et aidé pendant le déroulement de ma thèse au sein du Laboratoire de Mycologie du Service de Dermatologie du CHUV.

Le **Prof. M. Gilliet** pour m'avoir accueilli à la seine du Service de Dermatologie.

Le **Dr. K. Harshmann**, coordinateur du Genomic Technologies Facility, à l'Université de Lausanne, et notamment sa collaboratrice **Corinne** pour l'aide dans le control de qualité des extractions d'ARN.

Prof. Vincent Barras, pour avoir accepté d'être mon président du jury et **Dr P. Hauser** et **Dr. B Favre** pour avoir accepté d'être mes experts pour ma soutenance de thèse.

Je remercie de grand cœur également toutes les techniciennes du laboratoire de mycologie, **Mme Karine Salamin** pour l'aide dans le laboratoire; **Mme Marina Fratti** et **Mme Olympia Bontems** pour leur sympathie et leur soutien pendant ma thèse.

Je remercie aussi tous les gens du Département de Dermatologie: **Tobias**, **Anita**, **Elena**, **Daniel**, **Hyun Sook**, **Ana**, **Alessio**, **Olessya** et **Jeremy**.

Un grand merci à **ma Mère** pour ses sacrifices et de m'avoir toujours soutenu, comme mon frère **Matteo**. À mes amis **Josè**, **Josip** et **Gianluca** pour m'avoir aussi soutenu et aidé pendant ma thèse et aussi dans autres moments de ma vie.

En fin, merci à tous ceux qui, de près ou de loin, m'ont permit d'agrandir mes expériences soit dans le domaine scientifique que dans ma vie en générale.

Summary

Dermatophytes are highly specialized filamentous pathogenic fungi that are able to digest keratinized substrates. Pathogenic species are the most common agents of superficial mycoses but their virulence mechanisms are poorly understood. Since dermatophytes almost exclusively infect the *stratum corneum*, nails and hairs, research into the mechanisms of invasion has primarily focused on secreted proteases. Nothing was known about other secreted hydrolases (e.g. ceramidases and lipases) that are possibly involved in the degradation of the cutaneous barrier, and possible transcription factors specifically modulated during the infection process.

The aim of the present thesis was to identify the proteins (in particular proteases) secreted by dermatophytes during infection that are putative virulence factors and antigenic molecules. A complete gene expression profile of the dermatophyte *Arthroderma benhamiae* was obtained during infection of its natural host (guinea pig) using RNA-sequencing technology. This profile was compared to those of the fungus cultivated *in vitro* in two media containing keratin and soy meal protein as the sole source of nitrogen, and in Sabouraud medium. The expression profiles of genes encoding secreted proteins in infected guinea pigs were found very different from that during *in vitro* growth when using keratin as substrate. Especially, the sets of the 12 most highly expressed genes encoding proteases with a signal sequence during infection and in keratin medium only had the putative vacuolar aspartic protease gene *PEP2* in common. The most upregulated gene encoding a secreted protease during infection was that encoding subtilisin SUB6, which is a known major allergen in the related dermatophyte *Trichophyton rubrum*.

Different tools were recently developed to improve genetic analyses of dermatophytes. In our study, the *Agrobacterium tumefaciens*-mediated transformation system was used to transform *A. benhamiae* in order to produce recombinant proteins such as SUB6, SUB7 and SUB8 which are potentially involved in infection for further characterization.

Comparing gene expression during infection on guinea pigs versus keratin degradation *in vitro*, which is supposed to mimic the host environment, revealed the critical importance of using real *in vivo* conditions for investigating virulence mechanisms. The analysis of genes expressed *in vivo*, encoding cell surface and secreted proteins, particularly proteases, led to the identification of new allergen and virulence factor candidates.

Résumé

Les dermatophytes sont des champignons filamenteux pathogènes capables de digérer des substrats kératinisés. Ils sont la cause du plus grand nombre de mycoses cutanées. Comme les dermatophytes infectent la peau, les ongles et les cheveux, la recherche sur les facteurs de virulence de ces champignons s'est concentrée sur leurs protéases secrétées. Aucune donnée n'était disponible sur d'autres hydrolases sécrétées (e.g. céramidases et lipases) certainement impliquées dans la dégradation de la barrière cutanée. L'objectif de cette thèse était d'identifier les protéines (en particulier les protéases) qui sont sécrétées par les dermatophytes lors d'une infection. Ces protéines sécrétées sont des facteurs de virulence potentiels et des molécules impliquées dans des réactions immunologiques.

Un profil d'expression de tous les gènes (transcriptome) du dermatophyte *Arthroderma benhamiae* lors d'infections de cochons d'Inde a pu être obtenu en utilisant des techniques récentes de séquençage de l'ARN. Ce profil a été comparé avec ceux du champignon cultivé *in vitro* dans différents milieux contenant de la kératine ou des protéines de soja comme seule source d'azote, et dans du milieu de Sabouraud. De fortes différences entre les transcriptomes ont été révélées. En particulier, les sets des 12 gènes les plus exprimés codant pour des protéases avec un peptide signal *in vitro* et *in vivo* n'avaient en commun que la protéase aspartique PEP2 qui est en fait une protéase vacuolaire. Le gène codant pour une protéase sécrétée le plus exprimé *in vivo* était celui d'une subtilisine, SUB6. Cette protéase était connue pour être un antigène majeur de l'espèce *Trichophyton rubrum*.

Nous avons pu transformer *A. benhamiae* avec des plasmides pour sur-exprimer les gènes codant pour SUB6 et SUB7 en utilisant la bactérie *Agrobacterium tumefaciens.* Ces subtilisines qui sont potentiellement impliquées dans l'infection ont été obtenues dans du surnageant de culture du champignon alors qu'il avait été impossible de les obtenir avec d'autres systèmes d'expression.

En conclusion, la comparaison des transcriptomes *d'A. benhamiae* pendant l'infection et pendant sa croissance dans un milieu contenant de la kératine a démontré l'importance d'utiliser des vraies conditions *in vivo* pour investiguer les mécanismes de virulence des dermatophytes. L'analyse des gènes qui codent pour des protéines sécrétées et qui sont exprimés *in vivo* a permis d'identifier des facteurs de virulence et des allergènes potentiels des dermatophytes.

Abbreviations

Accession number (AC)

Agrobacterium tumefacens-mediated transformation (ATMT)

Caspase recruitment domain containing (CARD)

Common in fungal extracellular membrane domain (CFEM)

Delayed-type hypersensitivity (DTH)

Dimethsylsulfoxid (DMSO)

Dipeptidyl-peptidases (DPP)

False discovery rate (FDR)

From complementary DNA (XXXc)

From genomic DNA (XXXg)

Glycophosphatidyinositol (GPI)

Guinea pig (Gp)

Human immunodeficiency virus (HIV)

Immediate hypersensitivity (IH)

Interferon γ (IFN-γ)

Interleukin (IL)

Keratin (K)

Keratin liquid medium (KSP)

Leucine aminopeptidases (LAP)

Lysogeny Broth (LB)

Mass spectronomy (MS)

Metalloprotease (MEP)

Open reading frame (ORF)

Phenol/guanidine isothiocyanate (TRIzol)

p-nitroanilide (p-NA)

Polymerase chain reaction (PCR)

Principal component analysis (PCA)

RNA integrity number (RIN)

RNA quality number (RQN)

Round per minute (RPE)

Sabouraud (Sa)

Signal peptid (SIG)

Sodium dodecyl sulfate polyacrylamide gel electrophoresis (SDS-PAGE)

Soja (S)

Soy protein liquid medium (SP)

Subtilisn (SUB)

Swiss institute of bioinformatic (SIB)

Tandem mass spectronomy (MS/MS)

T-helper (Th)

Transcripts Per Kilobase Million (TPM)

Translation elongation factor 1 (TEF1)

Trichloroacetic acid (TCA)

Yeast extract beef (YEB)

1. Introduction

1.1. Fungi Overview

Fungi show a great diversity. Nowadays about 100’000 species have been described but an estimated number of more than 1 million species are still to be characterized. The kingdom of Fungi includes different species of mushrooms, yeasts, dermatophytes, truffles, moulds, and more others. Fungi, due the lack of photosynthetic pigments, are forced to follow a saprophytic or a parasitic existence. As saprophytic they are essential to the process of decay of complex animal and plant remains in the soil needed to renew the source of nutriments for further generation of plants and others organisms. As parasitic they could lead to a broad spectrum of diseases on humans, animals and plants causing important damages. Fungi are present almost everywhere in the air, on the soil, and in/on plants and animals.

Fungi are eukaryotic and heterotrophic organisms (they do not posses chlorophyll and use only organic carbon source as nutriment). They could be free-living organisms but most of them establish a relationship with other organisms (plants, insects, humans) in a parasitic or mutualistic way. Some fungi grow as a single cell (yeasts) but the majority of them grow by making multicellular filaments (hyphae). The network formed by different hyphae is called mycelium. The cell membrane is enclosed in a cell wall composed principally by chitin and glucans (1-3β and 1-6β). It contains ergosterol that differs from cholesterol present in the mammalian cell membrane. Each fungal cell contains one or several haploid or diploid nuclei.

The reproduction of fungi depends on the species and on the environmental conditions. They can reproduce both sexually and asexually often leading to the production of spores which produced on hyphae or in micro or macro sporangia. The asexual and sexual forms in the same species are morphologically very different. The asexual form is called anamorph and the sexual form is called teleomorph. The two forms had different names. However, according to the recent rules proposed by the Amsterdam declaration on Fungal Nomenclature, only one name species should be retained for a fungal species (one fungus=one name) (1). "Authors should choose the oldest generic name, irrespective of whether it is typified by a species name with a teleomorphic or an anamorphic type, except where the younger generic name is far better known".

The sexual life cycle of fungi is different from other eukaryotic organisms because the zygote is the only diploid cell and when two mating type fuse. If the conditions are not optimal, the nuclei do not fuse until the conditions change.

1.2. Classification

The kingdom of Fungi was only created in 1969 by Whittaker (2). They were before together with Plants. Then they were moved into the Protista kingdom composed primarily by unicellular organisms (Figure 1). Nowadays, the classification of fungi is not anymore based only on morphological characteristics but is also based on biochemical and genetics features.

The fungi were divided in 5 major classes based on their reproduction and the characteristics of their sporangia: the Chitridiomyces, the Zygomycetes, the Ascomycetes and the Basidiomycetes and the Deuteromycetes. However, the

Chitridiomyces and the Zygomycetes were shown to be polyphyletic and new classes were created (3)

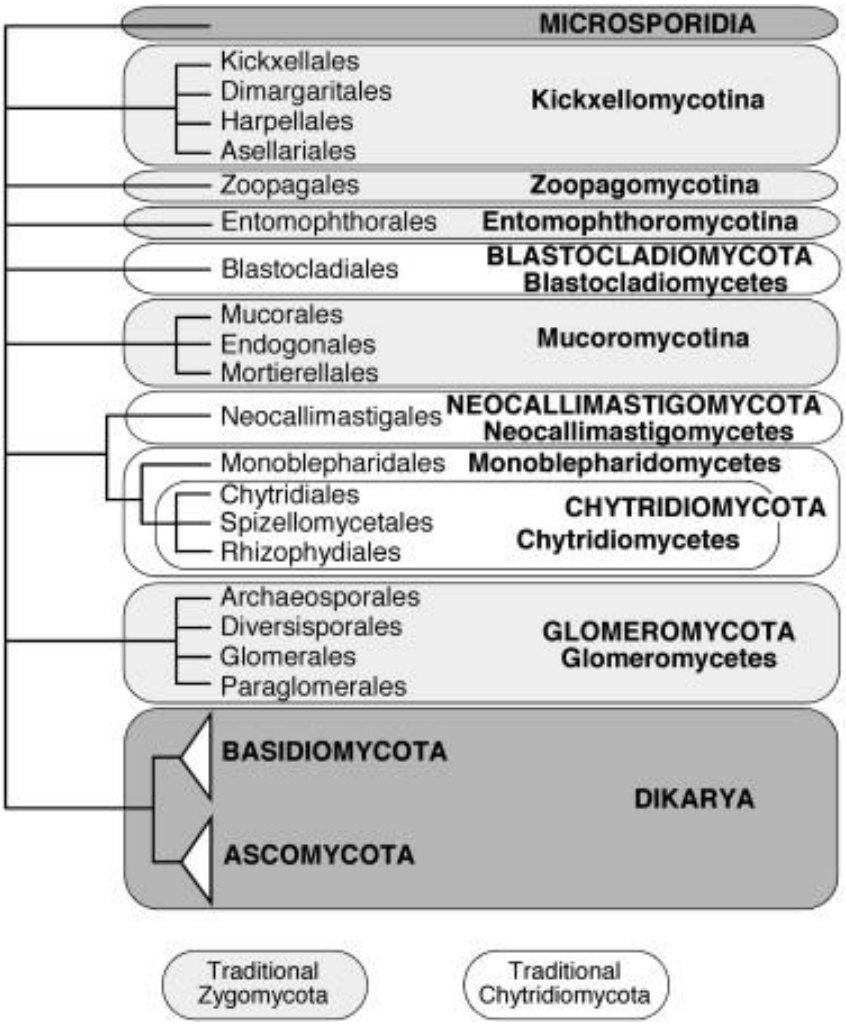

Figure 1 Phylogeny and classification of *Fungi*. Basal *Fungi* and *Dikarya*. Branches lengths are not proportional to genetic distance. From Hibbett *et al*. (4).

1.2.1. The Ascomycetes

The majority of the ascomycetes reproduce sexually with spores borne internally in specialized cells called asci. For some ascomycete species, only asexual reproduction is known. The Ascomycetes is the largest group of fungi. Many of these fungi interact with plant roots forming mycorrhizae. This symbiosis is so important due the fact that almost every plant interacts with one or more fungi in a mutualistic way. Fungi such as cup fungi, morels and truffles belong to the Ascomycetes.

1.2.2. The Basidiomycetes

Basidiomycetes reproduce sexually with spores borne externally on specialized cells called basidia. However, some of the species in this class do not reproduce sexually. Most of the fungi present in the Basidiomycetes are filamentous fungi. The majority of comestible fungi (mushrooms) belong to this class. However, the species of some genus such as *Malasezzia* and Cryptococcus are yeasts. Species of *Malasezzia* are human skin commensals.

1.2.3. The Zygomycetes

The Fungi belonging to Zygomycetes are mainly terrestrial saprophytes, parasite or predator of protozoa and nematodes. Approximately 1000 species have been identified. All zygomycetes reproduce both sexually and asexually. The sexual spores are called zygospores and are really resistant to harsh conditions thanks to a thick chitin wall. The asexual spores are borne internally in a sporangium.

1.2.4. The Chitridiomycetes

They are considered to be the most primitive fungi. They differ from the species of the other classes by the presence of flagellated spores and the chemical composition of the cell wall with cellulose. Chitrides are microscopic and the flagellum of the spores permits them to move toward nutriments or away from non-optimal environments. The species of this phylum are found mostly in an aquatic environment but also in some anaerobic conditions (e.g. digestive tract of ruminants).

1.2.5. The Deuteromycetes

Deuteromycetes, also named Fungi imperfecti, grouped species where only the asexual reproduction was known. This taxon is not longer accepted nowadays but some of the fungi that were present in this class could be included in the ascomycetes and basididiomycetes using DNA sequence analysis.

1.3. Fungal secreted hydrolases

Only small molecules such as amino acids, short peptides or mono and di-glucosides can be absorbed by fungi and used as nutrient. To digest macromolecules such as proteins, starch and cellulose in smaller molecules outside of the fungal cell many fungi secreted a large panel of hydrolases. These secreted enzymes require humid environment for their diffusion to reach different macromolecules. Consequently growing fungi are often restricted in moist environments.

1.4. Fungal secreted proteases

1.4.1. Classification of Proteases

The term protease is synonymous with peptidase, proteolytic enzyme and peptide hydrolase. The proteases include all enzymes capable to cleave the peptide bonds (CO-NH) of proteins. All the different proteases are classified and the nomenclature of proteases can be found together with information about them in the Handbook of proteolytic enzyme (5) and online in the MEROPS database accessible on the website (http://merops.sanger.ac.uk/). The proteases are firstly classified following their mode of action and their active site. Aspartatic, cystein, glutamic, metallo, serine, and threonine proteases as well as proteases with unknown catalytic mechanism are recognized. Then, each protease is assigned to a family that is a set of homologous enzymes.

The proteases are also divided into endoproteases (or endopeptidases) and exoproteases (or exopeptidases). The endoproteases cleave peptide bonds internally within a polypeptide chain. The exoproteases instead cleave peptide bonds only at the N- or C- terminus of a polypeptide chain.

1.4.2. Secreted proteases

Like most secreted proteins, secreted proteases are synthesized as a precursor containing a hydrophobic N-terminal extension of 15-30 amino acids, known as the prepeptide or signal peptide (6). The signal peptide is needed to correctly enter the secretory pathway by allowing the transport of the protease across the endoplasmic reticulum membrane (7), where it is subsequently cleaved by a signal peptidase (8). Not all the proteins with a secretion signal will be released in the environment. Some of

these proteases are vacuolar and remain intracellular or bind to the membrane through a transmembrane domain or a glycophosphatidyinositol (GPI)-anchor.

Several secreted proteases are synthesized as a precursor with a peptide (30 to 250 amino acids in length), which is located between the signal peptide and the N-terminus of the mature enzyme (propeptide). It is known to be essential and specific for the correct folding and the secretion of the enzyme (9–11). Upon copmpletion of folding, the propeptide is removed by an auto- or exogenous proteolytic reaction to generate the active enzyme (12–15).

1.4.3. Fungal endo and exopeptidases

Fungi secrete different sets of proteases (endo and exopetidases) suitable to digest protein source present in a specific environment. The secreted fungal endo and exopeptidases are found in 14 families (Table 1). The main fungal secreted endoproteases are aspartic proteases of the A1 family or pepsins (16), metalloproteases of the M35 and M36 families (deuterolysins and fungalisins, respectively), and serine proteases of the S8 family (subtilisins). Fungal secreted exopeptidases are aminopeptidases and carboxypeptidases. The main aminopeptidases are leucine aminopeptidases of the M28 family, tripeptidyl peptidases of the S53 family and dipeptidyl peptidases of the S9 family. The main carboxypeptidases are metalloproteases of the M14 family and serine proteases of the S10 family (17).

Table 1 Fungal protease families with distribution among taxonomic kingdoms. Aspartatic (A); Glutamatic (G); Metallo (M); Serine (S).

Protese family	Fungi	Plants	Animal	Bacteria	Protozoans	Archea
A1	+	+	+	-	+	-
G1	+	-	-	+ (few)	-	-
M12	+	-	+	+	+	-
M20	+	+	+	+	-	+
M28	+	+	+	+	-	+
M35	+	-	-	+ (few)	-	-
M36	+	-	-	+ (few)	-	-
M43	+	-	+	+	-	+
S1	+	+	+	+	+ (few)	+ (few)
S8A	+	+	+	+	+	+
S9	+	+	+	+	+	+
S10	+	+	+	+	-	-
S28	+	+	+	-	-	-
S33	+	+	+	+	+	+
S53	+	-	+	+	-	+

1.5. Dermatophytes

1.5.1. General properties

Dermatophytes are highly specialized filamentous pathogenic fungi that are able to digest and grow on keratinized substrates (18). Pathogenic species are the most common agents of superficial mycoses infecting almost exclusively the stratum corneum, nails and hairs.

Dermatophytes are ascomycete fungi, but only anamorphs (or asexual forms) are isolated from infected patients, animals or soil. Mating studies in laboratory conditions led to the discovery of the perfect states of dermatophyte species. Dermatophyte anamorphs are classified in three genera, *Trichophyton*, *Microsporum*, and *Epidermophyton* on the basis of macroscopic and microscopic characteristics of the organism grown in culture. When sexual reproduction has been observed in the dermatophytes, their teleomorph states have been classified in the genus *Arthroderma* of the Ascomycetes.

Three broad ecological groups of dermatophyte species are recognized that are anthropophilic, zoophilic and geophilic depending on their major reservoir in nature. Anthropophilic species naturally colonize humans, while zoophilic species are found predominantly in animals. Geophilic species of dermatophytes are simply saprophytes existing in the soil without or sporadically causing disease.

1.5.2. Dermatophyte genomes

Genomes of seven dermatophyte species were sequenced and annotated (19–21). The dermatophyte genomes are comprised between 22.5 and 24 Mb and are highly collinear. They are smaller in size than those of *Coccidioides* spp., *Histoplasma* spp. and *Aspergillus* spp. but are enriched for particular families of genes encoding secreted proteases and fungal specific kinases. The dermatophytes also contain a large number of genes coding for enzymes that synthesize secondary metabolites. Genes encoding enzymes involved in sugar metabolism and plant cell wall breakdown are lacking. For instance, there are no genes encoding glycoside hydrolases and alpha-amylases. These deficiencies attest for high specialization of dermatophytes and adaptation to particular substrates other than vegetal debris. The number of predicted protein-coding genes was found to vary from 7,980 in *A. benhamiae* to 8,915 in *M. canis*. (20, 21)

Different tools were recently developed to improve genetic analyses of dermatophytes, including efficient systems for targeted gene inactivation, gene silencing and broad transcriptional profiling techniques.

1.5.3. Dermatophyte Infections

The ability to digest keratin allows the dermatophyte to invade the human keratinized tissue. The diseases are described with the word "tinea" followed by a term for the particular infected body site (22). In case of highly inflammatory tinea corpis, tinea faciei and tinea capitis, it is essential to identify precisely the etiologic agent to choose the best therapeutic approach and to consider pets as the possible source of infection in order to avoid recurrence of new infections.

Dermatophytes are the most common cause of fungal infections worldwide affecting on millions of individuals annually. This led, in several countries, to an impact on the health care system estimated around millions of dollars a year for the treatment only. Nevertheless the research and the medical community still lack a sophisticated biological knowledge and diagnostic methods to prevent and treat these infections.

1.5.4. Dermatophytosis Symptoms

Dermatophytoses vary depending on the causative agent and the body site affected. Anthropophilic species (e.g. *T. rubrum*, *T. interdigitale*, and *T. tonsurans*), tend to be associated with more chronic infections which are less inflammatory. In contrast, zoophilic and geophilic species of dermatophytes (e.g. *A. benhamiae, A. vanbreuseghemii*, *Trichophyton erinacei*, *T. verrucosum*, *M*. *canis* and *M. gypseum*) often cause highly inflamed lesions in humans (Figure 2).

The classical ringworm lesions occur in tinea capitis, tinea corporis, and tinea barbae, which are the most common sites for zoophilic dermatophyte infections. The typical lesions are more or less circumscribed circular areas of variable erythema that are centrifugally growing, with scaling and desquamation. Alopecia accompanies infection due to the increased fragility of infected hairs. The lesions vary in size and may be singular or multiple. In areas such as the foot and in body folds lesions with *T. rubrum* or *T. interdigitale* may be more diffuse. Nail infections (tinea unguium) leads to dystrophic nails.

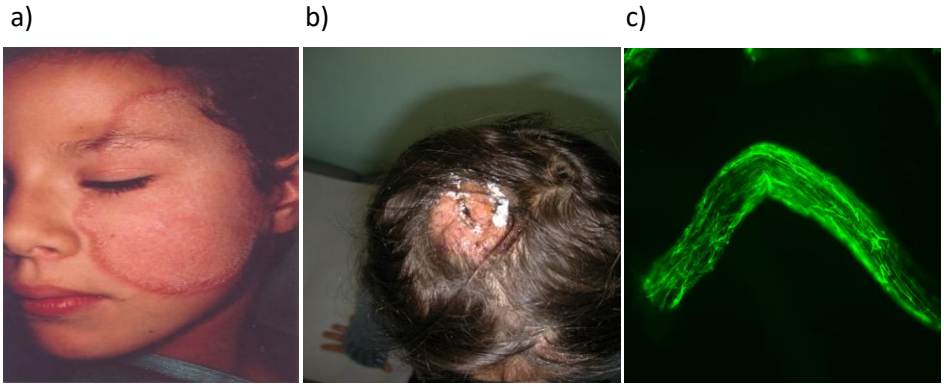

Figure 2 Examples of infections by dermatophyte (*A. benhamiae*). *Tinea faciei* (a); *Tinea capititis* (b); direct mycological examination of a hair infected by *A. benhamiae* (400x) (c)

1.6. Virulence factors

Since dermatophytes are almost exclusively localized in keratinized tissues, research into the mechanisms of invasion has primarily focused on secreted proteases. Dermatophytes grow well in a medium containing protein as sole nitrogen source and secrete proteolytic activity. The major secreted endoproteases have been found to be two subtilisins (SUB3 and SUB4) and two metalloproteases of the fungalisin family (MEP3 and MEP4) (23, 24). In addition, dermatophytes secrete various aminopeptidases that are leucine aminopeptidases (LAP1 and LAP2) and dipeptidyl-peptidases (DPPIV and DPPV), for which an ortholog exists in *Aspergillus* spp., as well as a major metallocarboxypeptidase homologous to the human pancreatic carboxypeptidase A (25, 26).

Currently, knowledge regarding dermatophyte gene expression during infection remains poor. The first transcriptome analyses of a dermatophyte during infection were performed using a cDNA microarray based on transcripts of *A. benhamiae* grown in a protein medium covering approximately 20–25% of its genome and on few selected

protease-coding genes (27). As a striking result, most major proteases secreted by the fungus during its growth *in vitro* in a protein medium (e.g., SUB3, SUB4, MEP3, MEP4, LAP2, and DPPIV) were not detected and, therefore, appeared not to be involved during the establishment of infection. In contrast, a gene encoding another subtilisin (SUB6) was found to be highly expressed during skin infection, but not when the fungus grew in any culture medium. As a general conclusion, most proteases secreted in vitro in a keratin medium appeared to be not involved during the establishment of an infection, at least in the tested model. In contrast, other secreted proteases not involved in keratin degradation likely fulfill important functions in virulence.

Nothing is currently known about the other secreted hydrolases (e.g. ceramidases and lipases), which are also certainly involved in the degradation of the skin barrier.

Microarrays analysis revealed strong upregulation of key enzymes of the glyoxylate cycle (e.g. isocitrate lyase and malate synthase). The glyoxylate cycle, which is absent in mammals, was previously found to support the pathogenicity of other microbial pathogens, e.g. *Mycobacterium tuberculosis* and the yeast *Candida albicans* (28, 29). In dermatophytes, however, similar to *A. fumigatus* (30), the analyses of knock-out mutants defective in key enzymes of this metabolic pathway have excluded its contribution to fungal pathogenicity *in vivo*, at least in the analyzed animal infection models (31).

1.7. Host defense mechanisms

Zoophilic and geophilic species of dermatophytes (e.g. *Arthroderma benhamiae, Trichophyton erinacei*, *Trichophyton verrucosum*, and *Microsporum canis*) cause highly inflamed lesions in humans. A dermatophyte often provokes a more intense inflammatory reaction on a host to which it is not adapted than to its natural host, but on the other hand such lesions more rapidly lead to spontaneous clearance. Both innate and adaptive immunity are involved in host defense mechanisms against dermatophytes.

1.7.1. Innate immunity

Innate immunity in superficial dermatophytosis implies the action of keratinocytes and neutrophils. A broad spectrum of cytokines is produced by keratinocytes upon exposure to a dermatophyte (32), including IL-8, a potent chemo-attractant for neutrophils which can kill dermatophytes, and the pro-inflammatory tumour-necrosis factor α (TNF-α) (33). Production is higher in zoophilic than in anthropophilic dermatophytes (32, 34) which is consistent with the clinical features by the respective dermatophyte groups. Keratinocytes also secrete a wide variety of antimicrobial peptides (AMP) with antifungal properties. Human β-defensin (35), cathelicidin LL-37 (36), psoriasin (37), and disulphide-reduced psoriasin (38) were proven to be either fungistatic or fungicidal *in vitro* against *T. rubrum.* Disulphide-reduced psoriasin was isolated from psoriasis lesions and conveys resistance to fungal infections (38).

Rare cases of deep dermatophytosis have been described in HIV and immunosuppressed patients (39, 40), but also in immunocompetent people, mainly from

North Africa of families with consanguinity (41). These patients were found to bear homozygous mutations in the gene coding for a caspase recruitment domain containing protein (CARD9). A stop codon mutation (Q289*) was detected in 15 patients from seven Algerian and Tunisian families (41). Two missense mutations, R101C and R101L, were detected in two Moroccan siblings and a Brazilian patient, respectively (42). The mutation Q289* was also detected in a patient of Egyptian origin with extensive skin and nail dermatophytosis (43). CARD9 is an adaptator protein in the signaling pathway downstream from lectin receptors, such as dectin 1 and dectin 2 involved in the recognition of pathogenic fungi. Mainly in myeloid cells and involved in the stimulation of pro-inflammatory responses, CARD9 plays an important role in the innate immune response against fungal pathogens. CARD9-deficient cells showed low levels of IL6 production after stimulation with zymosan, an agonist of dectin 1 (41).

1.7.2. Adaptive immunity

Zoophilic and geophilic dermatophytes induce a delayed type hypersensitivity (DTH) cell-mediated response, which usually results in recovery and subsequent protection against re-infection. The response is characterized by elevated levels of the key cytokines interleukin-12 (IL-12) and IFN-γ, which trigger T-helper 1 (Th1) cells for the activation of macrophages as effector cells. The overexpression of transforming growth factor-b, interleukin (IL)-1b and IL-6 mRNA during infection of *A. benhamiae* in a mouse model also suggests a role of the Th17 pathway in the establishment of immunity with recruitment of polymorphonuclear neutrophils (44). In contrast, anthropophilic species (e.g. *T. rubrum*, *T. interdigitale*, and *T. tonsurans*) tend to be associated with less inflammatory, but more chronic and persistent infections. These infections are

correlated with poor specific DTH, elevated specific IgE and IgG4, and IgE-mediated immediate hypersensitivity (IH), with the production of Th2 cytokines by mononuclear leukocytes (45, 46). While cell-mediated Th1 response to dermatophytes is effective in eradicating the infection, Th2-mediated IH responses are not protective.

1.8. Important clinical manifestations distant from dermatophyte infections: Asthma and skin dermatophytids

1.8.1. Dermatophytids

Kerions were recognized as the cause of generalized cutaneous eruption of the skin by Jadassohn in 1918 (47). Allergic exzematous skin reactions to dermatophytosis at a distant area of the body were the object of many papers in the first part of the twentieth century. Since then, the literature on the subject is relatively scarce, but this topic was recently reviewed by Ilkit (48).

In analogy to the name tuberculid, the suffix id was retained for the terminology of any cutaneous allergic reaction caused by a microorganism at a distant area of the body. The word dermatophytid was proposed to designate secondary allergic reactions to infections caused by dermatophytes by Williams in 1926 (49). Dermatophytids encompassed trichophytids as well as Microsporids, Epidermophytids used in the ancient literature following the etiologic agent of the secondary allergic reaction (50). Dermatophytids reactions have been described with many dermatophyte infections including tinea pedis, tinea corporis, and tinea cruris (51). Vesicular eruptions on the hands were experimentally induced by Peck in 1930 (52) by infecting the toes of a previously unaffected person.

The clinical presentations are often characterized by symmetric widespread eczematous eruptions in body sites (53). Dyshidrotic and vesicular eczema on the hands (palms and/or fingers) associated with tinea pedis and/or tinea unguium in adults (generally caused by *T. rubrum* and *T. interdigitale*) are common dermatophytids (53). Eczema with grouped or scattered follicular papules on the chest, trunk and back associated with scalp ringworm due to zoophilic and anthrophilic species are less frequent but were the object of many reports. The dermatophytids go away once the dermatophytes infection has been cured.

A set of diagnostic criteria were retained to identify a dermatophytid reaction (48, 51, 52):

(i) There is a proven dermatophytic infection in a body site other than the eczematous skin reaction

(ii) The eczema appeared after the dermatophytes infection. The fungus is not present in the site of the cutaneous eruption that is it cannot be isolated in cultures or detected by direct mycological examination.

(iii) The dermatophytid symptoms only disappear after eradication of the primary focus of fungal infection

(iv) The patients are sensitized to dermatophytes antigens and show a positive skin test response to fungal extracts (termed *Trichophytin*). Positive delayed reaction is the more often recorded but immediate reaction can occur (48, 51).

1.8.2. Asthma

Allergic disease in the respiratory tract has been linked to chronic dermatophytosis with anthropophilic *Trichophyton* species in individuals with immediate hypersensitivity (54) although the fungus only colonizes the skin and the nails. There is a strong association between sensitization to proteins from the fungus and the severity of asthma (55). Like dermatophytids (of the skin), *Trichophyton* asthma can be controlled with systemic antifungal therapy (45, 54, 56, 57)

The first described major allergens in *T. rubrum* that cause sensitization were called Tri r2 and Tri r4. These antigens were found to induce dual immune responses and elicit either immediate (IH) or delayed-type (DTH) hypersensitivity skin test reactions in different individuals (45, 54, 58, 58). Tri r 2 and Tri r 4 were the two proteases later called SUB6 and DPPV in the annotation of the dermatophyte secreted proteases.

In contrast to dermatophytids *Trichophyton* asthma is not very common but is possibly underestimated because the lack of fungal extracts for intradermal skin tests to demonstrate sensitization.

2. Thesis project

2.1. Statement of the problem and objectives of this work

Knowledge regarding dermatophyte gene expression during infection was poor. The first transcriptome analyses of a dermatophyte during infection were performed using a cDNA microarray based on transcripts of *A. benhamiae* grown in a protein medium covering approximately 20–25% of its genome and on few selected protease-coding genes (27). As a striking result, genes encoding major proteases secreted by the fungus *in vitro* appeared not to be expressed during the establishment of infection. In contrast, a gene encoding another subtilisin (SUB6) was found to be highly expressed during skin infection. Of important note, SUB6 is the ortholog of the gene encoding the major allergen Tri r2 in *T. rubrum* (59). In addition, nothing is known about other secreted hydrolases (e.g. ceramidases and lipases) that are possibly involved in the degradation of the cutaneous barrier, and possible transcription factors specifically modulated during the infection process.

As numerous antigenic molecules eliciting the host immune responses still remain to be discovered, and in view of the importance of secreted proteins, both as antigens and as possible virulence factors, the goals of this work were the following: (i) to obtain a complete gene expression profile of *A. benhamiae* during infection using state-of-the-art RNA-seq technology, (ii) to compare it with the expression profiles of the fungus grown *in vitro* in different media; (iii) to identify which proteins and in particular individual proteases are secreted *in vivo* during infection as possible new virulence factors and (iv) to produce and characterize the main proteases secreted during infection.

We explored the complete transcriptome of *A. benhamiae* genes during experimental infection in the guinea pig (animal model) using the state-of-the-art RNA-seq technology. We compared it with the transcriptomes of the fungus growing *in vitro* in Sabouraud, soja and keratin medium.

The results of the RNA-seq were used to identify putative virulence factors of pathogenic dermatophytes. We focused on *the A. benhamiae* secretome with an emphasis on proteases. A dermatophytes expression system was developed to produce the main proteases secreted during infection.

3. Material and Methods

3.1. Strains and growth media

A. benhamiae Lau2354-2 (CBS 112371) (60, 61) was used in this study. This strain, deposited in the Belgian Coordinated Collections of Microorganisms (BCCM/IHEM) under IHEM20161, is the reference strain that was chosen for *A. benhamiae* genome sequencing (61). It was isolated from a patient suffering from a highly inflammatory dermatophytosis in the Centre Hospitalier Universitaire Vaudois (CHUV). The *A. benhamiae* strain was maintained at 28 °C on Sabouraud dextrose agar medium.

A. benhamiae was grown *in vitro* in Sabouraud liquid medium, soy protein liquid medium (SP), and keratin liquid medium (KSP) as previously described (27). SP medium was prepared by dissolving 2 g of soy protein (Supro 1711, Protein Technologies International) in 1 L of distilled water. Aliquots of 100 mL of KSP were prepared by adding 0.2 g of keratin (Merck, Darmstadt, Germany; keratin is derived from animal hooves and horns) and 5 mL of SP medium to 95 mL of distilled water. A low amount of SP in KSP medium was found to be necessary to initiate the growth of dermatophytes with keratin as the sole substrate (27). A plug of fresh *A. benhamiae* mycelia grown on Sabouraud agar was inoculated in 100 mL of liquid Sabouraud, SP, and KSP medium and incubated for 5, 10 and 24 days, respectively, at 30 °C without shaking. At the indicated time points, growth in protein media was accompanied by substantial proteolytic activity along with clarification of the media and, in the case of keratin–soy cultures, also by visible dissolution of the water-insoluble keratin granules.

3.2. Animal infection

All animal experiments were performed by Elana Batut under the guidance of Bernard Mignon at the University of Liège. Animal experiments were approved by the local ethics committee (University of Liège, ethics protocol no. 1052).

Specific pathogen-free, 3-month-old female guinea pigs (cross-bred white albinos, Dunkin Hartley strain-Charles River Laboratories International, Wilmington, USA) were infected with *A. benhamiae* Lau2354-2. *A. benhamiae* mycelia scraped from freshly grown 18-day-old Sabouraud plates and suspended in 5% (w/w) poloxamer 407 (BASF, Germany) was applied to a 16-cm^2 back skin surface that had been clipped and scarified previously. Each guinea pig was infected with 6×10^9–2×10^{10} CFU. Non-infected control guinea pigs were subjected to the same procedure, except that the poloxamer 407 mixture did not contain any fungal elements. Three guinea pigs were sacrificed after 8, 14, 27, 44 days and 14 days after reinfection once healed. The infected skin from sacrificed animals was frozen at -80 °C for subsequent total RNA isolation. Both the hair and *stratum corneum* were examined for the presence of fungal elements by direct mycological examination.

3.3. RNA extraction

The extraction of RNA from infected guinea pig skin required a specific procedure to yield sufficient amount of RNA with sufficient quality. The kits commercially available provided low-quality and quantity RNA. These results were possibly due by the presence of hairs in the samples that obstructed the column used for extraction. After

different tests, we established the following optimized protocol. The fungal mycelia or guinea pig skin infected by *A. benhamiae* was frozen in liquid nitrogen and then crushed in a grinder in the presence of glass beads (200 – 300 µL) and phenol/guanidine isothiocyanate (TRIzol, Life Technology, Carlsbad, USA) to avoid RNA degradation. The resulting powder (250 µL) was placed in an Eppendorf tube with approximately 700 µL of glass beads and 500 µL of TRIzol. The fungal elements were mechanically broken down further using a FastPrep®-24 homogenizer (MP Biomedicals, LLC) for 15 s at a speed of 4 m/s, and then immediately put on ice. Next, 250 µL of phenol:chloroform:isomyl alcohol (24:24:1) (Life Technologies) were added to the whole mixture. After vigorous mixing, a centrifugation step was performed for 6 min at 13,000 rpm (19,000 g). Two hundred microlitres of the aqueous phase were extracted and added to the same volume of 80% ethanol, mixed by pipetting, and then added to a RNeasy Mini Spin Columns (QIAGEN©, Venlo, Netherlands). After 15 s of centrifugation, the collector tube was removed (for the entire protocol after each centrifugation, the collector tubes were replaced), and then 350 µL of wash buffer RW1 (QIAGEN©) was added and the column centrifuged for 15 s. Subsequently, one unit of RNasin© Plus RNase inhibitor (Promega) in 20 µL of water was added, and the column was left for 5 min at room temperature. The column was then washed again with 350 µL of RW1 and centrifuged for 15 s.

In a next step, a solution of RNAfree DNase (QIAGEN©) (10 µL of DNase in 70 µL of RNA-free water) was added to the column, and the column incubated for 15 min at room temperature. The column was washed with 350 µL of RW1 and twice with 500 µL of RPE buffer (QIAGEN©), according to the manufacturer's recommendations. The

column was further centrifuged for 2 min at maximum speed (13000 rpm, 19000 g) to eliminate traces of buffers. The total RNA was collected in an RNAse-free Eppendorf tube after adding 25–40 µL of RNA-free water to the column, a 5-min incubation, and a centrifugation step for 1 min at 13000 rpm. Eluted RNA was stored at -80 °C with the addition of 0.4 µL of RNasin© to increase stability.

The concentration and the quality of RNA samples were assessed using an ND-1000 spectrophotometer (NanoDrop Technologies) and a Fragment Analyzer™ Automated CE System (Advanced Analytical), respectively. The quality of the RNA was evaluated using RNA quality number (RQN). The RQN correspond to an integrity score from 1 to 10 of the 18S and 28S peak and is equivalent to the broadly accepted RNA integrity number (RIN). The final quality of the RNA was at least roughly 7 RQN to ensure good cDNA library preparations and subsequent RNA-seq analysis.

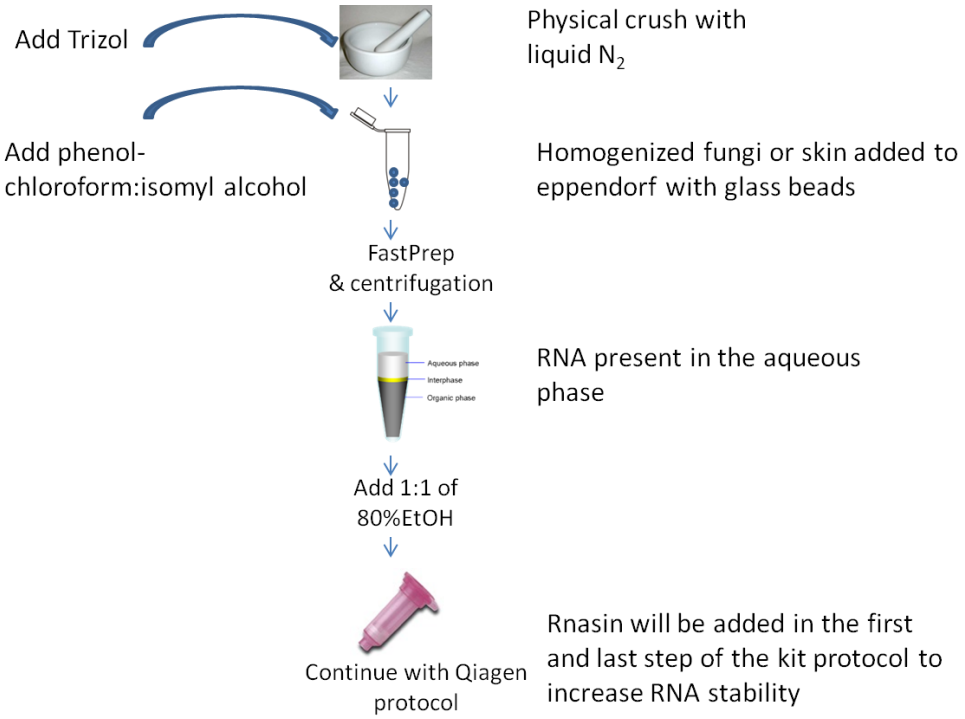

Figure 3 Schema of the lab RNA extraction protocol. We took care to increase the lysis of fungal cells avoiding possible RNA degradation through the addition of Rnasin (RNase inhibitor.)

3.4. RNA sequencing

In close collaboration with the Lausanne Genomic Technologies Facility, and using the Illumina technology (HiSeq 2000 sequencer), we performed a TruSeq stranded single read total RNA analysis using one lane with a multiplex level of 15, acquiring approximately 30 million 'strand-specific' reads with a length of 100 bp for each sample (Table 4)

Reads were aligned against the *A. benhamiae* and guinea pig genomes using *tophat2* (version 2.0.9) (62).

3.5. Gene prediction and annotation

The bioinformatics work needed to achieve the new gene prediction and the re-annotation of *A. benhamiae* was performed in collaboration with the Swiss Institute of Bioinformatics (SIB), with the special help of Thuong Van Du Tran and Marco Pagni.

Gene prediction was made with *augustus* (version 3.0.2) (63) using a specific gene model obtained as follows. Gene transcripts and intron locations were obtained using *cufflinks* (version 2.2.1) (64). The transcripts were three-frame translated into potential amino-acid sequences using *transeq* from EMBOSS (version 6.5.7) (65). The complete proteomes of *Saccharomyces cerevisiae* and *Aspergillus nidulans* (reviewed by Swiss-Prot) were mapped onto the potential amino acid sequences with *glsearch36*, from the FASTA alignment tools (version 3.6) (66) to identify coding phase and CDS location within transcripts. Based on the alignment quality and on the presence of start

and stop codons near alignment extremities (+/- 10 amino acids), a set of confidently predicted CDS was gathered and converted into gene annotations using intron locations previously given by *cufflinks*. These annotations were used as a training set to build a gene model with the scripts supplied in the *augustus* distribution.

3.6. In silico identification of putative cell surface and secreted proteases

The identification of putative secreted proteases was performed in collaboration with the SIB, with the special help of Marc Feuremann.

To identify putative secreted proteins, we checked for the presence of an N-terminal signal sequence using both *Phobius* (version 1.01) (67) and *SignalP* (version 4.1) (68). Signal peptides have been confirmed by the prediction of N-terminal transmembrane spans using *TMHMM* (version 2.0) (69, 70). The presence of a potential glycosylphosphatidylinositol (GPI) anchor has been checked by using *PredGPI* (version 1.0) (71). Using the transmembrane span predictors *TMHMM* (version 2.0), *ESKW* (version 1.0) (72), and *MEMSAT* (version 1.8) (73), we refined the secretome prediction by removing the proteins that contain one or more transmembrane spans in addition to the signal peptide and that are probably targeted to membranes. All the secreted proteins have been subjected to Blast analysis against the UniProtKB database (74) as well as to InterPro scanning (75, 76) to associate and reveal some putative functions.

3.7. Mass spectrometry and experimental validation of new secreted proteins

Precipitation and separation of proteins from *A. benhamiae* cultures at pH 4 and pH 7 along with shotgun mass spectrometry (MS) experiments have been described by Sriranganadane et al. (77). A new search of MS/MS spectra against the sequences of our new predicted proteome was performed.

3.8. Transcriptome analysis

The number of reads mapped onto each newly predicted gene locus was obtained with *htseq-count* (version 0.5.4p3) (78). Genes with counts fewer than one per million in all samples were removed from the statistical analyses (e.g., 81 genes). Gene expression was normalized using the TMM-normalized Voom transformation (79); hierarchical clustering and principal component analysis was done using R (version 3.1.1). Differential gene expression analysis was performed with the R Bioconductor package *limma* (80). The cut-offs of 1e-3 for FDR (BY-adjusted *p*-value) (81) and 2 for fold change were applied to identify genes relevant to each contrast. The R software package *WGCNA* (82) was used for correlation network analysis, using the Pearson correlation.

3.9. Plasmids construction for gene expression in *A. benhamiae*

The plasmid pNDC10 (Table 3) was designed for the production of dermatophyte secreted proteins. This plasmid was constructed by cloning in pAg1 (83) an expression

cassette with the hygromycin B phosphotransferase gene (*hph*) as a selection marker and the *A. benhamiae* SUB3 encoding gene under the *A. benhamiae* Translation elongation factor 1 (TEF1) promoter. The expression cassette was generated by gene synthesis (Genecust, Dunedange, Luxembourg). An *Xho*I site was inserted in pNDC1 just downstream the sequence coding for the *A. benhamiae* SUB3 signal sequence. A *Bgl*II site and a *Spe*I site were inserted just after the stop sequence TAG of the SUB3 ORF. The expression plasmids pNDC1, pNDC2 and pNDC3 (Table 3) to produce SUB4, SUB6 and SUB7, respectively, were constructed as following: the *A. benhamiae* SUB6 and SUB7 genes were amplified by polymer chain reaction (PCR) using the primer pairs P3/P4, P5/P6 and P7/P8, respectively (Table 2). The PCR products were digested with either *Sal*I *or Xho*I and either *Bam*HI or *Spe*I for which a site was previously designed at the 5' end of the primers, and fused to the large 7.5 kb fragment of pNDC10 digested with *Xho*I and either *Bgl*II or *Spe*I to generate expression plasmids pNDC1, pNDC2 and pNDC3.

The expression plasmid pNDC10_G418 was generated by replacing in pNDC10 the *hph* gene by the *Escherichia coli* neomycin phosphotransferase gene *neo* conferring resistance to the gentamycin 418. To perform this construction, a *neo* gene cassette was amplified with primers P1 and P2 (Table 2) for which a restriction site *Pci*I and *Aci*I site was designed at the 5' end, and the plasmid pDTV3 as a target (84). The PCR product was digested with the restriction enzyme *Pci*I and *Acl*I and inserted with the large fragment of pNDC10 cut with the same enzymes.

The expression plasmids pNDC5, pNDC6 and pNDC7 (Table 3) were constructed as following: the *A. benhamiae* genes encoding SUB4, SUB6, SUB7 and SUB8 were

amplified by PCR using the primer pairs P3/P4 P5/P6 P7/P8 and P9/P10, respectively (Table 2). *SUB4*, *SUB6* and *SUB7* and *SUB8* genomic DNA (gDNA) was obtained using *A. benhamiae* genomic DNA as a target. Deduced cDNA of *SUB6* and *SUB8* corresponding to gDNA minus introns was synthesized by Genecust (Dunedange, Luxembourg) and cloned in pUC57. The generated plasmids were used as targets for producing cDNA fragments to be cloned in pNDC10_G418.

The PCR products were digested with either SalII or XhoI and either BamHI or SpeI, and fused to the large 7.5 kb fragment of pNDC0_G418 digested with XhoI and either BglII or SpeI to generate expression plasmids pNDC4 to pNDC7 (Table 3).

The sequence of pNDC10 was deposited in the NCBI database with the accession number LN866853, the other expression plasmids will be deposited soon.

Table 2 Primers used for the production of the expression plasmids pNDCs with hygromycin cassette. Underlined are the restriction enzyme sites.

Name	Sequence	Restriction enzyme	Function
P1	GTCACATGTAGAAGATGATATTGAAGGA	*Pci*I	Insertion of *neo* cassette
P2	GTCGGATCCAGATGATTCATGACGTATA	*Bam*HI	
P3	CTTGTCGACTTGATGCCCGCGCAGTCTTCAAG	*Sal*I	SUB4 expression
P4	CTTGGATCCCTACTGGCCACTTCCGTTGTAGAG	*Bam*HI	
P5	GTGCTCGAGATGGTGCTAGAATCCTTGAGGCCGGT	*Xho*I	SUB6 expression
P6	GTTACTAGTTTATTTGCCGCTGCCGTTGTA	*Spe*I	
P7	GTTGCTCGAGCTGAGATCATGGAGACTCGCGCTGGT	*Xho*I	SUB7 expression
P8	GTTGGATCCTTACATGCCAGATCCGTTGTTGATGAGCTTGC	*Bam*HI	
P9	GTCCTCGAGCCTCCCCCATGATCGTTGAC	*Xho*I	SUB8 expression
P10	GTTACTAGTTTATGCGACGACGGCGTCCT	*Spe*I	

Table 3 Plasmid nomenclature and their type of resistance cassette and the target recombinant protein

Plasmid name	**Resistance cassette**	**Protein expressed**
pNDC10	*hph*	SUB3
pNDC1	*hph*	SUB4
pNDC2	*hph*	SUB6
pNDC3	*hph*	SUB7
pNDC10_G418	*neo*	SUB3
pNDC4	*neo*	SUB4
pNDC5	*neo*	SUB6
pNDC6	*neo*	SUB7
pNDC7	*neo*	SUB8

a)

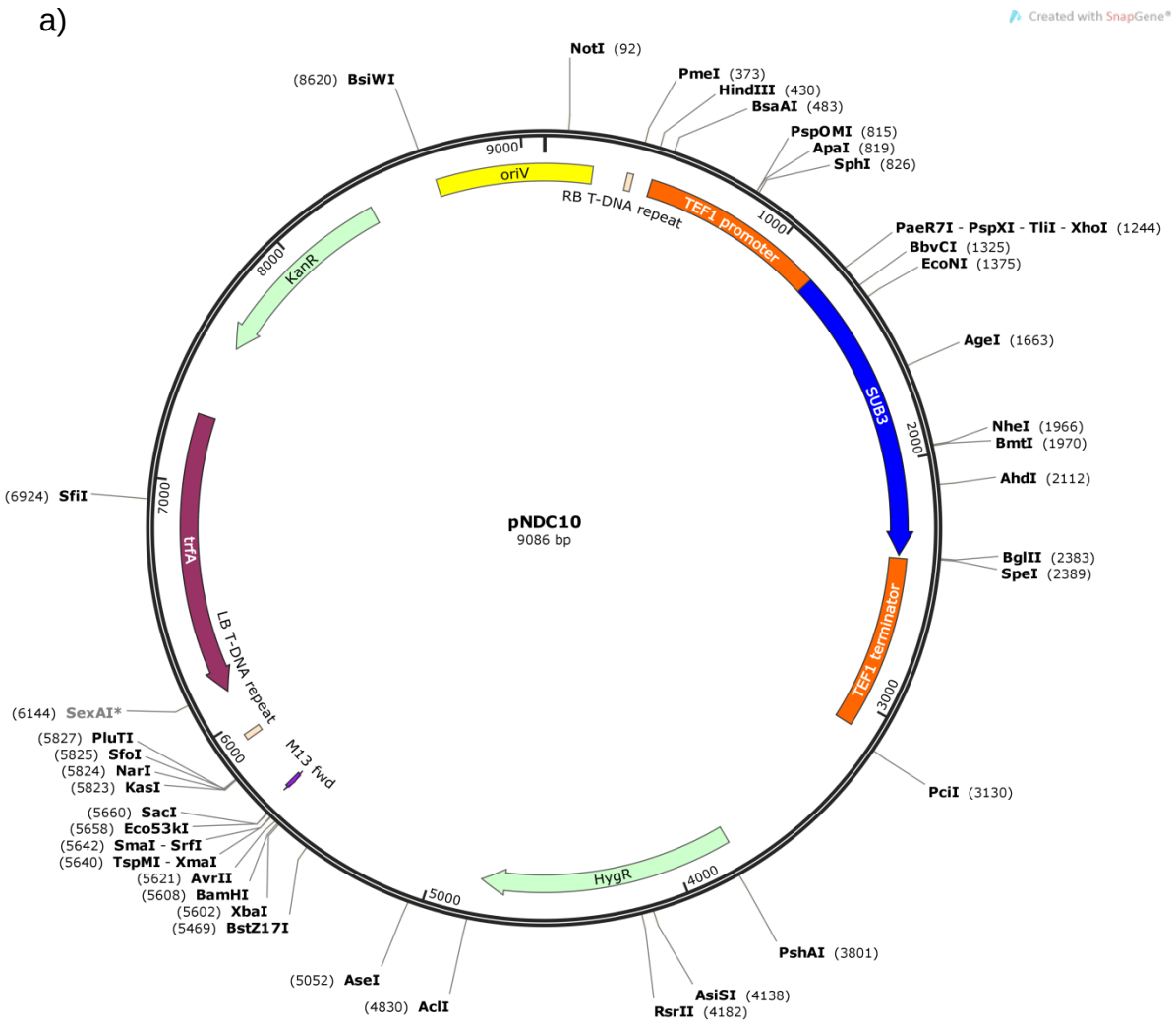

Feature	Location	Size (bp)	Description	
RB-T DNA repeat	335-359	25	right delimitation insert	
TEF1 promoter	436-1188	753	TEF1 promoter	
SUB3	1189-2382	1194	gene of interest	
TEF1 terminator	2395-3094	700	terminator	
HygR	3774-4799	1026	hygromycin resistance	
M13 fwd	5668-5684	17	cloning site	
LB T-DNA repeat	5920-5944	25	left delimitation insert	
trfA	6128-7279	1149	replication in *A. tumefaciens*	
KanR	7575-8369	795	kanamycin resistance	
oriV	8651-196	632	replication in *E. coli*	

b)

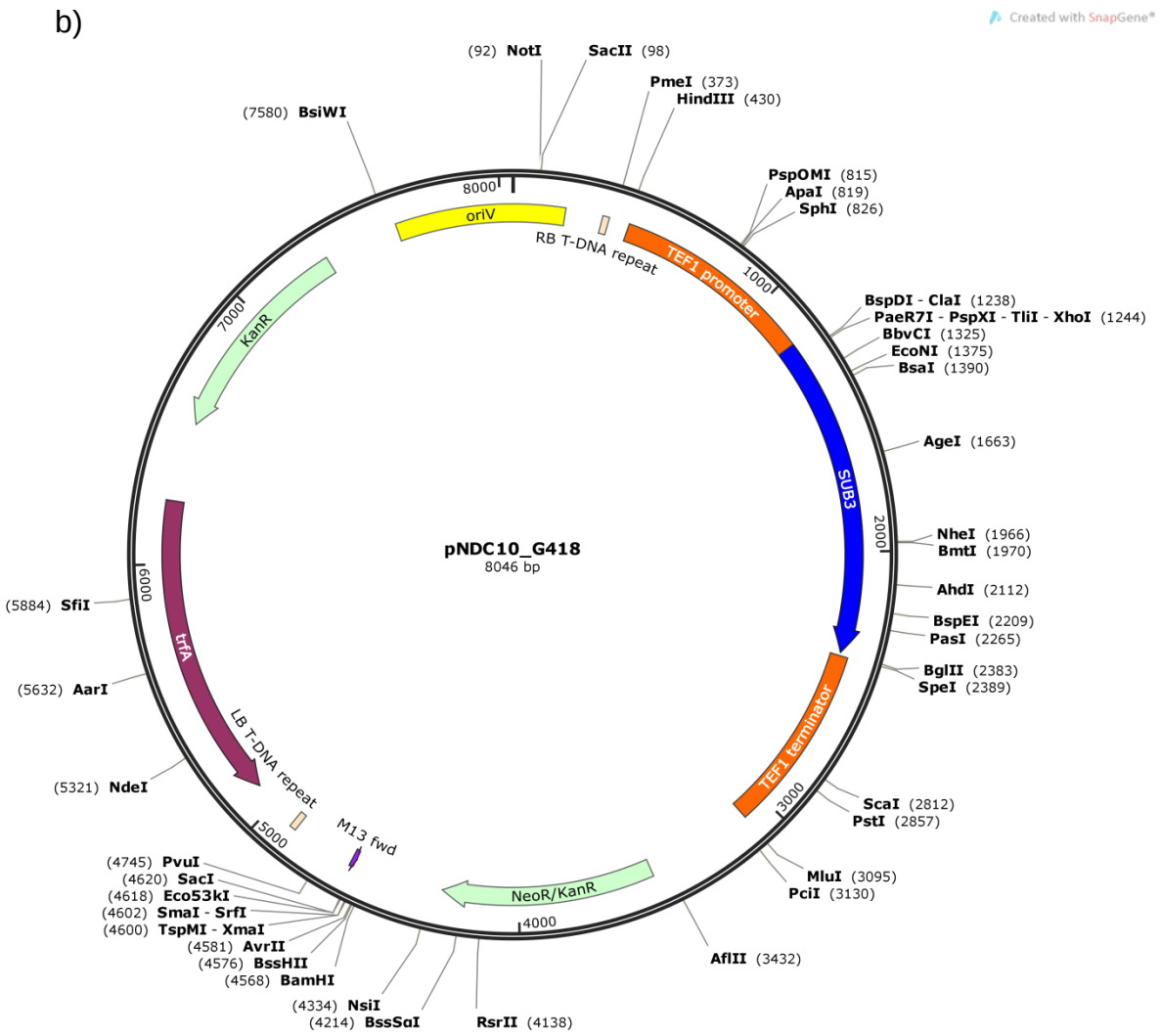

Feature	Location	Size (bp)	Description	
RB-T DNA repeat	335-359	25	right delimitation insert	
TEF1 promoter	436-1188	753	TEF1 promoter	
SUB3	1189-2382	1194	gene of interest	
TEF1 terminator	2395-3094	700	terminator	
NeoR/KanR	3494-4288	1026	neomycin resistance	
M13 fwd	4628-4644	17	cloning site	
LB T-DNA repeat	4880-4904	25	left delimitation insert	
trfA	5088-6236	1149	replication in *A. tumefaciens*	
KanR	6535-7329	795	kanamycin resistance	
oriV	7611-196	632	replication in *E. coli*	

Figure 4 Map of the plasmid pNDC0 harboring the *hph* cassette (a) and pNDC0_G418, harboring the *neo* cassette (b). Under the map the respective features of the two plasmids.

3.10. *Agrobacterium tumefaciens*-mediated transformation (ATMT)

This technique is widely used in plant molecular biology, but recently it was introduced also in the fungal molecular biology. In fact this technique allows to transform almost every fungus avoiding difficult steps of the currently transformation techniques in fungus. First of all, competent *E. coli* (DH5α strain) was transformed by heat shock with our pNDC plasmid containing the gene of interest. To select *E. coli* DH5α harboring the pNDC bacteria were grown on selective media (50 µg/ml kanamycin), PCR analysis with primers within our gene of interest was performed as additional control. The transformed *E. coli* DH5α were grown in Lysogeny Broth (LB) medium over night (ON) to amplify the pNDC and a midi purification was performed (Qiagen). The midi was used to transform *Agrobacterium tumefaciens* strain EHA105 by electroporation (2.5 V, 400 Ω, 25 µF) and to select the strains harboring our pNDC the bacteria were grown in a selective YEB media containing 50 µg/ml kanamycin, 50 µg/ml rifampicin and 25 µg/ml chloramphenicol; PCRs within our genes of interest were performed as additional control. The *A. tumefaciens* strains harboring appropriate binary vector which had been grown on soli YEB medium supplemented with appropriate antibiotics at 28°C for 2-3 days, were suspended in 10ml dH_2O. The bacterial cells were collected and resuspended in 1ml of AIM medium and let grown until an OD_{660} of ~0.7, at this point the bacterial suspension was supplemented with 2mM of acetosyringone and cultured on a shaker (160rpm) at 28°C for 6h.

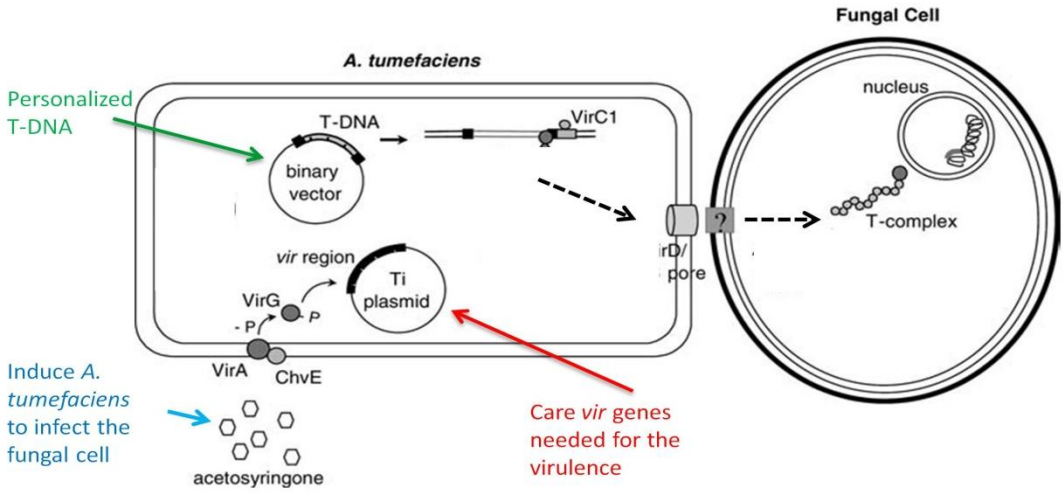

Figure 5 A schema of the *Agrobacterium tumefaciens*-mediated transformation (ATMT) showing the binary vector harboring the gene of interest (green) and the Ti plasmid harboring all the genes needed for the infection of the host in *Agrobaterium tumefaciens* (red). The membrane protein allowing the entry of the T-DNA is not yet known. (http://www.rasmusfrandsen.dk/atmt.htm).

Meanwhile *Arthroderma benhamiae* strain LAU2354-2 was grown in a modified SDA medium to induce the fungus to produce conidiae for 7-12 days. Conidiae were recolted in a 100 µL volume of dH_2O (1 x 10^7 conidia) and mixed with the same volume of *Agrobacterium* suspension. The mixture was spread onto sterilized nylon membrane (GeneScreen Hybridization Transfer Membrane, PerkinElmer, Massachusetts, USA) and placed on solid *Agrobacterium* induction medium to allow the attachment of the bacterial cell to the surface of the fungal cell (Figure 5). Plates containing the membranes were incubated for 48h at 28°C; subsequently the membranes were transferred onto plates containing 200 µg/ml of cefotaxime sodium to kill the *Agrobacterium* cells, and 300 µg/ml of hygromycin B to select for transformants. Plates were overlaid with 10 ml of SDA complemented with the previous mentioned antibiotics and incubated for 3-4 days and to increase the selection 10 ml of SDA containing 350-

400 µg/ml of hygromycin B were re-overlaid each days of the incubation. Colonies appearing on the plates were selected and analyzed by molecular biological methods (e.g. PCR).

3.11. Proteolytic activity test

Exoproteolytic activities were tested with the synthetic substrate N-Suc-Ala-Ala-Pro-Phe-p-nitroanilide supplied by Genecust (Dunedange, Luxembourg) and with the casein resorufin-labeled universal protease substrate supplied by Rohe (Mannheim, Germany).

The N-Suc-Ala-Ala-Pro-Phe-p-nitroanilide stock solution was freshly prepared at a concentration of 50 mM in DMSO and used immediately. The reaction mixture contained a concentration of 6 mM substrate and the enzyme preparation in 50 µL of 50 mM citrate buffer (pH values from 2.0 to 7.0) or in 50 mM of Tris buffer (pH values from 7.0 to 9.0). After incubation at 37°C for 10-240 min (depending on the activity of the enzyme preparation), the reaction was terminated by adding 5 µL of glacial acetic acid and then 0.9 mL of water. The released pNA was measured by spectrophotometry at λ= 405 nm. A control with substrate but without enzyme was carried out in parallel. SUB activities are expressed as mU (µmoles of released substrate/min) using -Suc-Ala-Ala-Pro-Phe-p-nitroanilide as the substrate.

Casein resorufin-labeled universal protease substrate stock solution was prepared at a concentration of 0.4% (w/v) in distilled water. 100 µL of substrate solution and 10 µL of 50 mM Tris-HCl at different pH (from 7 to 9) were added to 1 mL of distilled water to produce the reaction mix. Subsequently 50 µL of 10 days old liquid culture supernatant of the different transformants were added to 40 µL of reaction mix

and incubated at 37° C for 20-100 min (depending on the activity). After incubation the solution is precipitated by the addition of trichloroacetic acid (4% final concentration (v/v)) and incubates on ice for 5 min. After centrifugation 40 µL of Tris-HCl (500mM; pH 9.4) were added to the collected supernatant (neutralizing step). The absorbance at 574 nm of mixture was measured by spectrophotometry. The wild type strain was used as negative control and a *Pichia pastoris* modified strain producing SUB4 as positive control.

One arbitrary unit (U) of proteolytic activity was defined as that producing an absorbance of 0.01 per min.

3.12. Western blot analysis

SDS-PAGE of the different protein extracts was performed on a 10% separating gel. The gels were stained with Coomassie brilliant blue R-250 (Bio-Rad, Hercules, CA, USA). Western blots were revealed using available rabbit anti SUB6 and anti SUB7 antisera (85) and alkaline phosphatase conjugated goat anti-rabbit IgG (Bio-Rad).

4. Results

4.1. *Arthroderma benhamiae* experimental infections in guinea pigs

Skin samples from experimentally infected animals were used for transcriptomic analysis of *A. benhamiae* during infection. As shown in Table 4, at day 8 after infection, the animals showed no or minimal skin symptoms. The direct mycological examination showed numerous filaments present on the hair and skin samples with the presence of a low number of conidia (data not shown). At 14 days, the guinea pigs exhibited macroscopic skin lesions, but direct mycological examination showed fewer fungal filaments on the infected skin samples with thicker septa than at 8 days. We considered day 8 as the time point for the peak of infection and day 14 as the time point for the peak of inflammation. After 27 days, the skin lesions were still present but regressing, while very few fungal elements were observed by direct mycological examination. At day 44, the guinea pigs had fully recovered from infection, and no *A. benhamiae* filaments were observable. At this time, three animals that had recovered from primary infection were reinfected by *A. benhamiae* but did not develop a new infection. Three guinea pigs were sacrificed for each time points for RNA extraction (three replicate experiments).

4.2. RNA extraction

A large amount of high-quality RNA could be extracted from *A. benhamiae* mycelia grown in liquid cultures by use of the QIAGEN© RNeasy Plant Mini Kit following the instructions of the manufacturer. However, the QIAGEN© protocol of RNA extraction

was not suitable for extracting total RNA from infected guinea pig skin. The quality of the RNA extracted from infected guinea pig skin had an RQN of 2–4, which is sub-optimal for cDNA library construction and subsequent RNA-seq analysis. Therefore, two modifications were made to the extraction protocol, as described in the Materials and Methods (M+M) section, to increase the RNA quality from the *in vivo* samples: (i) frozen pieces of collected guinea pig skin scrapings were mechanically broken with glass beads in TRIzol, and (ii) RNAsin was used in the first and final steps of extractions to stabilize and increase the quality of extracted RNA (see M+M)). This protocol was also used for RNA extraction from *A. benhamiae* mycelia grown *in vitro* and in average gave a higher RQN compared to the kit protocol as shown in Figure 6.

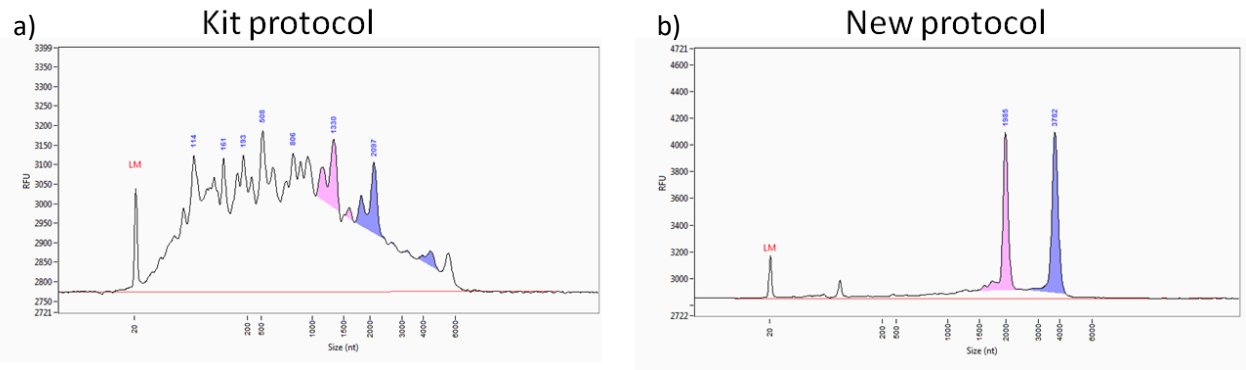

Figure 6 Bioanalyser results showing the increase in RNA quality using the modified RNA extraction protocol. Qiagen protocol (a) and modified protocol (b). Control peak (LM); Pink peak shows the 18S; Blue peak shows the 28S. A good profile should show only 3 distinct peaks (LM, 18S and 28S). Multiple peaks represent RNA degradation or/and contamination.

4.3. RNA sequencing

RNA was extracted in triplicate from the fungus grown in KSP medium, SP medium, and Sabouraud's medium and from each infected animal. Approximately 13 million reads were obtained for each RNA sample extracted from the fungus growing in the three tested culture media (Table 5). Approximately 30 million 'strand-specific' reads were acquired from each RNA sample extracted from infected skin samples, consisting of a mixture of reads from the fungus and from its mammalian host (Table 4). As a result, roughly 1 million fungal reads (2.8%) were obtained with RNA extracted from skin samples of guinea pigs at day 8 of infection, while 91.3% of the reads could be aligned with the guinea pig genome. The number of fungal reads (about 50,000) obtained with RNA extracted at day 14 of infection was not suitable to perform powerfull statistical analysis of gene expression, but were still enough to be indicative.

Table 4 RNA data summary Representation of the total reads obtained from the RNAseq (second column) of the different conditions (first column); the number of reads aligning to *A. benhamiae* genome (third column); percentage of the aligned reads from the total reads obtained (fourth column); percentage of reads aligning to the guinea pig (*Cavia porcellus*) genome (fifth column) and the representative percentage (sixth column). In green are represented the data which could be used for the analysis; in yellow are data which still could be used for the analysis but were not as good as those in green; in red are data we could not use for our analysis; NA stands for not applicable. All given read numbers are means obtained from three different guinea pigs. Below, images of guinea pig infected skins at the different time points showing the degree of the lesion caused by the dermatophyte.

Days	Total clean reads	# reads aligned to *A. benhamiae*	(%)	**# reads aligned to *C. porcellus***	**(%)**
8	30,733,918	858,530	2.79	28,082,022	91.30
14	31,271,442	40,153	0.13	29,451,220	94.18
27	34,539,337	577	0.00	32,338,000	93.60
44	30,960,429	708	0.00	28,733,038	92.81
WT	26,066,193	637	0.00	24,337,355	93.37
keratin	13,260,733	7,322,903	55.22	NA	NA
soy	9,904,026	4,433,104	44.76	NA	NA
Sabouraud	11,435,711	5,303,987	46.38	NA	NA

Day : 0 8 14 27 44

Table 5 Designation of samples and growth conditions

RNA sample	Growth condition	
	Code	**Description**
Cb1	Gp8	*In vivo*: Guinea pig 8 days post infection
Cb2		
Cb3		
Cb4	Gp14	*In vivo*: Guinea pig 14 days post infection
Cb5		
Cb6		
K1	K	*In vitro*: Keratin medium
K2		
K3		
S1	S	*In vitro*: Soy medium
S2		
S4		
Sa1	Sa	*In vitro*: Sabouraud medium
Sa2		
Sa3		

4.4. New gene annotation of the *Arthroderma benhamiae* genome

The annotation work of the *A. benhamiae* genome was performed by the bioinformatic collaborators Thuong Van Du Tran and Marco Pagni from the SIB.

A preliminary investigation of the RNA-seq reads mapped onto the *A. benhamiae* genome revealed that many gene and intron locations from the original genome annotations were not supported by our experimental data. Hence, re-annotating the CDS of the genome appeared to be a prerequisite before further analyzing the transcriptome expression. Particular attention was paid to the location of the start codons because of our high interest in secreted proteins, which should be endowed with a signal peptide at the N-terminus.

augustus (63), a program for gene prediction in eukaryotic organisms that relies on a statistical model of an organism's gene structure was used. The correctness of *augustus* predictions is, however, highly dependent on this model, and great care must be used at the time of training this model (e.g., establishing the model using a training dataset). Practically, we mapped all RNA-seq reads onto the genome, deduced full-length gene transcripts, and retained only those with sufficient coverage. Then, we translated the filtered transcripts into their three possible coding frames. Full-length CDS were detected by aligning the transcripts against a set of high-quality protein sequences, namely the protein sequences reviewed by Swiss-Prot of the model organisms *S. cerevisiae* and *A. nidulans*. The CDS annotations were back-propagated onto the genome, introducing intron descriptions, and supplied as a training set to

augustus to generate a new gene model. With the latter, the *A. benhamiae* genome was re-annotated and yielded 7387 protein-coding genes.

Table 6 compares our 7387 newly predicted genes with the original set of 7979 and shows that about 65% of the genes have been affected one way or another, for example the intron boundaries within 1242 genes were corrected and 383 new genes were recorded. In addition, 39 genes in the existing annotation were split into two genes, and, in contrast, 297 genes in the new annotation corresponded to fusions of previously annotated genes.

Table 6 Comparison between the new gene set and the original one. *Matched*: identical old and new gene annotations; *Alternative*: conserved start and stop codons but different splicing; *Different*: different start or stop codons, possibly different splicing; *Merged*: more than one old gene merged into a single new one; *Split*: old gene split into several new ones; *New*: genes only found in the new predictions (708 original genes were lost, see text). *Auto*: gene annotations as produced by *augustus*; *Manual*: manual correction of the start codon. The number of genes whose products were confirmed by mass spectrometry in culture supernatants is given between parentheses. GPI: Glycosylphosphatidylinositol.

New vs old gene prediction	**Gene count in complete genome**	**Gene count in secretome only**							
		With GPI				**Without GPI**			
		Auto		**Manual**		**Auto**		**Manual**	
Matched	2628	47	(**13**)	1	(**1**)	154	(**55**)	0	
Alternative	1242	19	(**6**)	0		49	(**19**)	0	
Different	2761	31	(**6**)	1		85	(**19**)	9	(**4**)
Merged	297	6	(**3**)	0		8	(**2**)	1	
Split	76	1	(**1**)	0		5	(**2**)	0	
New	383	6		0		34	(**8**)	0	
	7387	110	(**29**)	2	(**1**)	335	(**105**)	10	(**4**)

4.5. *In silico* definition of the secretome

In collaboration with Marc Feuermann from the SIB, we decided to define the *secretome* as the set of all secreted proteins, which is made of all proteins with a signal peptide, excluding trans-membrane proteins. In practice, this set is not trivial to define. The presence/absence of a signal peptide depends on the tools used to predict it, on the strength of the signal itself, and on its presence at the N-terminus, which ultimately relies on the correct detection of the start codon. Hence, all genes predicted by *augustus* were further subjected to prediction refinements

A total of 634 proteins with a signal peptide, including 112 probable GPI-anchored proteins, have been predicted. Using transmembrane predictors, we removed all proteins that contained one or more transmembrane spans in addition to the signal peptide and that were probably targeted to membranes. This refinement led to a final *A. benhamiae* predicted secretome, made of 457 proteins that are listed and characterized in Table S1.

MS data were previously published regarding proteins secreted by cells grown in soy protein liquid medium (77). A new analysis of these data was conducted, using the new secretome definition. The presence of 139 proteins in the supernatant at either pH 4 or 7 was confirmed (Table S1), including 8 of the newly predicted ones. Moreover, among the 708 proteins from the original annotation that were lost in our new prediction, 31 were supposed to be secreted, but none of them could be detected in the MS data.

4.6. *Arthroderma benhamiae* gene expression in different growth conditions

The nomenclature used for the samples and the corresponding growth conditions are given in Table 5. Figure 7 presents an overview of the gene expression in the different samples, considering either the complete genome or the secretome subset. Both hierarchical clustering and principal component analysis indicate that the biological replicates are closer to each other than to other conditions. The only exception is possibly with the Gp samples, where the distinction between the conditions observed at 8 and 14 days post infection does not really exceed the inter-Gp variations (Figure 8). The expression differences are strongly dominated by the contrast between *in vivo* Gp8+Gp14 and *in vitro* S+Sa+K conditions. This result confirms and generalizes the observations made previously on a much smaller gene set (27). The analysis of the expression data from the complete genome (including the secretome) and of the secretome yielded the same strong contrast, possibly even slightly reinforced for the secretome.

Among the *in vitro* conditions, the gene expressions in the soy and Sabouraud media appeared closer to each other in the complete gene set, while soy and keratin appeared closer in the secretome subset. None of the three *in vitro* conditions tested is a good proxy for *in vivo* growth conditions, despite the keratin medium being supposed to mimic the host environment. To address this question in more depth, we enumerated all possible partitions of growth conditions into two subsets, to contrast a subset of conditions versus the remaining ones. The list of all possible contrasts is given in Figure 7, with the corresponding amounts of differentially expressed genes. This confirms that

the *in vivo* versus *in vitro* contrast is dominant and that not much information can be expected to be gathered by separating Gp8 from Gp14. Interestingly, two other contrasts seem to carry additional signals: K:Gp8+Gp14+Sa+S in the genome complete gene set and Gp8+Gp14+Sa:S+K in the secretome subset.

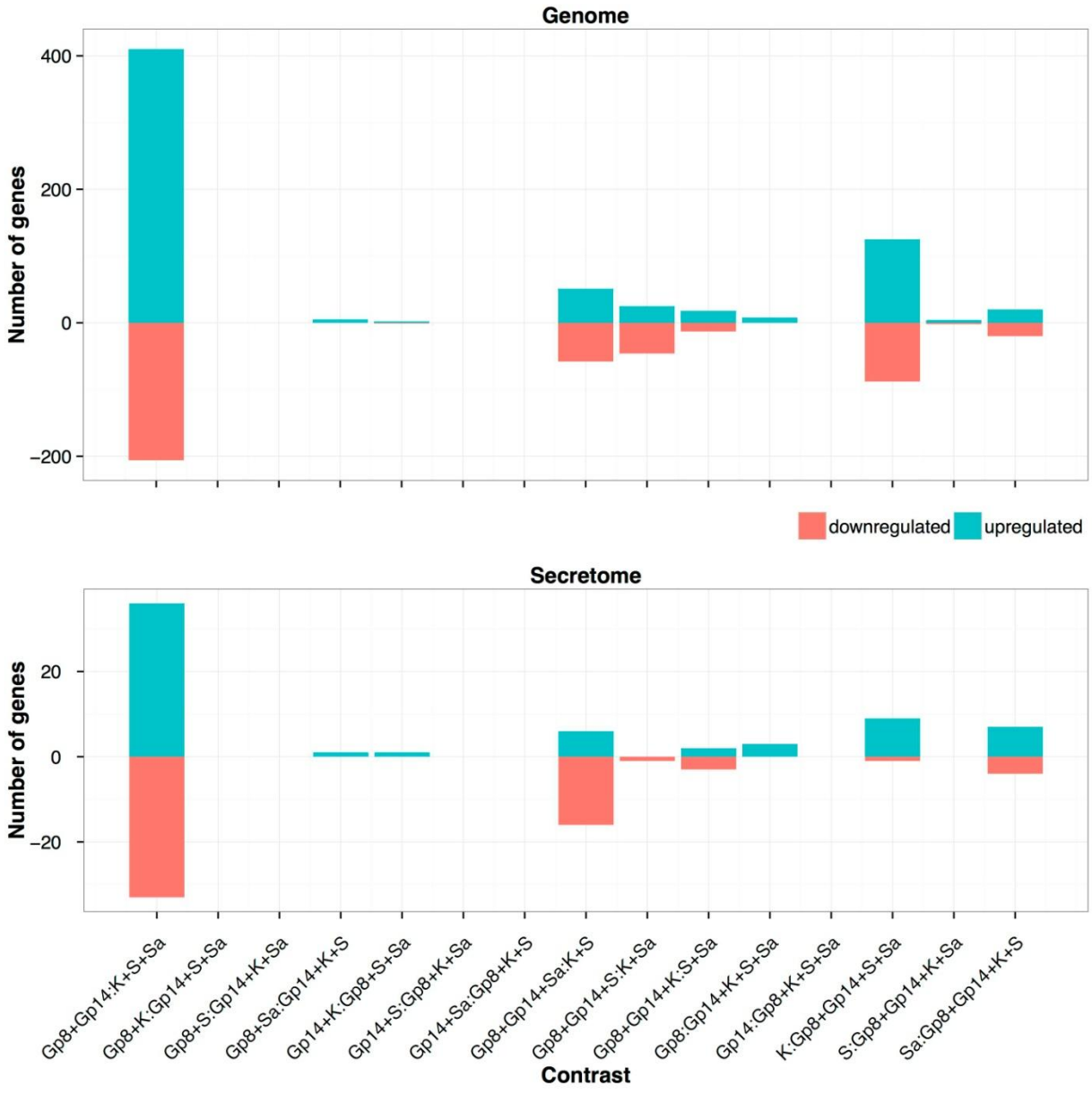

Figure 7 Number of differentially expressed genes versus the enumeration of all possible contrasting conditions in the genome and the secretome, using a cut-off of 1e-3 for FDR and 2 for the fold change.

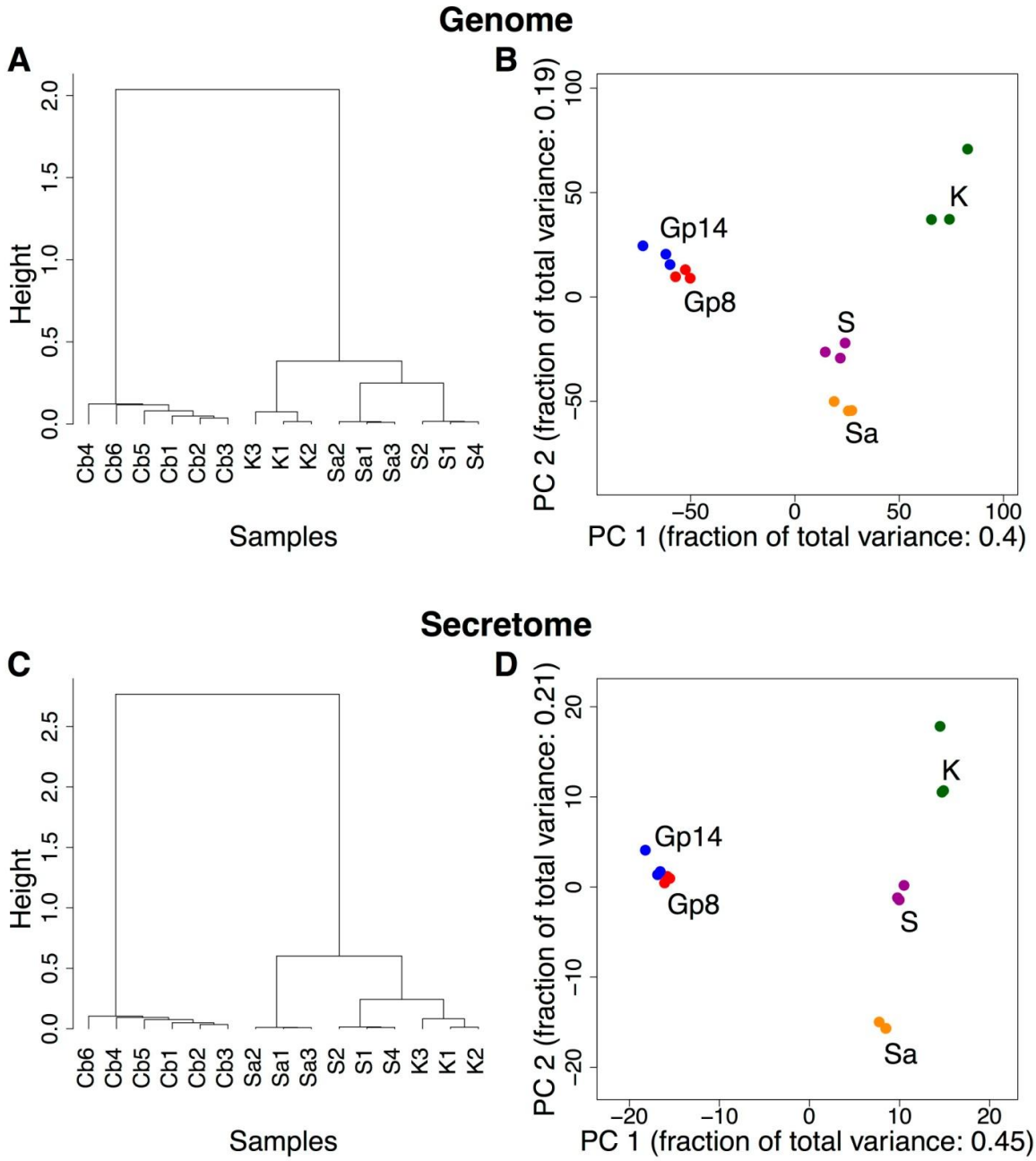

Figure 8 Hierarchical clustering (A, C) and principal component analysis (B, D) of RNA sequencing samples considering the genes from the complete genome (A, B) or only the secretome subset (C, D). The sample names reflect the growth conditions: Cb, *in vivo* in guinea pig; S, *in vitro* in soy medium; Sa, *in vitro* in Sabouraud medium; K, *in vitro* in keratin medium. The *in vivo* samples cluster together.

4.7. Gene expression profile of *Arthroderma benhamiae* cell surface/secreted proteins during inflammatory cutaneous infection

Table 7A lists the 25 most highly expressed secretome-related genes *in vivo* (8 and 14 days after infection). Only a few gene products have been clearly identified: ARB_00653 encoding a putative NAD-dependent malate dehydrogenase, ARB_02206 for a putative sialidase, two genes for putative 1,3-beta-glucanosyltransferases (ARB_07487 and ARB_05253), and five for putative proteases including three subtilisins (SUB6 encoded by ARB_05307, SUB8 by ARB_00777, and SUB10 by ARB_06467), ARB_04336 for a neutral protease of the deuterolysin family (M35), and ARB_02919 for the aspartic protease PEP2.

In silico analysis of the protein sequences led to the identification of some features that might point to their putative roles (Figure 9A). The most highly expressed gene, ARB_01183, encodes a protein which has not been characterized but which contains a thaumatin domain. Three gene products are predicted to contain GPI-anchors (ARB_01627, ARB_2697, and ARB_7696), two contain a common in fungal extracellular membrane (CFEM) domain (ARB_02741, ARB_01545), one with a glycoside hydrolase domain (ARB_07954), and one with a carboxylesterase domain (ARB_02369). Moreover, a sequence similarity search provided some additional clues about the function or localization of a few more gene products: ARB_06538 might encode a putative stress-responsive protein, ARB_06390 a cell wall protein and ARB_06538 an extracellular matrix protein. ARB_06463 shows similarities to ribosomal

proteins. Four genes encode proteins for which we did not find any functional data. These include ARBNEW_231, a newly predicted gene and the third most highly expressed gene *in vivo*. Table 7A also reveals that the expression pattern is not significantly different between the two *in vivo* conditions, suggesting that no remarkable metabolic changes occur between day 8 and day 14 of infection, at least at the secretome level.

The secretome expression pattern was completely different during growth on keratin, an *in vitro* condition supposed to mimic the host environment (Table 7B, Figure 9C). As an example, even if about 20% of the 100 most expressed secreted proteins are proteases in both *in vivo* and in keratin (Figure 9B), the batch of proteins expressed in these different conditions is clearly different (Figure 9C). This is in accordance with our above-mentioned WGCNA analysis in which relevant correlation groups were found only when *in vivo* and keratin conditions were contrasted (Gp8+Gp14:Sa+S+K, Gp8+Gp14+Sa:S+K, Gp8+Gp14+S:Sa+K, or Gp8+Gp14+Sa+S:K). Expression patterns in soy and Sabouraud are closer to that in keratin, yet they are distinct from each other (Figure 7), which explains their relatively neutral impact in the WGCNA contrasts. Among the 25 most highly expressed secretome-related genes, only five were found to be in common: two encoding putative GPI-anchored proteins (ARB_01627 and ARB_07696), ARB_02741 encoding a CFEM domain protein, ARB_06390 for a putative cell wall protein, and ARB_02369 for a carboxylesterase domain-containing protein. Eight putative secreted proteases were found to be encoded among the 25 most highly expressed genes on keratin; however, none is in common with those highly expressed during infection.

Table 8 lists the 12 most highly expressed genes encoding proteases during infection and those expressed on keratin. The genes encoding SUB6 (ARB_05307), SUB10 (ARB_06467), and the deuterolysin (ARB_04336) are highly and specifically upregulated during the infection phase with fold changes of 2000x, 60x, and 100x, respectively. The gene encoding SUB8 (ARB_00777) was relatively downregulated in keratin. PEP2 (ARB_02919), which is a putative ortholog of the vacuolar aspartic protease of *S. cerevisiae* PrA and has been subsequently identified in other filamentous fungi, was found to be highly expressed under all the *in vivo* and *in vitro* conditions.

On the other hand, the protease genes upregulated in keratin include subtilisins SUB3 (encoded by ARB_00701) and SUB4 (ARB_01032), the metallocarboxypeptidase MCPA of the M14 family (ARB_07026_07027), the leucine aminopeptidases LAP1 (ARB_03568) and LAP2 (ARB_00494), the aspartic protease OPSB (ARB_04170), and two extracellular metalloproteases (ARB_05085, ARB_05317).

Likewise, in the soy culture, only four protease genes were highly expressed: SUB4 (encoded by ARB_01032), LAP2 (ARB_00494), PEP2 (ARB_02919), and DPPV (ARB_06651) (Table S6). With the Sabouraud culture, in addition to PEP2, SUB8 (ARB_00777) and OPSB (ARB_04170) showed relatively high expression.

Table 7 Twenty-five most highly expressed genes encoding secreted proteins during infection compared to *in vitro* expression; (B) Twenty-five most highly expressed genes encoding secreted proteins *in vitro* (KPS medium) compared to *in vivo* expression. Expression levels are in transcripts per kilobase millions (TPM). Standard deviaton average: ±141 for Gp8; ±401 for Gp14; ± 595 for K, ± 172 for S and ± 233 for Sa in (a). ± 1806 for K; ±66 for Gp8; ±97 for Gp14, ± 425 for S and ± 343 for Sa in (b)

(a)

	Gp8	Gp14	K	S	Sa
Antigenic thaumatin−like protein : ARB_01183	6131.2	7203.45	30.04	34.6	257.26
Subtilisin−like protease SUB6 (peptidase S8 family) : ARB_05307	5036.99	2631.96	1.21	1.7	2.79
Uncharacterized protein conserved in filamentous fungi : ARBNEW_231	4218.62	1752.17	0.34	0.1	1375.82
Uncharacterized protein : ARB_03496	4021.16	3952.23	11.68	9.2	17.83
GPI−anchored CFEM domain protein : ARB_02741	3503.48	3821.21	14805.46	8079.51	2149.45
Uncharacterized protein : ARB_05215_05217	3074.2	3499.98	41.92	107.17	215.76
Uncharacterized protein : ARB_02803	3064.4	3092.76	7272.66	6071.91	10321.25
Glycoside hydrolase : ARB_07954	2746.09	4707.54	163.59	866.05	2986.3
GPI−anchored cell wall protein : ARB_01627	2663.98	2756.38	2548.84	1539.09	2111.72
GPI−anchored cell wall protein : ARB_02697	2413.1	3204.93	1052.9	1075.17	1072.41
Ribosomal protein−like : ARB_06463	2092.63	1674.07	827.51	2732.89	3796.79
GPI anchored serine−threonine rich protein : ARB_07696	1628.54	1424.67	3462.73	2765.99	7210.23
1,3−beta−glucanosyltransferase (glycosyl hydrolase 72 family) : ARB_07487	1464.52	1220.67	612.62	529.91	439.93
GPI−anchored CFEM domain protein : ARB_01545	1229.73	1192.05	41.93	331.29	352.46
Neutral protease 2 homolog (peptidase M35 family) : ARB_04336	1156.36	1120.08	12.73	13.09	9.48
1,3−beta−glucanosyltransferase (glycosyl hydrolase 72 family) : ARB_05770	947.52	1298.82	461.92	368.72	411.9
Aspartic−type endopeptidase PEP2 (peptidase A1 family) : ARB_02919	843.45	970.31	691.09	1136.3	549.54
Secreted lipase (type−B carboxylesterase family) : ARB_02369	828.2	291.04	1727.24	561.67	10.69
Subtilisin−like protease SUB10 (peptidase S8 family) : ARB_06467	791.13	789.18	11.62	13.26	12.92
PGA52−like protein (Asp f 4 homolog) : ARB_06390	759.55	749.58	2380.81	1307.5	2003.33
Sialidase : ARB_02206	692.21	1026.03	10.2	5.39	5.24
Extracellular matrix protein : ARB_06538	669.18	911.13	193.05	281.04	699.93
Subtilisin−like protease SUB8 (peptidase S8 family) : ARB_00777	642.2	682.55	188.06	669.86	437.99
Putative stress−responsive protein : ARB_05496	640.41	945.37	16.64	111.83	47.77
NAD−dependent malate dehydrogenase : ARB_00653	615.04	591.45	499.85	820.57	1216.75

(b)

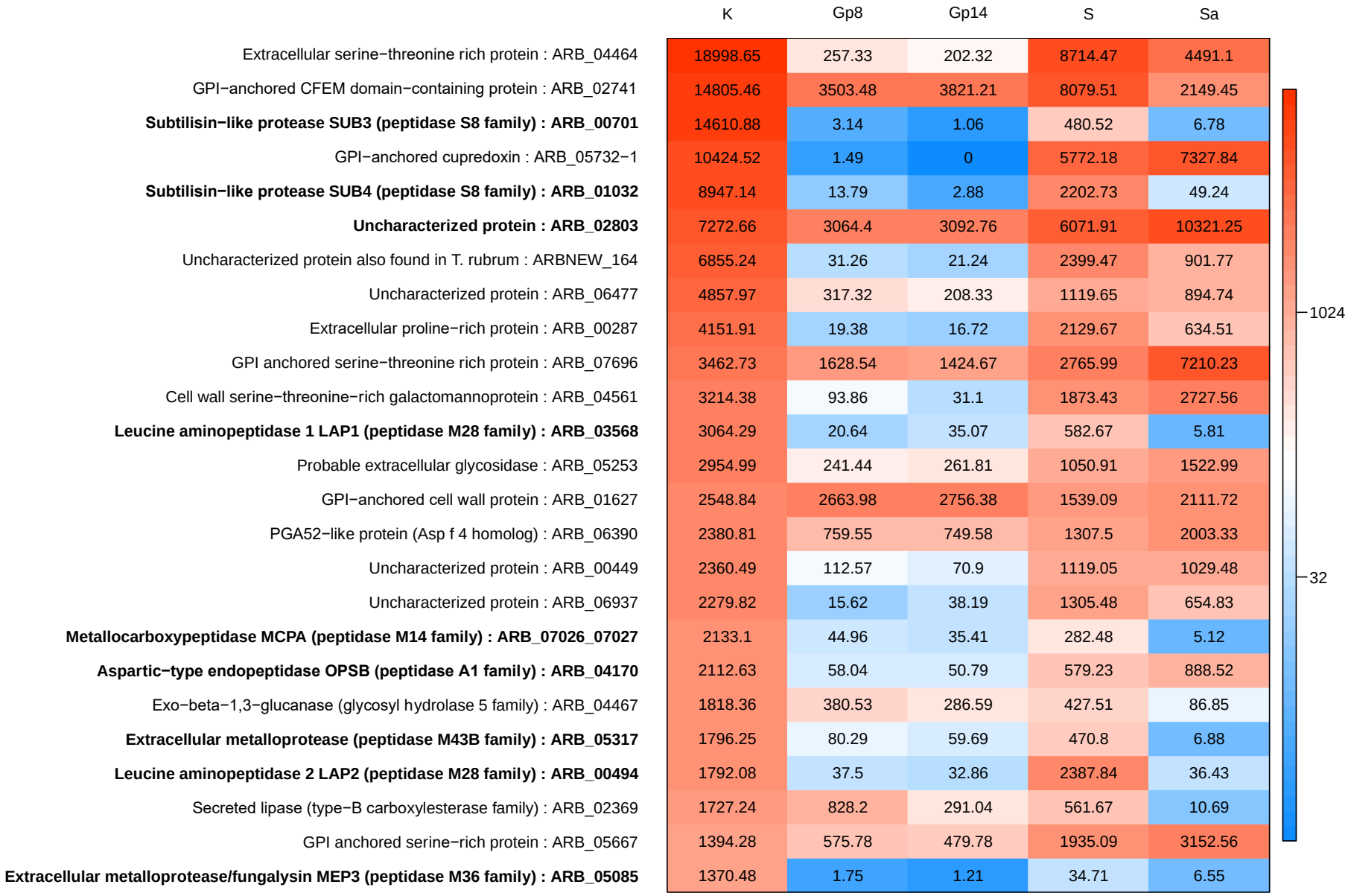
K
Gp8
Gp14
S
Sa
Extracellular serine−threonine rich protein : ARB_04464
18998.65
257.33
202.32
8714.47
4491.1
GPI−anchored CFEM domain−containing protein : ARB_02741
14805.46
3503.48
3821.21
8079.51
2149.45
Subtilisin−like protease SUB3 (peptidase S8 family) : ARB_00701
14610.88
3.14
1.06
480.52
6.78
GPI−anchored cupredoxin : ARB_05732−1
10424.52
1.49
0
5772.18
7327.84
Subtilisin−like protease SUB4 (peptidase S8 family) : ARB_01032
8947.14
13.79
2.88
2202.73
49.24
Uncharacterized protein : ARB_02803
7272.66
3064.4
3092.76
6071.91
10321.25
Uncharacterized protein also found in T. rubrum : ARBNEW_164
6855.24
31.26
21.24
2399.47
901.77
Uncharacterized protein : ARB_06477
4857.97
317.32
208.33
1119.65
894.74
Extracellular proline−rich protein : ARB_00287
4151.91
19.38
16.72
2129.67
634.51
GPI anchored serine−threonine rich protein : ARB_07696
3462.73
1628.54
1424.67
2765.99
7210.23
Cell wall serine−threonine−rich galactomannoprotein : ARB_04561
3214.38
93.86
31.1
1873.43
2727.56
Leucine aminopeptidase 1 LAP1 (peptidase M28 family) : ARB_03568
3064.29
20.64
35.07
582.67
5.81
Probable extracellular glycosidase : ARB_05253
2954.99
241.44
261.81
1050.91
1522.99
GPI−anchored cell wall protein : ARB_01627
2548.84
2663.98
2756.38
1539.09
2111.72
PGA52−like protein (Asp f 4 homolog) : ARB_06390
2380.81
759.55
749.58
1307.5
2003.33
Uncharacterized protein : ARB_00449
2360.49
112.57
70.9
1119.05
1029.48
Uncharacterized protein : ARB_06937
2279.82
15.62
38.19
1305.48
654.83
Metallocarboxypeptidase MCPA (peptidase M14 family) : ARB_07026_07027
2133.1
44.96
35.41
282.48
5.12
Aspartic−type endopeptidase OPSB (peptidase A1 family) : ARB_04170
2112.63
58.04
50.79
579.23
888.52
Exo−beta−1,3−glucanase (glycosyl hydrolase 5 family) : ARB_04467
1818.36
380.53
286.59
427.51
86.85
Extracellular metalloprotease (peptidase M43B family) : ARB_05317
1796.25
80.29
59.69
470.8
6.88
Leucine aminopeptidase 2 LAP2 (peptidase M28 family) : ARB_00494
1792.08
37.5
32.86
2387.84
36.43
Secreted lipase (type−B carboxylesterase family) : ARB_02369
1727.24
828.2
291.04
561.67
10.69
GPI anchored serine−rich protein : ARB_05667
1394.28
575.78
479.78
1935.09
3152.56
Extracellular metalloprotease/fungalysin MEP3 (peptidase M36 family) : ARB_05085
1370.48
1.75
1.21
34.71
6.55
1024
32

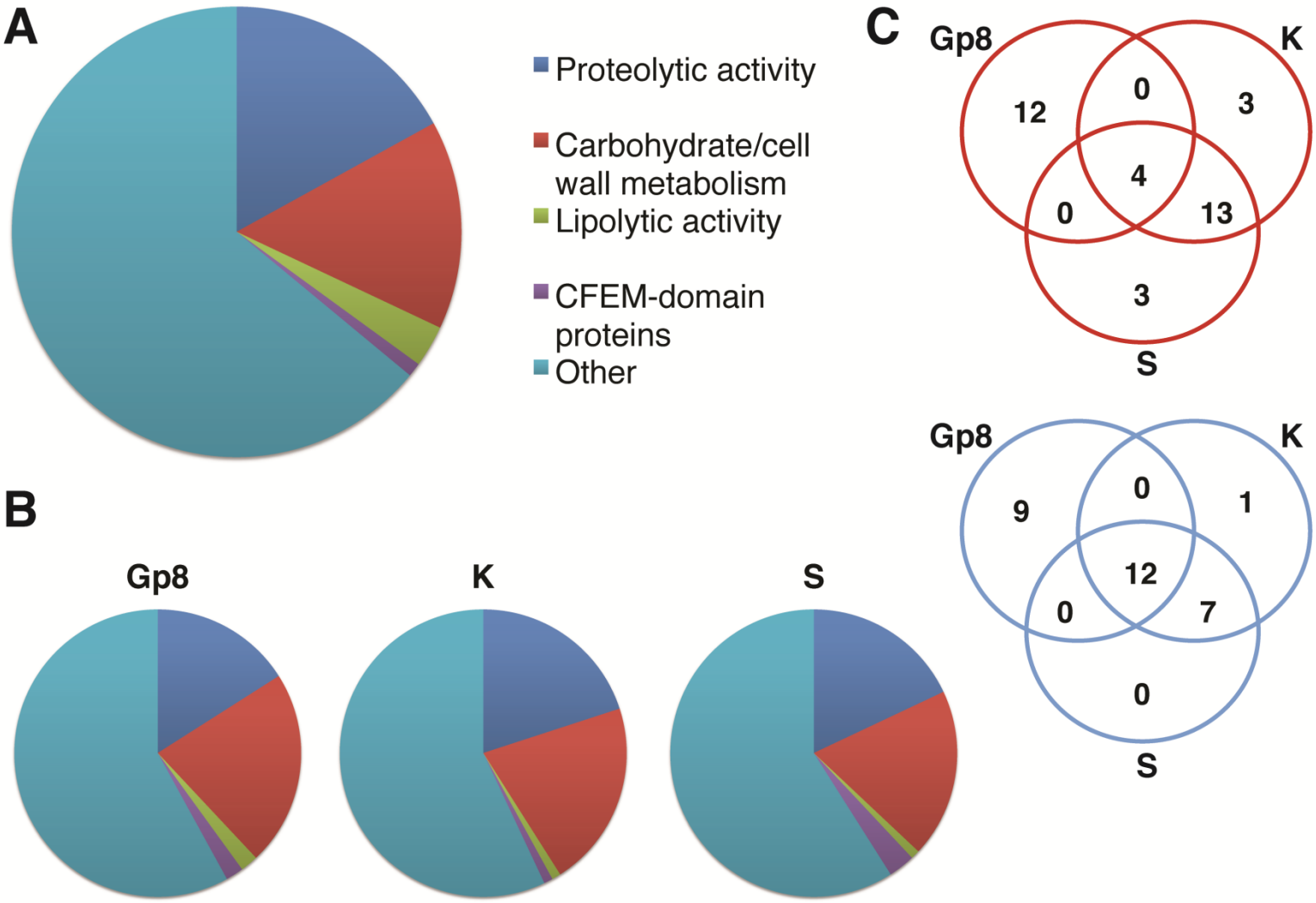

Figure 9 Characterization of the secretome. (A) Pie chart showing the main functional groups identified within the 457 proteins of the secretome. See also detailed description in supplementary material. (B) Pie charts showing the same functional groups as in (A), but within the most 100 expressed genes *in vivo* (8 days) (V), on keratin, a condition supposed to mimic *in vivo* conditions (K), and on soy, a classical *in vitro* condition (S). (C) Venn diagram of proteases (below) and carbohydrate/cell wall metabolim proteins (above) present in the 100 most expressed secreted proteins in the 3 conditions described in (B). Proteases represent about 20% of the 100 most expressed proteins in the 3 conditions, however, the batch of proteins is clearly different *in vivo* when compared to keratin and soy. This trend is not as significant when comparing carbohydrate/cell wall metabolim proteins.

Table 8 Twelve most highly expressed genes encoding secreted proteases during infection (left table) and during *in vitro* growing in keratin medium (right table). In bolt the only protease (PEP2) present in both conditions in the first 12 more expressed genes encoding for secreted proteases.

	Gp8	K	
Subtilisin−like protease SUB6 : ARB_05307	5036.99	14610.88	ARB_00701 : Subtilisin−like protease SUB3
Neutral protease 2 homolog : ARB_04336	1156.36	8947.14	ARB_01032 : Subtilisin−like protease SUB4
Aspartic−type endopeptidase PEP2 : ARB_02919	843.45	7272.66	ARB_02803 : Uncharacterized protein
Subtilisin−like protease SUB10 : ARB_06467	791.13	3064.29	ARB_03568 : Leucine aminopeptidase LAP1
Subtilisin−like protease SUB8 : ARB_00777	642.2	2133.1	ARB_07026_07027 : Metallocarboxypeptidase MCPA
Carboxypeptidase Y homolog A CPYA : ARB_01491	528.34	2112.63	ARB_04170 : Aspartic−type endopeptidase OPSB
Probable serine carboxypeptidase : ARB_06414	459.6	1796.25	ARB_05317 : Probable metaloproteinase
Subtilisin−like protease SUB1 : ARB_04944	422.02	1792.08	ARB_00494 : Leucine aminopeptidase LAP2
Peptidase S41 family protein : ARB_02997	181.69	1370.48	ARB_05085 : Extracellular metalloprotease MEP3 (fungalysin)
Probable glutamate carboxypeptidase : ARB_02390	150.69	792.98	ARB_06110 : Dipeptidyl peptidase 4 DPPIV
Carboxypeptidase S1 homolog A SCPA : ARB_04046	133.52	760.65	ARB_06651 : Dipeptidyl peptidase 5 DPPV
Putative metallocarboxypeptidase ECM14 : ARB_04942	125.9	691.09	**ARB_02919 : Aspartic−type endopeptidase PEP2**

4.8. Production of recombinant subtilisin proteases in *A. benhamiae*

Several attempts to produce recombinant SUB4, SUB6 and SUB7 were performed using *Pichia pastoris* as an expression system. SUB4 was produced as recombinant protein, while no recombinant protein was detected for SUB6 and SUB7 in *P. pastoris* culture supernatant (86). The failure to produce recombinant *A. benhamiae* subtilisins in *P. pastoris* led us to establish a homologous expression system in *A. benhamiae*. *Arthroderma benhamiae* SUB4, SUB6 and SUB7 were produced by overexpressing their encoding gene in *A. benhamiae* strain LAU2354-2.

In a first step we constructed the plasmid pNDC1 with the gene *SUB4* as described in Material and Method section. This plasmid carried the *HGH* gene as a selection marker. Then, *SUB4* in pNDC1 was replaced by genomic DNA encoding SUB6 and SUB7 to generate pNDC2 and pNDC3. However, we had difficulties to distinguish Hygromycin resistant *A. benhamiae* transformants from a fungal background in Petri dishes. In fact, hygromycin B selection was first used with *Arthroderma vanbreuseghemii* by Yamada in 2009 (83) but we noticed that the MIC to hygromycin B of *A. benhamiae* was higher than that of *A. vanbreuseghemii*. Therefore, another selection marker was tested and we constructed another expression plasmid, pNDC4-7, carrying the *E. coli* neomycin phosphotransferase gene conferring resistance to the gentamycin 418. Hygromycin B and Gentamycin (G418) are aminoglycoside which inhibit protein synthesis, but gentamycin revealed to be more efficient to select *A. benhamiae* transformants from the background. *A. benhamiae* was unable to grow in

the presence of more than 200 µg/mL of G418 (Figure 10), while it was still slowly growing using hygromycin B at a concentration of 600 µg/mL.

More than 25-30 hygromycin resistant *A. benhamiae* transformants were obtained with *A. tumefaciens*-mediated transformation using each constructed expression plasmid. The transformants were purified by performing subcultures on Sabouraud's agar containing hygromycin at a concentration of 400 µg/ mL, and subsequently grown in Sabouraud's liquid medium for 9 days without hygromycin. The transformants producing the maximum of SUB4, SUB6 or SUB7 activity (0.42 mU and 0.72 mU per mL, respectively) were called AbeSUB4, AbeSUB6 and AbeSUB7, respectively (Figure 12a). As a control, *A. benhamiae* LAU2354-2 and a transformant obtained with a plasmid where the SUB4 gene was deleted did not produce appreciable proteolytic activity. Western blot analyses revealed that SUB4, SUB6 and SUB7 were secreted by the selected transformants as strong signals were obtained using (specific) antibodies raised against orthologous subtilisins in *T. rubrum* (85) (Figure 13).

A similar number of transformants (15-20) were obtained with ATMT using the neomycin phosphotransferase cassette. They were isolated and cultured in Sabouraud liquid medium for 9 days. The transformants with the maximum proteolytic activity (0.38 mU, 0.66 mU and 0.46 mU per mL) were selected for further characterization and named AbeSUB6_G418, AbeSUB7_G418 and AbeSUB8_G418 respectevly (Figure 12b).

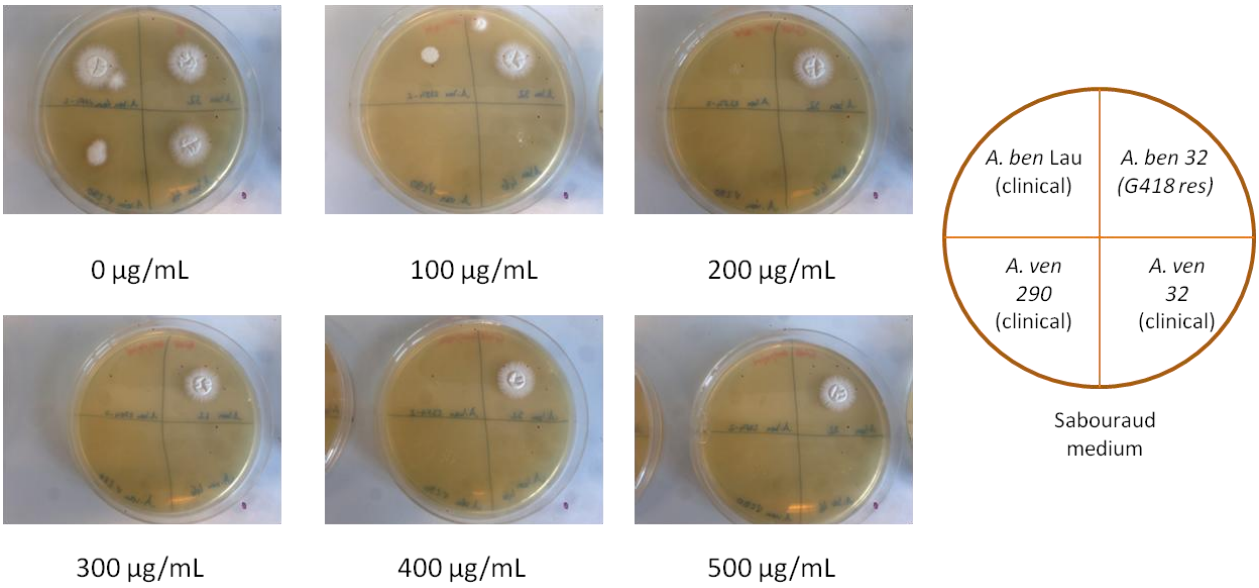

Figure 10 Minimum inhibitory concentration test with gentamycin 418. Our strain *(A. benhamiae* Lau2354-2), two others clinical strains (*A. vanbreuseghemii* 290 and 32) and a modified *A. benhamiae* resaistant to G418 (*A. benhamiae* 32). Different concentration of gentamycin 418 were used. Sabouraud media were use to perform the MIC test.

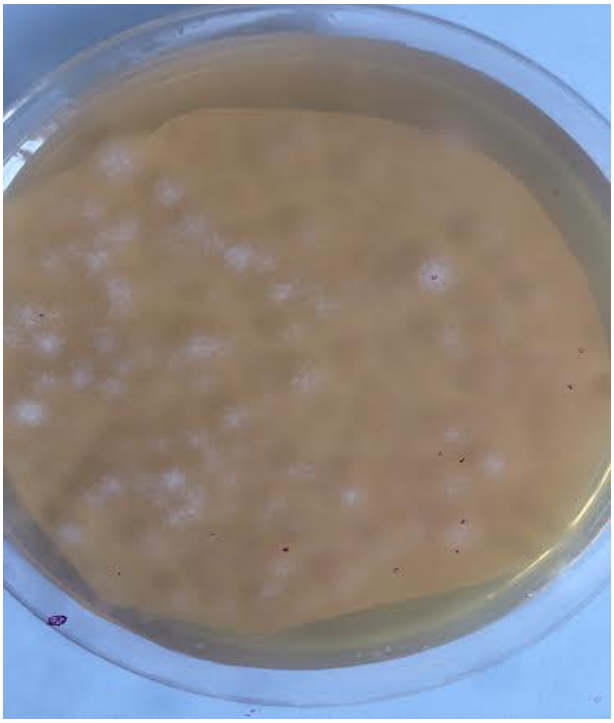

Figure 11 As explain in MM; after the last coverage with 10mL of selective Sabouraud medium containing 200 µg/mL G418, the transformants were incubated at 30 °C for 3-4 days until the appearance of colonies..

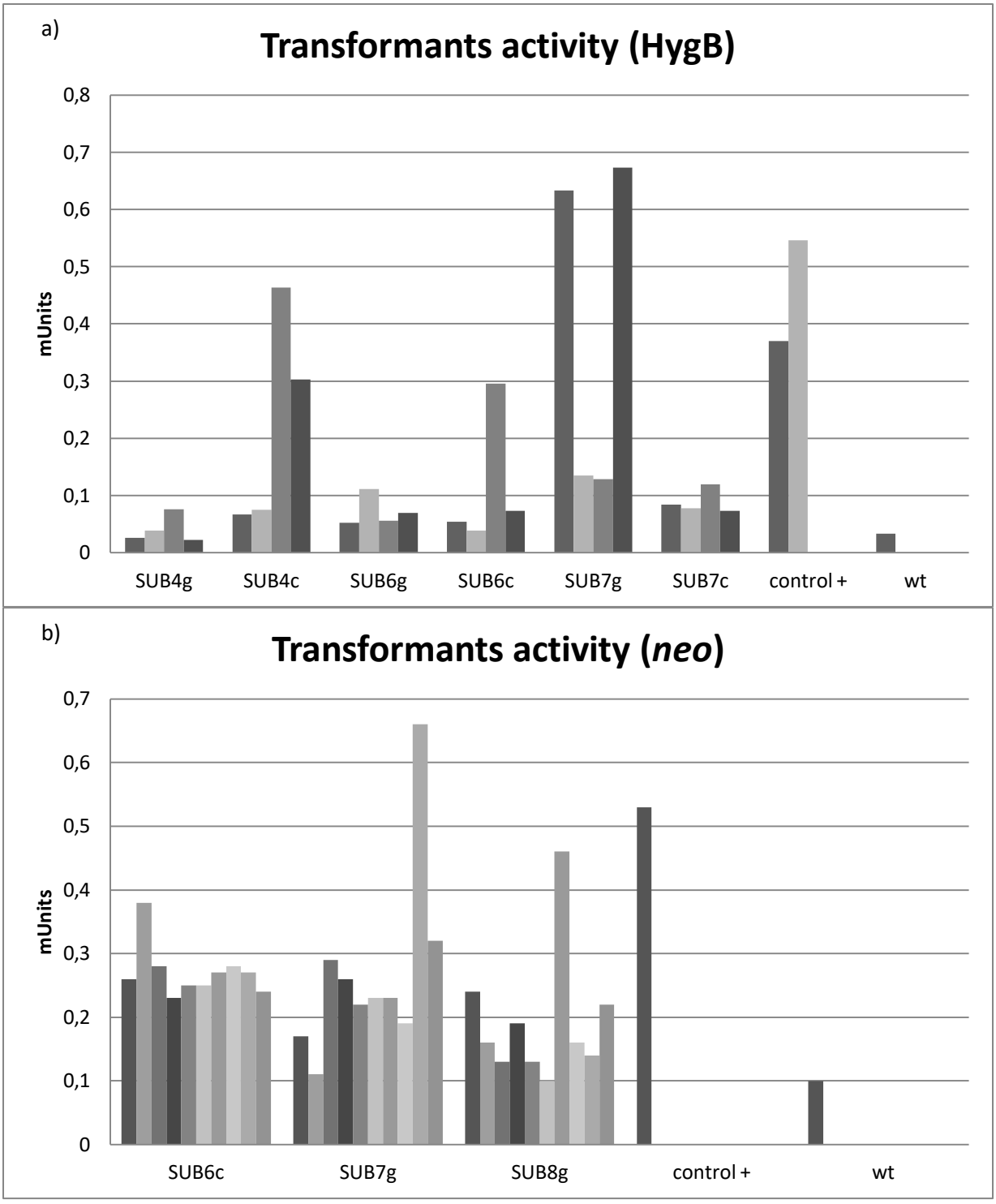

Figure 12 Activity tests, using casein resorufin-labeled, of *A. benhamiae* transformants a) with *hph* cassette and b) with *neo* cassette. 80µL of supernatant from 9 days old liquid culture in Sabouraud were used. We measure absorbance at 475 nm after 90min incubation at 37°C. The activity is given in Units (see MM). Genomic DNA is represented with g and complementary DNA with a c. Positive control is a *Pichia pastoris* strain producing recombinant SUB4.

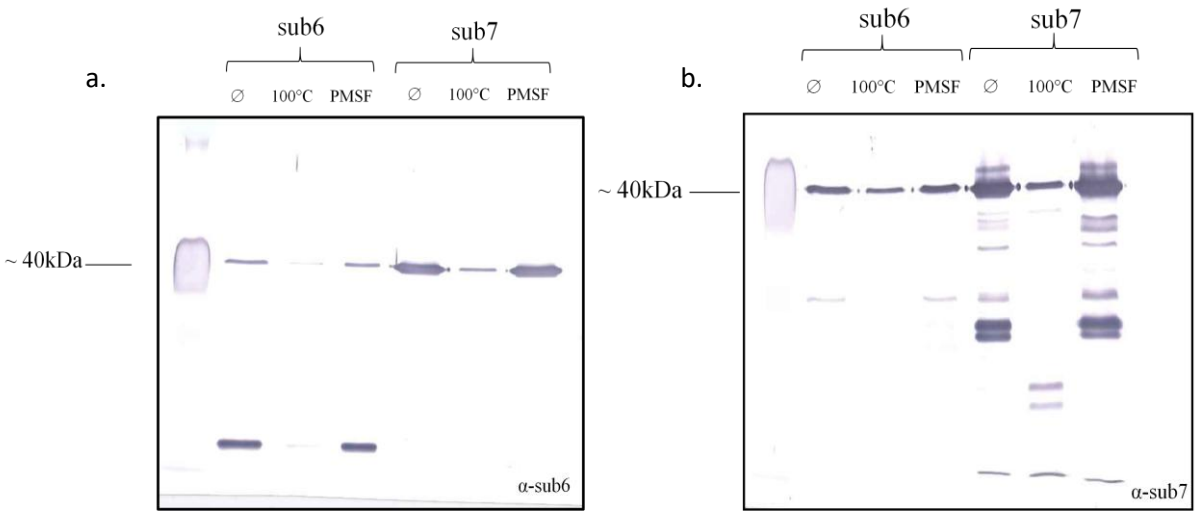

Figure 13 Western blot analysis of 5µl supernatant extracted from 2 weeks old liquid cultures of *A. Benhamiae* using antibodies against SUB6 (a) and against SUB7 (b). The samples were treated as fallow: (i) not treated as a control; (ii) warmed up to 100°C for 2 minutes and (iii) 5mM of PMSF, a specific subtilisin inhibitor, was added. The recombinants proteins SUB6 and SUB7were produced by AbeSUB6 and AbeSUB7 strains respectively.

4.9. pH-dependance of different subtilisn activities

The *A. benhamiae* transformants with the highest activity, from both transformations, were cultured in liquid Sabouraud for 9 days. Subsequently the supernatant was collected and stored at -20°C.

The pH-dependant proteolytic activity of the recombinant SUBs was determined in citrate buffer for pH range from pH 2 to pH 7 and in Tris HCl buffer from pH 7 to pH 9 as explained in material and methods. The four enzymes were active in Tris-HCl buffer between pH 7 and 9.5 on resorufin labeled Casein with a broad peak of activity between 7.5 and 9.0 (Figure 14).

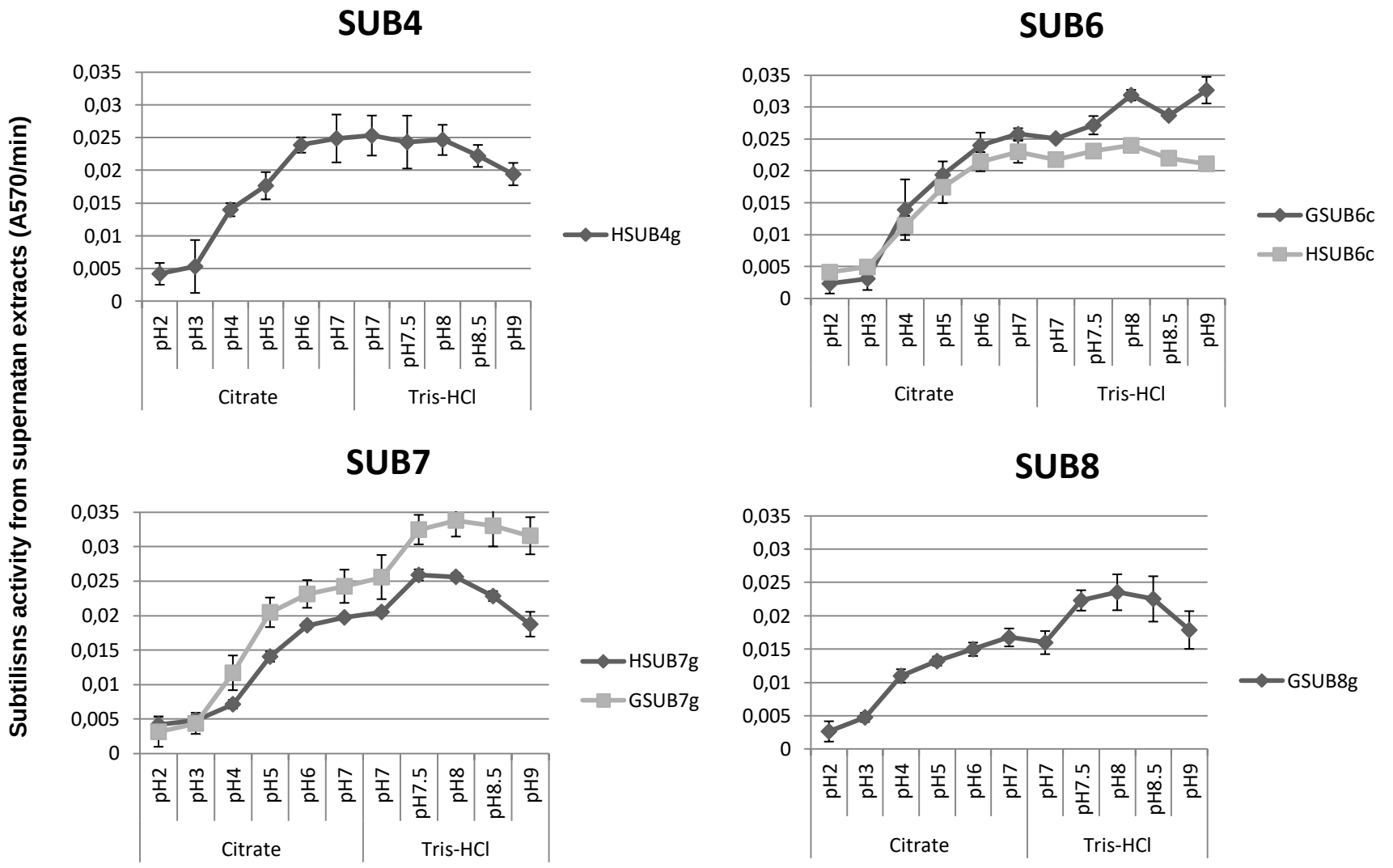

Figure 14 Activity per minute of SUBs from 10 days old culture supernatant in Sabouraud. 50 µL of supernatant was used. Recombinant proteins from pNDC1-3 are labeled with an H; Recombinant proteins from pNDC5-7 are labeled with a G**.** lower case g stand for genomic DNA and lower case c stand for complementary DNA.

5. Discussion

RNA-seq data obtained from *A. benhamiae* grown in various liquid culture conditions and during infection in guinea pigs led to a new gene prediction and annotation of its genome. A complete gene expression profile of *A. benhamiae* was obtained during infection of its natural host. Most dermatophyte ORFs available to date were deduced by cDNA analysis and by expressed sequence tag sequencing using RNA extracted from dermatophytes grown *in vitro* together with automatic annotation and comparison with other annotated genomes.

5.1. New *Arthroderma benhamiae* gene annotation

About 65% difference and, particularly, 383 new protein-coding genes were detected compared to the existing gene prediction. We used previously acquired MS data to validate *a posteriori* the presence of the predicted ORFs in culture supernatant. A comparable approach with emphasis on proteogenomics has been recently used to review the genome and proteome of *T. rubrum* (87). In this study, the identification of 323 new peptides by MS in culture supernatant led to the refinement of 161 genes and the prediction of nine new genes. However, the RNA-seq analysis to validate the whole-genome proteomics was only performed with RNA extracted from *T. rubrum* cultured *in vitro* on potato glucose agar, but not during infection. This previous study and our results have in common the combination of experimental data with bioinformatics software and manual curation to generate an improved gene annotation. Our study is more focused on the biology of infection.

In silico analysis of our predicted proteome led to the identification of 457 putative cell surface and secreted proteins. Our list of probable secreted proteins is likely to also contain proteins targeted to intracellular organelles, such as the endoplasmic reticulum or vacuole, since the exploited prediction tools cannot distinguish between such proteins and secreted ones. The Fungal Secretome and Subcellular Proteome KnowledgeBase (http://proteomics.ysu.edu/secretomes/fungi2/index.php) tries to address this concern by providing the prediction of secreted and organellar localization of proteins. It basically utilizes the same tools as we used in our strategy and reveals the same functional groups (88). In addition, they use WoLF PSORT (http://www.genscript.com/wolf-psort.html) that converts protein sequences into numerical localization features, based on sorting signals, amino acid composition and functional motifs. Nevertheless, this tool can produce a high number of false positives. Moreover, homologs of well-known intracellular proteins have been found in the secretome proteomic data. As an example, ARB_02919 is the closest *A. benhamiae* homolog of the *A. fumigatus* vacuolar aspartic peptidase (PEP2) and *S. cerevisiae* vacuolar proteinase A (PEP4). The latter is a vacuolar enzyme required for the processing of vacuolar precursors (89), whereas the former plays an additional role linked to the cell wall (90). ARB_02919 was found as a secreted protein by MS (77), and is one of the most expressed proteins in all the five studied conditions. Contaminations cannot be ruled out, but our strategy ensures the best coverage of cell surface and secreted proteins, even if some false positives are probably still present.

5.2. Reprogramming of gene expression from a saprophyte to a parasite lifestyle

Striking differences were revealed between transcriptomes of *A. benhamiae* during growth under various conditions *in vitro* and during infection of its natural host. Such differences emphasize the importance of performing transcriptional analysis directly during infection, instead of using *in vitro* conditions that mimic the host environment. We also identified several newly predicted genes, as well as genes with unknown functions, that were differentially expressed *in vivo* versus *in vitro*, and, thus, might have a relevant role in infection. To sum up, the ability of dermatophytes to switch from a saprophyte to a parasite lifestyle is attested by an important reprogramming of gene expression.

Several comparative RNA-seq analyses were performed for other species of human pathogenic fungi (91–94), but as these studies rely on infection-mimicking conditions and not on the real *in vivo* situation, we think that they should be considered with caution. Only few studies were performed in real infection conditions. Gene expression profiles of *C. albicans* were obtained during infection in both the mouse kidney and the insect *Galleria mellonella* (95). Interestingly, gene expressions in these very distinct hosts were much closer to each other than in the *in vitro* liquid cultures used as controls. More recently, transcriptional profiling of *Blastomyces* was performed in co-cultures with human bone marrow-derived macrophages and during *in vivo* pulmonary infection in a mouse model (96). They identified a number of functional categories upregulated exclusively *in vivo*, including secreted proteins, zinc acquisition proteins, as well as cysteine and tryptophan metabolism. Nine secreted protein were identified, including products of five of the ten most upregulated genes during infection. One of these genes,

BDFG_00717, encodes a CFEM-domain-containing protein, highlighting the importance of those proteins in virulence.

5.3. Potential non-protease virulence factors of *Arthroderma benhamiae*

Numerous genes that were highly expressed during infection encode uncharacterized proteins. Highly expressed protein-coding genes with a putative function other than proteolysis included ARB_01183, encoding a putative antigenic thaumatin domain protein, and two genes encoding 1,3-beta-glucanosyltransferases (ARB_07487 and ARB_05770). ARB_01183 was the most expressed secreted protein-coding gene *in vivo*. Thaumatin-like proteins (TLPs) are found in many eukaryotes and have been particularly studied in plants, in which they are involved in defense against fungal pathogens. Plant TLPs also have been shown to act as important allergens (97). TLPs are also found in fungi, such as *Moniliophtora perniciosa*, and may be involved in the inhibition of growth of fungal competitors and pathogenicity (98). The 1,3-beta-glucanosyltransferases play an important role in fungal cell wall morphology and pathogenicity. Deletion of the gene *GEL2* encoding a 1,3-beta-glucanosyltransferase in *A. fumigatus* leads to altered cell wall composition as well as to reduced virulence in a murine model of invasive aspergillosis (99). GAS1 of the entomopathogenic fungus *Beauveria bassiana* contributes similarly to its mycoinsecticide activity (100).

ARB_02741, like *Blastomyces* BDFG_00717, encodes a GPI-anchored CFEM domain protein which is highly expressed *in vivo* and *in vitro* conditions. Its function has not been characterized yet, but it is interesting to note that the closest homologs of

ARB_02741 in the human fungal pathogen *Coccidioides posadasii* are the proline-rich antigens Ag2/PRA and Prp2, which have been reported to be leading vaccine candidates (101, 102). CFEM-domain proteins have been shown to be important for haem uptake and virulence in *C. albicans* (103). The ability to acquire iron from host tissues is a major virulence factor of pathogenic microorganisms. The three *A. fumigatus* CFEM-domain proteins have been shown to be important for cell wall stability, not for virulence (104). Other proteins may also be involved in immune escape, such as ARB_06975, whose *A. fumigatus* hydrophobin homolog was shown to prevent immune recognition by forming a hydrophobic layer on the cell surface (105).

5.4. *Arthroderma benhamiae* secreted proteases during infection

SUB6 was the most highly expressed gene encoding a secreted protease during infection in guinea pigs. In addition to *SUB6*, other *A. benhamiae* protease genes encoding the subtilisins SUB7, SUB8, and SUB10 as well as a neutral protease of the deuterolysin family (M35) were also specifically upregulated. RNA-seq analysis results also confirmed that genes encoding major proteases secreted by the fungus during growth in a protein medium (e.g., SUB3, SUB4, MEP3, MEP4, LAP1, and DPPIV) were expressed at a basic level during infection like in Sabouraud medium and were not upregulated. These results are in accordance with recent findings by proteomic analysis (LC-MS/MS) in *T. rubrum*-infected nails that revealed SUB6 as the major protein secreted by the fungus in onychomycosis (106). The closely related SUB7 (subtilisin-like protease 7, Q8NID9) and DPPV (dipeptidyl-peptidase 5, Q9UW98) were also detected. Likewise, most major proteases secreted by the fungus during its growth *in vitro* in a

protein medium (26, 107) were not detected and, therefore, appeared not to be involved during the establishment of onychomycosis. As a general conclusion, the proteases secreted *in vitro* during protein degradation and *in vivo* during infection are different, regardless of the dermatophyte species and the *tinea*. The view that the proteases isolated from dermatophytes grown *in vitro* in a protein medium are virulence attributes and exert a major role during infection appears to be too naïve and can no longer be accepted. Dermatophytes evolved from soil saprophytic fungi that are able to efficiently degrade hard keratin into amino acids and into short peptides in the process of recycling nitrogen, and the pathogenic phase of dermatophytes has to be dissociated from their saprophytic phase. Some of the multiple members of protease gene families in dermatophytes are dedicated exclusively to protein degradation while others, such as SUB6, likely fulfill specific roles during infection. The notion that proteases secreted in proteinaceous media correspond to virulence attributes has also been discarded for other pathogenic fungi. Two different *A. fumigatus* mutants unable to secrete proteolytic activity in a protein growth medium did not show attenuated virulence when tested in a leukopenic mouse model. In the first mutant, the genes coding for the two major secreted proteases ALP and MEP (108) were deleted. In the other mutant, the gene coding for a transcriptional activator (PRTT) which regulates transcription of genes encoding the major proteases secreted in a protein medium was deleted. Noteworthily, no homolog of PRTT in *Aspergillus* spp. (109, 110) has been identified in *A. benhamiae*.

Genes encoding major proteases secreted by dermatophytes during *in vitro* growth in a protein medium are tightly controlled by *DNR1*, the ortholog of *AREA* in *Aspergillus nidulans* (111). In the absence of ammonium and glutamine, this transcription factor was

found to be required for the expression of genes involved in nitrogen metabolism. Although dermatophytes infect keratinized tissues, our results suggest that the panel of proteases secreted during infection depends on other transcription factors that remain to be discovered.

5.5. *Arthroderma benhamiae* secreted proteins as allergens and their use in diagnostic

Secreted proteins are allergens that play a key role in the pathogenic process. SUB6, DPPV, and the beta-glucosidase ARB_05770 (encoded by three of the most expressed genes of *A. benhamiae* during infection) are orthologs of the three known major dermatophyte allergens Tri t1, Tri r2, and Tri r4, which are involved in bronchial sensitization and symptomatic asthma (59, 112, 113). Dermatophyte antigens are also involved in eczematous skin reactions at a location distant from the area of dermatophyte infection (dermatophytids). The etiology of common dyshidrotic and vesicular eczema on the hands (palms and fingers) is rarely investigated and may remain elusive because no commercially standardized antigens are available to perform routine skin tests and antibody detection. At a time when quality in laboratory techniques is a key issue, it is not possible to use trichophytin, a fungal extract that greatly varies in its preparation and composition (114). The secreted proteins encoded by genes highly expressed during infection are the best candidates for the detection of dermatophyte allergic diseases, and it would be relevant to perform skin test reactions using standardized antigens in cases of eczematous skin reactions of unknown origin. A positive reaction could be indicative of a non-detected dermatophyte infection and could suggest possible antifungal treatment.

5.6. Arthroderma benhamiae transformation

An improvement in the selection of transformants to allow further transformations with non proteolytic activity inserts was required. We change the hygromycin B phosphotransferase cassette to a neomycin phosphotransferase (G418) resistnace cassette. Both antibiotics are aminoglycoside, inhibiting protein synthesis but gentamycin was known to be more suitable for transformant selection. The resistance at different level of gentamycin of different *A. benhamiae* and *A. vanbreuseghemii* strains was tested on Sabouraud medium (Figure 10). Our strain Lau2354-2 was unable to grow in the presence of more than 200 µg/mL of G418. In contrast the same strain was able to grow in presence of hygromycin B at a concentration over 600 µg/mL.

6. Conclusion

Comparing gene expression during infection phase versus keratin degradation *in vitro* shows the importance of using real *in vivo* conditions to further investigate the virulence mechanisms of dermatophytes, instead of using some *in vitro* conditions supposed to mimic the host environment. Focusing our analysis on genes encoding cell-associated and secreted proteins, in particular proteases, led to the identification of strong candidates as allergens and putative virulence factors. The new genome annotation provided in this study might serve as a reference for annotation or re-annotation of other dermatophyte species and evolutionary related filamentous fungi. The established dermatophytes expression system allowed the production of SUB6, SUB7 and SUB8 for the first time, and will be suitable to produce other antigens and proteins of interest.

7. References

1. Hawksworth DL, Crous PW, Redhead SA, Reynolds DR, Samson RA, Seifert KA, Taylor JW, Wingfield MJ, Abaci O, Aime C, Asan A, Bai F-Y, de Beer ZW, Begerow D, Berikten D, Boekhout T, Buchanan PK, Burgess T, Buzina W, Cai L, Cannon PF, Crane JL, Damm U, Daniel H-M, van Diepeningen AD, Druzhinina I, Dyer PS, Eberhardt U, Fell JW, Frisvad JC, Geiser DM, Geml J, Glienke C, Gräfenhan T, Groenewald JZ, Groenewald M, de Gruyter J, Guého-Kellermann E, Guo L-D, Hibbett DS, Hong S-B, de Hoog GS, Houbraken J, Huhndorf SM, Hyde KD, Ismail A, Johnston PR, Kadaifciler DG, Kirk PM, Kõljalg U, Kurtzman CP, Lagneau P-E, Lévesque CA, Liu X, Lombard L, Meyer W, Miller A, Minter DW, Najafzadeh MJ, Norvell L, Ozerskaya SM, Oziç R, Pennycook SR, Peterson SW, Pettersson OV, Quaedvlieg W, Robert VA, Ruibal C, Schnürer J, Schroers H-J, Shivas R, Slippers B, Spierenburg H, Takashima M, Taşkın E, Thines M, Thrane U, Uztan AH, van Raak M, Varga J, Vasco A, Verkley G, Videira SIR, de Vries RP, Weir BS, Yilmaz N, Yurkov A, Zhang N. 2011. The amsterdam declaration on fungal nomenclature. IMA Fungus 2:105–112.

2. Whittaker RH. 1969. New concepts of kingdoms or organisms. Evolutionary relations are better represented by new classifications than by the traditional two kingdoms. Science 163:150–160.

3. Hibbett DS, Binder M, Bischoff JF, Blackwell M, Cannon PF, Eriksson OE, Huhndorf S, James T, Kirk PM, Lücking R, Thorsten Lumbsch H, Lutzoni F, Matheny PB, McLaughlin DJ, Powell MJ, Redhead S, Schoch CL, Spatafora JW,

Stalpers JA, Vilgalys R, Aime MC, Aptroot A, Bauer R, Begerow D, Benny GL, Castlebury LA, Crous PW, Dai Y-C, Gams W, Geiser DM, Griffith GW, Gueidan C, Hawksworth DL, Hestmark G, Hosaka K, Humber RA, Hyde KD, Ironside JE, Kõljalg U, Kurtzman CP, Larsson K-H, Lichtwardt R, Longcore J, Miadlikowska J, Miller A, Moncalvo J-M, Mozley-Standridge S, Oberwinkler F, Parmasto E, Reeb V, Rogers JD, Roux C, Ryvarden L, Sampaio JP, Schüssler A, Sugiyama J, Thorn RG, Tibell L, Untereiner WA, Walker C, Wang Z, Weir A, Weiss M, White MM, Winka K, Yao Y-J, Zhang N. 2007. A higher-level phylogenetic classification of the Fungi. Mycol Res 111:509–547.

4. Hibbett DS, Binder M, Bischoff JF, Blackwell M, Cannon PF, Eriksson OE, Huhndorf S, James T, Kirk PM, Lücking R, Thorsten Lumbsch H, Lutzoni F, Matheny PB, McLaughlin DJ, Powell MJ, Redhead S, Schoch CL, Spatafora JW, Stalpers JA, Vilgalys R, Aime MC, Aptroot A, Bauer R, Begerow D, Benny GL, Castlebury LA, Crous PW, Dai Y-C, Gams W, Geiser DM, Griffith GW, Gueidan C, Hawksworth DL, Hestmark G, Hosaka K, Humber RA, Hyde KD, Ironside JE, Kõljalg U, Kurtzman CP, Larsson K-H, Lichtwardt R, Longcore J, Miadlikowska J, Miller A, Moncalvo J-M, Mozley-Standridge S, Oberwinkler F, Parmasto E, Reeb V, Rogers JD, Roux C, Ryvarden L, Sampaio JP, Schüssler A, Sugiyama J, Thorn RG, Tibell L, Untereiner WA, Walker C, Wang Z, Weir A, Weiss M, White MM, Winka K, Yao Y-J, Zhang N. 2007. A higher-level phylogenetic classification of the Fungi. Mycol Res 111:509–547.

5. Alan J., Neil D. R. Handbook of Proteolytic EnzymesThird Edition.

6. Blobel G, Dobberstein B. 1975. Transfer of proteins across membranes. II. Reconstitution of functional rough microsomes from heterologous components. J Cell Biol 67:852–862.

7. Pfeffer SR, Rothman JE. 1987. Biosynthetic protein transport and sorting by the endoplasmic reticulum and Golgi. Annu Rev Biochem 56:829–852.

8. Milstein C, Brownlee GG, Harrison TM, Mathews MB. 1972. A possible precursor of immunoglobulin light chains. Nature New Biol 239:117–120.

9. Fabre E, Nicaud JM, Lopez MC, Gaillardin C. 1991. Role of the proregion in the production and secretion of the Yarrowia lipolytica alkaline extracellular protease. J Biol Chem 266:3782–3790.

10. Eder J, Fersht AR. 1995. Pro-sequence-assisted protein folding. Mol Microbiol 16:609–614.

11. Fukuda R, Umebayashi K, Horiuchi H, Ohta A, Takagi M. 1996. Degradation of Rhizopus niveus aspartic proteinase-I with mutated prosequences occurs in the endoplasmic reticulum of Saccharomyces cerevisiae. J Biol Chem 271:14252–14255.

12. Togni G, Sanglard D, Quadroni M, Foundling SI, Monod M. 1996. Acid proteinase secreted by Candida tropicalis: functional analysis of preproregion cleavages in C. tropicalis and Saccharomyces cerevisiae. Microbiol Read Engl 142 (Pt 3):493–503.

13. Newport G, Agabian N. 1997. KEX2 influences Candida albicans proteinase secretion and hyphal formation. J Biol Chem 272:28954–28961.

14. Marie-Claire C, Roques BP, Beaumont A. 1998. Intramolecular processing of prothermolysin. J Biol Chem 273:5697–5701.

15. Zaugg C, Jousson O, Léchenne B, Staib P, Monod M. 2008. Trichophyton rubrum secreted and membrane-associated carboxypeptidases. Int J Med Microbiol IJMM 298:669–682.

16. Hanzi M, Shimizu M, Hearn VM, Monod M. 1993. A study of the alkaline proteases secreted by different Aspergillus species. Mycoses 36:351–356.

17. Monod M, Staib P, Borelli C. 2013. Candidapepsin, p. 160–165. *In* Handbook of Proteolytic EnzymesThird edition. Neil D. Rawlings & Guy S. Salvesen.

18. Ajello L. 1974. Natural history of the dermatophytes and related fungi. Mycopathol Mycol Appl 53:93–110.

19. The Broad Institute. 2011. Dermatophyte comparative database.

20. Burmester A, Shelest E, Glöckner G, Heddergott C, Schindler S, Staib P, Heidel A, Felder M, Petzold A, Szafranski K, Feuermann M, Pedruzzi I, Priebe S, Groth M, Winkler R, Li W, Kniemeyer O, Schroeckh V, Hertweck C, Hube B, White TC, Platzer M, Guthke R, Heitman J, Wöstemeyer J, Zipfel PF, Monod M, Brakhage AA. 2011. Comparative and functional genomics provide insights into the pathogenicity of dermatophytic fungi. Genome Biol 12:R7.

21. Martinez DA, Oliver BG, Gräser Y, Goldberg JM, Li W, Martinez-Rossi NM, Monod M, Shelest E, Barton RC, Birch E, Brakhage AA, Chen Z, Gurr SJ, Heiman D, Heitman J, Kosti I, Rossi A, Saif S, Samalova M, Saunders CW, Shea T, Summerbell RC, Xu J, Young S, Zeng Q, Birren BW, Cuomo CA, White TC. 2012. Comparative genome analysis of Trichophyton rubrum and related dermatophytes reveals candidate genes involved in infection. mBio 3:e00259-212.

22. Degreef H. 2008. Clinical forms of dermatophytosis (ringworm infection). Mycopathologia 166:257–265.

23. Jousson O, Léchenne B, Bontems O, Capoccia S, Mignon B, Barblan J, Quadroni M, Monod M. 2004. Multiplication of an ancestral gene encoding secreted fungalysin preceded species differentiation in the dermatophytes Trichophyton and Microsporum. Microbiol Read Engl 150:301–310.

24. Jousson O, Léchenne B, Bontems O, Mignon B, Reichard U, Barblan J, Quadroni M, Monod M. 2004. Secreted subtilisin gene family in Trichophyton rubrum. Gene 339:79–88.

25. Monod M, Léchenne B, Jousson O, Grand D, Zaugg C, Stöcklin R, Grouzmann E. 2005. Aminopeptidases and dipeptidyl-peptidases secreted by the dermatophyte Trichophyton rubrum. Microbiol Read Engl 151:145–155.

26. Zaugg C, Jousson O, Léchenne B, Staib P, Monod M. 2008. Trichophyton rubrum secreted and membrane-associated carboxypeptidases. Int J Med Microbiol IJMM 298:669–682.

27. Staib P, Zaugg C, Mignon B, Weber J, Grumbt M, Pradervand S, Harshman K, Monod M. 2010. Differential gene expression in the pathogenic dermatophyte Arthroderma benhamiae in vitro versus during infection. Microbiol Read Engl 156:884–895.

28. Lorenz MC, Fink GR. 2001. The glyoxylate cycle is required for fungal virulence. Nature 412:83–86.

29. McKinney JD, Höner zu Bentrup K, Muñoz-Elías EJ, Miczak A, Chen B, Chan WT, Swenson D, Sacchettini JC, Jacobs WR, Russell DG. 2000. Persistence of Mycobacterium tuberculosis in macrophages and mice requires the glyoxylate shunt enzyme isocitrate lyase. Nature 406:735–738.

30. Schöbel F, Ibrahim-Granet O, Avé P, Latgé J-P, Brakhage AA, Brock M. 2007. Aspergillus fumigatus does not require fatty acid metabolism via isocitrate lyase for development of invasive aspergillosis. Infect Immun 75:1237–1244.

31. Grumbt M, Defaweux V, Mignon B, Monod M, Burmester A, Wöstemeyer J, Staib P. 2011. Targeted gene deletion and in vivo analysis of putative virulence gene function in the pathogenic dermatophyte Arthroderma benhamiae. Eukaryot Cell 10:842–853.

32. Shiraki Y, Ishibashi Y, Hiruma M, Nishikawa A, Ikeda S. 2006. Cytokine secretion profiles of human keratinocytes during Trichophyton tonsurans and Arthroderma benhamiae infections. J Med Microbiol 55:1175–1185.

33. Nakamura Y, Kano R, Hasegawa A, Watanabe S. 2002. Interleukin-8 and tumor necrosis factor alpha production in human epidermal keratinocytes induced by Trichophyton mentagrophytes. Clin Diagn Lab Immunol 9:935–937.

34. Tani K, Adachi M, Nakamura Y, Kano R, Makimura K, Hasegawa A, Kanda N, Watanabe S. 2007. The effect of dermatophytes on cytokine production by human keratinocytes. Arch Dermatol Res 299:381–387.

35. Jensen J-M, Pfeiffer S, Akaki T, Schröder J-M, Kleine M, Neumann C, Proksch E, Brasch J. 2007. Barrier function, epidermal differentiation, and human beta-defensin 2 expression in tinea corporis. J Invest Dermatol 127:1720–1727.

36. López-García B, Lee PHA, Gallo RL. 2006. Expression and potential function of cathelicidin antimicrobial peptides in dermatophytosis and tinea versicolor. J Antimicrob Chemother 57:877–882.

37. Fritz P, Beck-Jendroschek V, Brasch J. 2012. Inhibition of dermatophytes by the antimicrobial peptides human β-defensin-2, ribonuclease 7 and psoriasin. Med Mycol 50:579–584.

38. Hein KZ, Takahashi H, Tsumori T, Yasui Y, Nanjoh Y, Toga T, Wu Z, Grötzinger J, Jung S, Wehkamp J, Schroeder BO, Schroeder JM, Morita E. 2015. Disulphide-reduced psoriasin is a human apoptosis-inducing broad-spectrum fungicide. Proc Natl Acad Sci U S A 112:13039–13044.

39. da Silva BCM, Paula CR, Auler ME, Ruiz L da S, Dos Santos JI, Yoshioka MCN, Fabris A, Castro LGM, Duarte AJ da S, Gambale W. 2014. Dermatophytosis and

immunovirological status of HIV-infected and AIDS patients from Sao Paulo city, Brazil. Mycoses 57:371–376.

40. Wu L-C, Sun P-L, Chang Y-T. 2013. Extensive deep dermatophytosis cause by Trichophyton rubrum in a patient with liver cirrhosis and chronic renal failure. Mycopathologia 176:457–462.

41. Lanternier F, Pathan S, Vincent QB, Liu L, Cypowyj S, Prando C, Migaud M, Taibi L, Ammar-Khodja A, Boudghene Stambouli O, Guellil B, Jacobs F, Goffard J-C, Schepers K, del Marmol V, Boussofara L, Denguezli M, Larif M, Bachelez H, Michel L, Lefranc G, Hay R, Jouvion G, Chretien F, Fraitag S, Bougnoux M-E, Boudia M, Abel L, Lortholary O, Casanova J-L, Picard C, Grimbacher B, Puel A. 2013. Deep dermatophytosis and inherited CARD9 deficiency. N Engl J Med 369:1704–1714.

42. Grumach AS, de Queiroz-Telles F, Migaud M, Lanternier F, Filho NR, Palma SMU, Constantino-Silva RN, Casanova JL, Puel A. 2015. A homozygous CARD9 mutation in a Brazilian patient with deep dermatophytosis. J Clin Immunol 35:486–490.

43. Jachiet M, Lanternier F, Rybojad M, Bagot M, Ibrahim L, Casanova J-L, Puel A, Bouaziz J-D. 2015. Posaconazole treatment of extensive skin and nail dermatophytosis due to autosomal recessive deficiency of CARD9. JAMA Dermatol 151:192–194.

44. Cambier L, Weatherspoon A, Defaweux V, Bagut ET, Heinen MP, Antoine N, Mignon B. 2014. Assessment of the cutaneous immune response during Arthroderma benhamiae and A. vanbreuseghemii infection using an experimental mouse model. Br J Dermatol 170:625–633.

45. Woodfolk JA. 2005. Allergy and dermatophytes. Clin Microbiol Rev 18:30–43.

46. Mignon B, Tabart J, Baldo A, Mathy A, Losson B, Vermout S. 2008. Immunization and dermatophytes. Curr Opin Infect Dis 21:134–140.

47. Jadassohn j. 1918. Über die Trichophytien. Berliner Klin Wochenschr 21:489–494.

48. Ilkit M, Durdu M, Karakaş M. 2012. Cutaneous id reactions: a comprehensive review of clinical manifestations, epidemiology, etiology, and management. Crit Rev Microbiol 38:191–202.

49. Williams AW. 1926. Case of Pityriasis Rubra Pilaris. Proc R Soc Med 19:3.

50. Bloch B. 1928. Allgemeine und experimentelle Biologie der Dermatomykosen und die Trichophytide, p. 300–376, 564–606. *In* Handbuch der Haut- und Gesclechtskrankheiten.

51. Cheng N, Rucker Wright D, Cohen BA. 2011. Dermatophytid in tinea capitis: rarely reported common phenomenon with clinical implications. Pediatrics 128:e453-457.

52. Peck S. 1930. Epidermophytosis of the Feet and Epidermophytids of the Hands. Rev Dermatol Syph 22.

53. Veien NK, Hattel T, Laurberg G. 1994. Plantar Trichophyton rubrum infections may cause dermatophytids on the hands. Acta Derm Venereol 74:403–404.

54. Woodfolk JA, Wheatley LM, Piyasena RV, Benjamin DC, Platts-Mills TA. 1998. Trichophyton antigens associated with IgE antibodies and delayed type hypersensitivity. Sequence homology to two families of serine proteinases. J Biol Chem 273:29489–29496.

55. Matsuoka H, Niimi A, Matsumoto H, Ueda T, Takemura M, Yamaguchi M, Jinnai M, Otsuka K, Oguma T, Takeda T, Ito I, Chin K, Amitani R, Mishima M. 2009. Specific IgE response to trichophyton and asthma severity. Chest 135:898–903.

56. Ward GW, Karlsson G, Rose G, Platts-Mills TA. 1989. Trichophyton asthma: sensitisation of bronchi and upper airways to dermatophyte antigen. Lancet 1:859–862.

57. Call RS, Ward G, Jackson S, Platts-Mills TA. 1994. Investigating severe and fatal asthma. J Allergy Clin Immunol 94:1065–1072.

58. Slunt JB, Taketomi EA, Woodfolk JA, Hayden ML, Platts-Mills TA. 1996. The immune response to Trichophyton tonsurans: distinct T cell cytokine profiles to a single protein among subjects with immediate and delayed hypersensitivity. J Immunol Baltim Md 1950 157:5192–5197.

59. Woodfolk JA, Wheatley LM, Piyasena RV, Benjamin DC, Platts-Mills TA. 1998. Trichophyton antigens associated with IgE antibodies and delayed type

hypersensitivity. Sequence homology to two families of serine proteinases. J Biol Chem 273:29489–29496.

60. Fumeaux J, Mock M, Ninet B, Jan I, Bontems O, Léchenne B, Lew D, Panizzon RG, Jousson O, Monod M. 2004. First report of Arthroderma benhamiae in Switzerland. Dermatol Basel Switz 208:244–250.

61. Burmester A, Shelest E, Glöckner G, Heddergott C, Schindler S, Staib P, Heidel A, Felder M, Petzold A, Szafranski K, Feuermann M, Pedruzzi I, Priebe S, Groth M, Winkler R, Li W, Kniemeyer O, Schroeckh V, Hertweck C, Hube B, White TC, Platzer M, Guthke R, Heitman J, Wöstemeyer J, Zipfel PF, Monod M, Brakhage AA. 2011. Comparative and functional genomics provide insights into the pathogenicity of dermatophytic fungi. Genome Biol 12:R7.

62. Kim D, Pertea G, Trapnell C, Pimentel H, Kelley R, Salzberg SL. 2013. TopHat2: accurate alignment of transcriptomes in the presence of insertions, deletions and gene fusions. Genome Biol 14:R36.

63. Stanke M. 2004. Gene prediction with a hidden markov model. University of Göttingen, Germany.

64. Trapnell C, Roberts A, Goff L, Pertea G, Kim D, Kelley DR, Pimentel H, Salzberg SL, Rinn JL, Pachter L. 2012. Differential gene and transcript expression analysis of RNA-seq experiments with TopHat and Cufflinks. Nat Protoc 7:562–578.

65. Rice P, Longden I, Bleasby A. 2000. EMBOSS: the European Molecular Biology Open Software Suite. Trends Genet TIG 16:276–277.

66. Pearson WR. 1991. Searching protein sequence libraries: comparison of the sensitivity and selectivity of the Smith-Waterman and FASTA algorithms. Genomics 11:635–650.

67. Käll L, Krogh A, Sonnhammer ELL. 2004. A combined transmembrane topology and signal peptide prediction method. J Mol Biol 338:1027–1036.

68. Petersen TN, Brunak S, von Heijne G, Nielsen H. 2011. SignalP 4.0: discriminating signal peptides from transmembrane regions. Nat Methods 8:785–786.

69. Sonnhammer EL, von Heijne G, Krogh A. 1998. A hidden Markov model for predicting transmembrane helices in protein sequences. Proc Int Conf Intell Syst Mol Biol ISMB Int Conf Intell Syst Mol Biol 6:175–182.

70. Krogh A, Larsson B, von Heijne G, Sonnhammer EL. 2001. Predicting transmembrane protein topology with a hidden Markov model: application to complete genomes. J Mol Biol 305:567–580.

71. Pierleoni A, Martelli P, Casadio R. 2008. PredGPI: a GPI-anchor predictor. BMC Bioinformatics 9:392.

72. Eisenberg D, Schwarz E, Komaromy M, Wall R. 1984. Analysis of membrane and surface protein sequences with the hydrophobic moment plot. J Mol Biol 179:125–142.

73. Jones DT, Taylor WR, Thornton JM. 1994. A model recognition approach to the prediction of all-helical membrane protein structure and topology. Biochemistry (Mosc) 33:3038–3049.

74. UniProt Consortium. 2015. UniProt: a hub for protein information. Nucleic Acids Res 43:D204-212.

75. Zdobnov EM, Apweiler R. 2001. InterProScan--an integration platform for the signature-recognition methods in InterPro. Bioinforma Oxf Engl 17:847–848.

76. Quevillon E, Silventoinen V, Pillai S, Harte N, Mulder N, Apweiler R, Lopez R. 2005. InterProScan: protein domains identifier. Nucleic Acids Res 33:W116-120.

77. Sriranganadane D, Waridel P, Salamin K, Feuermann M, Mignon B, Staib P, Neuhaus J-M, Quadroni M, Monod M. 2011. Identification of novel secreted proteases during extracellular proteolysis by dermatophytes at acidic pH. Proteomics 11:4422–4433.

78. Anders S, Pyl PT, Huber W. 2015. HTSeq--a Python framework to work with high-throughput sequencing data. Bioinforma Oxf Engl 31:166–169.

79. Law CW, Chen Y, Shi W, Smyth GK. 2014. voom: precision weights unlock linear model analysis tools for RNA-seq read counts. Genome Biol 15:R29.

80. Smyth GK. 2005. limma: Linear Models for Microarray Data, p. 397–420. *In* Gentleman, R, Carey, VJ, Huber, W, Irizarry, RA, Dudoit, S (eds.), Bioinformatics and Computational Biology Solutions Using R and Bioconductor. Springer New York.

81. Benjamini Y, Yekutieli D. 2001. The Control of the False Discovery Rate in Multiple Testing under Dependency. Ann Stat 29:1165–1188.

82. Langfelder P, Horvath S. 2008. WGCNA: an R package for weighted correlation network analysis. BMC Bioinformatics 9:559.

83. Yamada T, Makimura K, Satoh K, Umeda Y, Ishihara Y, Abe S. 2009. Agrobacterium tumefaciens-mediated transformation of the dermatophyte, Trichophyton mentagrophytes: an efficient tool for gene transfer. Med Mycol 47:485–494.

84. Yamada T, Makimura K, Hisajima T, Ito M, Umeda Y, Abe S. 2008. Genetic transformation of the dermatophyte, Trichophyton mentagrophytes, based on the use of G418 resistance as a dominant selectable marker. J Dermatol Sci 49:53–61.

85. Giddey K, Monod M, Barblan J, Potts A, Waridel P, Zaugg C, Quadroni M. 2007. Comprehensive analysis of proteins secreted by Trichophyton rubrum and Trichophyton violaceum under in vitro conditions. J Proteome Res 6:3081–3092.

86. Jousson O, Léchenne B, Bontems O, Mignon B, Reichard U, Barblan J, Quadroni M, Monod M. 2004. Secreted subtilisin gene family in Trichophyton rubrum. Gene 339:79–88.

87. Xu X, Liu T, Ren X, Liu B, Yang J, Chen L, Wei C, Zheng J, Dong J, Sun L, Zhu Y, Jin Q. 2015. Proteogenomic Analysis of Trichophyton rubrum Aided by RNA Sequencing. J Proteome Res 14:2207–2218.

88. Meinken J, Asch DK, Neizer-Ashun KA, Chang G-H, Cooper JR 4, Min XJ. 2014. FunSecKB2: a fungal protein subcellular location knowledgebase. Comput Mol Biol 4.

89. Ammerer G, Hunter CP, Rothman JH, Saari GC, Valls LA, Stevens TH. 1986. PEP4 gene of Saccharomyces cerevisiae encodes proteinase A, a vacuolar enzyme required for processing of vacuolar precursors. Mol Cell Biol 6:2490–2499.

90. Reichard U, Monod M, Odds F, Rüchel R. 1997. Virulence of an aspergillopepsin-deficient mutant of Aspergillus fumigatus and evidence for another aspartic proteinase linked to the fungal cell wall. J Med Vet Mycol Bi-Mon Publ Int Soc Hum Anim Mycol 35:189–196.

91. Irmer H, Tarazona S, Sasse C, Olbermann P, Loeffler J, Krappmann S, Conesa A, Braus GH. 2015. RNAseq analysis of Aspergillus fumigatus in blood reveals a just wait and see resting stage behavior. BMC Genomics 16:640.

92. Chen F, Zhang C, Jia X, Wang S, Wang J, Chen Y, Zhao J, Tian S, Han X, Han L. 2015. Transcriptome Profiles of Human Lung Epithelial Cells A549 Interacting with Aspergillus fumigatus by RNA-Seq. PloS One 10:e0135720.

93. Muszkieta L, Beauvais A, Pähtz V, Gibbons JG, Anton Leberre V, Beau R, Shibuya K, Rokas A, Francois JM, Kniemeyer O, Brakhage AA, Latgé JP. 2013. Investigation of Aspergillus fumigatus biofilm formation by various “omics” approaches. Front Microbiol 4:13.

94. Edwards JA, Chen C, Kemski MM, Hu J, Mitchell TK, Rappleye CA. 2013. Histoplasma yeast and mycelial transcriptomes reveal pathogenic-phase and lineage-specific gene expression profiles. BMC Genomics 14:695.

95. Amorim-Vaz S, Tran VDT, Pradervand S, Pagni M, Coste AT, Sanglard D. 2015. RNA Enrichment Method for Quantitative Transcriptional Analysis of Pathogens In Vivo Applied to the Fungus Candida albicans. mBio 6:e00942-915.

96. Muñoz JF, Gauthier GM, Desjardins CA, Gallo JE, Holder J, Sullivan TD, Marty AJ, Carmen JC, Chen Z, Ding L, Gujja S, Magrini V, Misas E, Mitreva M, Priest M, Saif S, Whiston EA, Young S, Zeng Q, Goldman WE, Mardis ER, Taylor JW, McEwen JG, Clay OK, Klein BS, Cuomo CA. 2015. The Dynamic Genome and Transcriptome of the Human Fungal Pathogen Blastomyces and Close Relative Emmonsia. PLoS Genet 11:e1005493.

97. Palacín A, Rivas LA, Gómez-Casado C, Aguirre J, Tordesillas L, Bartra J, Blanco C, Carrillo T, Cuesta-Herranz J, Bonny JAC, Flores E, García-Alvarez-Eire MG, García-Nuñez I, Fernández FJ, Gamboa P, Muñoz R, Sánchez-Monge R, Torres M, Losada SV, Villalba M, Vega F, Parro V, Blanca M, Salcedo G, Díaz-Perales A. 2012. The involvement of thaumatin-like proteins in plant food cross-reactivity: a multicenter study using a specific protein microarray. PloS One 7:e44088.

98. Franco S de F, Baroni RM, Carazzolle MF, Teixeira PJPL, Reis O, Pereira GAG, Mondego JMC. 2015. Genomic analyses and expression evaluation of thaumatin-like gene family in the cacao fungal pathogen Moniliophthora perniciosa. Biochem Biophys Res Commun 466:629–636.

99. Mouyna I, Morelle W, Vai M, Monod M, Léchenne B, Fontaine T, Beauvais A, Sarfati J, Prévost M-C, Henry C, Latgé J-P. 2005. Deletion of GEL2 encoding for a beta(1-3)glucanosyltransferase affects morphogenesis and virulence in Aspergillus fumigatus. Mol Microbiol 56:1675–1688.

100. Zhang S, Xia Y, Keyhani NO. 2011. Contribution of the gas1 gene of the entomopathogenic fungus Beauveria bassiana, encoding a putative glycosylphosphatidylinositol-anchored beta-1,3-glucanosyltransferase, to conidial thermotolerance and virulence. Appl Environ Microbiol 77:2676–2684.

101. Cox RA, Magee DM. 2004. Coccidioidomycosis: host response and vaccine development. Clin Microbiol Rev 17:804–839, table of contents.

102. Herr RA, Hung C-Y, Cole GT. 2007. Evaluation of two homologous proline-rich proteins of Coccidioides posadasii as candidate vaccines against coccidioidomycosis. Infect Immun 75:5777–5787.

103. Weissman Z, Kornitzer D. 2004. A family of Candida cell surface haem-binding proteins involved in haemin and haemoglobin-iron utilization. Mol Microbiol 53:1209–1220.

104. Vaknin Y, Shadkchan Y, Levdansky E, Morozov M, Romano J, Osherov N. 2014. The three Aspergillus fumigatus CFEM-domain GPI-anchored proteins (CfmA-C) affect cell-wall stability but do not play a role in fungal virulence. Fungal Genet Biol FG B 63:55–64.

105. Aimanianda V, Bayry J, Bozza S, Kniemeyer O, Perruccio K, Elluru SR, Clavaud C, Paris S, Brakhage AA, Kaveri SV, Romani L, Latgé J-P. 2009. Surface hydrophobin prevents immune recognition of airborne fungal spores. Nature 460:1117–1121.

106. Méhul B, Gu Z, Jomard A, Laffet G, Feuilhade M, Monod M. 2015. Sub6 (Tri r 2), an Onychomycosis Marker Revealed by Proteomics Analysis of Trichophyton rubrum Secreted Proteins in Patient Nail Samples. J Invest Dermatol.

107. Giddey K, Monod M, Barblan J, Potts A, Waridel P, Zaugg C, Quadroni M. 2007. Comprehensive analysis of proteins secreted by Trichophyton rubrum and Trichophyton violaceum under in vitro conditions. J Proteome Res 6:3081–3092.

108. Jaton-Ogay K, Paris S, Huerre M, Quadroni M, Falchetto R, Togni G, Latgé JP, Monod M. 1994. Cloning and disruption of the gene encoding an extracellular metalloprotease of Aspergillus fumigatus. Mol Microbiol 14:917–928.

109. Punt PJ, Schuren FHJ, Lehmbeck J, Christensen T, Hjort C, van den Hondel CAMJJ. 2008. Characterization of the Aspergillus niger prtT, a unique regulator of extracellular protease encoding genes. Fungal Genet Biol FG B 45:1591–1599.

110. Bergmann A, Hartmann T, Cairns T, Bignell EM, Krappmann S. 2009. A regulator of Aspergillus fumigatus extracellular proteolytic activity is dispensable for virulence. Infect Immun 77:4041–4050.

111. Yamada T, Makimura K, Abe S. 2006. Isolation, characterization, and disruption of dnr1, the areA/nit-2-like nitrogen regulatory gene of the zoophilic dermatophyte, Microsporum canis. Med Mycol 44:243–252.

112. Deuell B, Arruda LK, Hayden ML, Chapman MD, Platts-Mills TA. 1991. Trichophyton tonsurans allergen. I. Characterization of a protein that causes immediate but not delayed hypersensitivity. J Immunol Baltim Md 1950 147:96–101.

113. Woodfolk JA. 2005. Allergy and dermatophytes. Clin Microbiol Rev 18:30–43.

114. Grappel SF, Bishop CT, Blank F. 1974. Immunology of dermatophytes and dermatophytosis. Bacteriol Rev 38:222–250.

8. Annexes

8.1. Supplementary Tables

Table S1 the secretome: predicted cell surface/secreted proteins, putative functions, and expression obtain through the great work of Marc Feuermann.

[1] Open reading frame (ORF) names in this study

[2] The status indicates the changes between previous proteome annotation and our predictions

[3] ORF names in the previous genome annotation (Burmester et al. 2011)

[4] Names attributed to some proteases by Burmester et al. (2011) and Sriranganadane et al. (2011)

[5] UniProt accession numbers corresponding to the previous predictions. When two ORFs have been merged in the new prediction and both are present in UniProtKB, the two corresponding ACs are indicated.

[6] The presence of a signal peptide is indicated by SIG. SIG + GPI indicates that the gene product is predicted to have a GPI anchor.

[7] Mass spectrometry data were extracted from Sriranganadane et al. (2011). For each identified gene product, we indicate the medium pH in which it was detected (either pH 4 or 7).

[8] Function has been assigned based on homology search in well-characterized fungi and/or from InterPro scanning to identify specific domains and families. Green identifies proteins with a potential role in proteolytic activity; red, proteins involved in carbohydrate metabolism; and orange, proteins involved in lipid metabolism.

[9] Homologous fungal allergens extracted from the Allergome database (http://www.allergome.org/)

[10] Name of weighted gene correlation network analysis (WGCNA) gene co-expression module

[11] Summary of differential gene expressions *in vivo* versus *in vitro*. Cut-offs: FDR = 1e-3 and 2-fold change.

[12] Significant expression trends from RNA sequencing data are indicated. The cut-off of -1 for the *z*-score of transcripts per million was applied.

[13] Mean expression values expressed in transcripts per million for every growth condition.

New ORF[1]	Status[2]	Original ORFs[3]	Name in literature[4]	UniProt AC[5]	Signal/GPI[6]	Mass spectrometry pH[7]	Predicted function[8]	Close homolog allergens[9]	Regulation in vivo[11]	Expression trend[12]	TPM Gp8[13]	TPM Gp14[13]	TPM K[13]	TPM S[13]	TPM Sa[13]
ARB_00035	No changes	ARB_00035		D4AV26	SIG+ GPI	pH4 & pH7	Mannosidase (glycoside hydrolase, family 47)				32	48	125	61	28
ARB_00047	SIG at N-terminus manually restored	ARB_00047		D4AV38	SIG	pH4 & pH7	Alpha/Beta hydrolase fold-containing protein				22	22	27	39	23
ARB_00075	No changes	ARB_00075		D4AV66	SIG	pH4 & pH7	Cell wall protein	Asp f 34	down	induced in vitro	6	0	157	323	164
ARB_00087	No changes	ARB_00087		D4AV78	SIG+ GPI		SUN domain-containing protein		down		24	15	353	173	212
ARB_00107	No changes	ARB_00107		D4AV98	SIG	pH7	DUF4360 family protein			induced in keratin	4	8	1277	4	0
ARB_00120	No changes	ARB_00120		D4AVB1	SIG		Mannosyltransferase				18	9	6	7	9
ARB_00127	No changes	ARB_00127		D4AVB8	SIG		Aminoglycoside 3-phosphotransferase				13	24	21	16	9
ARB_00131	No changes	ARB_00131	KexB	D4AVC2	SIG		Pheromone processing endoprotease (KexB)				29	35	37	38	35
ARB_00147	No changes	ARB_00147		D4AVD4	SIG		Calnexin	Pen ch 31			146	181	138	255	241
ARB_00163	C-terminus modified	ARB_00163		D4AVF0	SIG		Carboxylesterase, type B				0	0	7	6	3
ARB_00194	No changes	ARB_00194		D4AVI0	SIG	pH4 & pH7	Guanine-specific ribonuclease				19	36	26	13	9
ARB_00204	Internal intron/exon prediction changes	ARB_00204		D4AVJ0	SIG	pH4 & pH7	Glycoside hydrolase, family 18		up	induced in vivo	118	97	6	0	0
ARB_00230	No changes	ARB_00230		D4AVL6	SIG		Glutamyl-peptide cyclotransferase (peptidase M28 family)				59	43	33	44	53
ARB_00233	Internal intron/exon prediction changes	ARB_00233		D4AVL9	SIG		Alkaline phosphatase D-related				15	9	32	12	29

							protein								
ARB_00277	N-terminus shortened	ARB_00277		D4AVR3	SIG		Uncharacterized protein				3	2	1	2	1
ARB_00287	No changes	ARB_00287		D4AVS3	SIG		Extracellular proline-rich protein		down		19	17	4152	2130	635
ARB_00311	No changes	ARB_00311		D4AVU7	SIG		Glycoside hydrolase, family 76				47	35	54	54	24
ARB_00313	No changes	ARB_00313		D4AVU9	SIG		Cutinase				85	50	20	6	3
ARB_00322	N-terminus shortened	ARB_00322		D4AVV8	SIG		Uncharacterized protein				73	87	56	169	118
ARB_00327	C-terminus modified and extended	ARB_00327		D4AVW3	SIG		LysM domain-containing protein				4	13	1	1	1
ARB_00328	N-terminus modified and extended	ARB_00328		D4AVW4	SIG		Chitinase (glycoside hydrolase, family 18)				13	11	16	13	9
ARB_00449	No changes	ARB_00449		D4AW84	SIG+GPI		Uncharacterized protein		down		113	71	2360	1119	1029
ARB_00454	No changes	ARB_00454		D4AW89	SIG		Uncharacterized protein				1	0	7	3	6
ARB_00481	No changes	ARB_00481		D4AWB6	SIG		Ribosomal protein				123	93	196	102	233
ARB_00494	No changes	ARB_00494	Lap2	D4AWC9	SIG	pH4 & pH7	Aminopeptidase (peptidase M28 family)				38	33	1792	2388	36
ARB_00532	N-terminus extended	ARB_00532		D4AWG7	SIG	pH7	Tyrosinase			induced in Sabouraud	2	1	3	11	98
ARB_00556-2	ORF split in 2 ORFs	ARB_00556		D4AWJ1	SIG		Beta-lactamase/transpeptidase-like protein				0	1	4	2	6
ARB_00566	C-terminus modified	ARB_00566		D4AWK0	SIG		Uncharacterized protein				5	17	2	0	0
ARB_00576	No changes	ARB_00576		D4AWL0	SIG+GPI		Leucine aminopeptidase (peptidase M28 family)				19	15	9	15	10

ARB_00582	N-terminus extended	ARB_00582		D4AWL6	SIG		Legume-like lectin				95	131	63	84	76
ARB_00595	No changes	ARB_00595		D4AWM9	SIG	pH4 & pH7	Uncharacterized protein				34	28	643	448	128
ARB_00603	N-terminus extended	ARB_00603		D4AWN7	SIG		Uncharacterized protein				36	26	94	85	66
ARB_00641	No changes	ARB_00641		D4AWS5	SIG		Histidine phosphatase superfamily				187	120	305	119	258
ARB_00650	No changes	ARB_00650		D4AWT4	SIG+GPI		Uncharacterized protein		down	induced in vitro	6	0	109	164	110
ARB_00653	N-terminus shortened	ARB_00653		D4AWT7	SIG		NAD-dependent malate dehydrogenase				615	591	500	821	1217
ARB_00691	Internal intron/exon prediction changes	ARB_00691		D4AWX5	SIG		Uncharacterized protein				9	4	14	15	10
ARB_00701	No changes	ARB_00701	Sub3	D4AWY5	SIG	pH4 & pH7	Subtilisin-like protease (peptidase S8 family)			induced in keratin and soy	3	1	14611	481	7
ARB_00755	C-terminus shortened	ARB_00755		D4AX28	SIG		Cbb3-type cytochrome oxidase component		up		335	245	56	114	107
ARB_00762	No changes	ARB_00762	Mep4	D4AX35	SIG	pH7	Extracellular metalloprotease/fungalysin (peptidase M36 family)			induced in vitro	5	9	328	736	42
ARB_00766	Internal intron/exon prediction changes	ARB_00766		D4AX39	SIG+GPI		Endo-chitosanase (glycoside hydrolase family 75)				55	23	372	163	80
ARB_00777	No changes	ARB_00777	Sub8	D4AX50	SIG	pH4 & pH7	Subtilisin-like protease (peptidase S8 family)	Asp f 18/Asp n 18/Pen c 2/Cla h 9/Cur l 4/Pen n 18/Rho m 1			642	683	188	670	438
ARB_00781	No changes	ARB_00781		D4AX54	SIG		Alpha/beta hydrolase				4	1	3	6	6

ARB_00790	No changes	ARB_00790		D4AX63	SIG		Alpha/Beta hydrolase fold-containing lipase				2	2	2	2	1
ARB_00805	N-terminus shortened	ARB_00805		D4AX78	SIG+ GPI		Uncharacterized protein				0	0	5	0	0
ARB_00806	N-terminus extended	ARB_00806		D4AX79	SIG		Uncharacterized protein				0	0	4	0	0
ARB_00807	No changes	ARB_00807		D4AX80	SIG		Uncharacterized protein				0	0	3	0	0
ARB_00824	C-terminus modified	ARB_00824		D4AX97	SIG+ GPI		Uncharacterized protein				0	0	0	1	12
ARB_00842	C-terminus modified	ARB_00842		D4AXB4	SIG		Acid phosphatase				48	61	53	101	41
ARB_00849	C-terminus modified	ARB_00849		D4AXC1	SIG		Metalloprotein ase (peptidase M35 family)				2	0	2	5	4
ARB_00890	Internal intron/exon prediction changes	ARB_00890		D4AXG2	SIG+ GPI		Gamma-glutamyltransp eptidase				3	1	3	5	6
ARB_00892	No changes	ARB_00892		D4AXG4	SIG		Uncharacterized protein				0	0	0	0	0
ARB_00912	N-terminus shortened	ARB_00912		D4AXJ3	SIG+ GPI		Uncharacterized protein		down		321	218	735	714	695
ARB_00915	Internal intron/exon prediction changes	ARB_00915		D4AXJ6	SIG		Glycosyl transferase, family 20				88	95	66	148	64
ARB_00926	C-terminus shortened	ARB_00926		D4AXK7	SIG	pH4	Uncharacterized protein			induced in soy and Sabouraud	2	4	79	922	863
ARB_00930	No changes	ARB_00930		D4AXL1	SIG	pH4 & pH7	Beta-lactamase				4	1	13	7	6
ARB_00933	Internal intron/exon prediction changes	ARB_00933		D4AXL4	SIG+ GPI		Carboxylester ase, type B				5	4	1	2	3
ARB_00998	No changes	ARB_00998		D4AXS9	SIG		Lipase				127	147	123	80	73
ARB_01017	No changes	ARB_01017		D4AXU8	SIG+ GPI		CFEM domain protein				53	46	253	307	92
ARB_01032	Internal intron/exon prediction changes	ARB_01032	Sub4	D4AXW3	SIG	pH4 & pH7	Subtilisin-like protease (peptidase S8 family)			induced in vitro	14	3	8947	2203	49

ARB_01041	No changes	ARB_01041		D4AXX2	SIG		Peptidase M20 family protein				15	25	15	47	20
ARB_01050	No changes	ARB_01050		D4AXY1	SIG		Uncharacterized protein				2	7	3	3	12
ARB_01071	N-terminus shortened	ARB_01071		D4AY02	SIG	pH7	Peptidyl-prolyl cis-trans isomerase				459	483	507	871	617
ARB_01072	Internal intron/exon prediction changes	ARB_01072		D4AY03	SIG		Carboxylesterase, type B				12	14	8	13	16
ARB_01122	Internal intron/exon prediction changes	ARB_01122		D4AY53	SIG		Lipopolysaccharide-modifying protein				21	19	28	14	21
ARB_01125	Internal intron/exon prediction changes	ARB_01125		D4AY56	SIG+GPI		Uncharacterized protein				150	114	183	158	177
ARB_01131	Internal intron/exon prediction changes	ARB_01131		D4AY62	SIG		Cytochrome P450 alkane hydroxylase		down		27	22	178	230	115
ARB_01140	Internal intron/exon prediction changes	ARB_01140		D4AY71	SIG+GPI		1,3-beta-glucanosyltransferase (glycoside hydrolase family 72)				9	6	1	2	1
ARB_01153	N-terminus modified	ARB_01153		D4AY84	SIG		Prenylcysteine oxidase				29	21	25	48	37
ARB_01155_01156	ORFs merged	ARB_01155 and ARB_01156		D4AY86/D4AY87	SIG+GPI		LysM domain-containing protein				11	10	96	53	23
ARB_01183	No changes	ARB_01183		D4AYB4	SIG		Antigenic thaumatin domain protein		up		6131	7203	30	35	257
ARB_01187	N- and C-termini extended	ARB_01187		D4AYB8	SIG		Uncharacterized protein				2	1	16	9	5
ARB_01220	N-terminus modified	ARB_01220		D4AYF1	SIG		Uncharacterized protein				8	13	18	33	32
ARB_01230	SIG at N-terminus manually restored	ARB_01230		D4AYG1	SIG	pH4	Kelch repeat protein-containing protein				43	40	131	119	77
ARB_01233	No changes	ARB_01233		D4AYG4	SIG+GPI		Uncharacterized protein				1	0	5	3	3

ARB_01325	No changes	ARB_01325		D4AYQ6	SIG	pH4 & pH7	MD-2-related lipid-recognition domain-containing protein				232	276	316	440	251
ARB_01333	C-terminus modified	ARB_01333		D4AYR4	SIG		Uncharacterized protein				4	7	2	5	5
ARB_01338	Internal intron/exon prediction changes	ARB_01338		D4AYR9	SIG		Thioredoxin domain-containing protein				109	99	95	100	131
ARB_01345	C-terminus modified and shortened	ARB_01345	S28B	D4AYS6	SIG+GPI	pH4	Serine peptidase (peptidase S28 family)				34	31	240	214	82
ARB_01347	Internal intron/exon prediction changes	ARB_01347		D4AYS8	SIG	pH4 & pH7	Ribonuclease				36	39	26	49	29
ARB_01353	No changes	ARB_01353		D4AYT4	SIG	pH7	β-N-acetylhexosaminidase (glycoside hydrolase, family 20)	Pen ch 20			341	227	477	455	163
ARB_01369	C-terminus shortened	ARB_01369		D4AYV0	SIG		Uncharacterized protein				2	9	1	1	4
ARB_01382	No changes	ARB_01382	Mep2	D4AYW3	SIG+GPI		Extracellular metalloprotease/fungalysin (peptidase M36 family)				18	15	13	16	17
ARB_01443	Internal intron/exon prediction changes	ARB_01443		D4AZ23	SIG		Leucine aminopeptidase (family M28)				6	0	11	13	10
ARB_01444	C-terminus modified	ARB_01444		D4AZ24	SIG	pH4 & pH7	Endo-1,3(4)-beta-glucanase (glycoside hydrolase, family 81)				142	103	69	30	23
ARB_01488	Internal intron/exon prediction changes	ARB_01488		D4AZ68	SIG		LysM domain-containing protein				5	2	1	1	2
ARB_01491	No changes	ARB_01491		D4AZ71	SIG		Serine carboxypeptidase (peptidase S10 family)				528	449	231	515	358

ARB_01495	No changes	ARB_01495	Sub2	D4AZ75	SIG	pH7	Subtilisin-like protease (peptidase S8 family)	Asp fl 13/Asp o 13/Asp v 13			0	0	0	0	0
ARB_01498	Internal intron/exon prediction changes	ARB_01498		D4AZ78	SIG	pH4	Carboxylesterase, type B				7	4	20	14	16
ARB_01545	N-terminus shortened	ARB_01545		D4AZC5	SIG+GPI	pH4	CFEM-domain containing extracelular proline-glycine rich protein				1230	1192	42	331	352
ARB_01551	Internal intron/exon prediction changes	ARB_01551		D4AZD1	SIG		Glycosyltransferase, family 4				25	18	5	15	16
ARB_01584	No changes	ARB_01584		D4AZG6	SIG		Uncharacterized protein				462	335	1112	775	1293
ARB_01587	No changes	ARB_01587		D4AZG9	SIG		Serine carboxypeptidase (peptidase S10 family)				18	12	3	8	11
ARB_01595	N-terminus extended	ARB_01595		D4AZH7	SIG		Cupredoxin				3	2	2	3	5
ARB_01619	Internal intron/exon prediction changes	ARB_01619	CtsD	D4AZK1	SIG+GPI		Aspartic-type endopeptidase (peptidase A1 family)				23	17	36	49	46
ARB_01627	No changes	ARB_01627		D4AZK9	SIG+GPI	pH4 & pH7	GPI-anchored cell wall protein				2664	2756	2549	1539	2112
ARB_01633	No changes	ARB_01633		D4AZL5	SIG		Serine endopeptidase (peptidase S1 family)				0	0	1	1	1
ARB_01650	N-terminus shortened	ARB_01650		D4AZN2	SIG		Uncharacterized protein				6	4	30	270	2129
ARB_01687	No changes	ARB_01687		D4AZR9	SIG		Uncharacterized protein				2	0	4	7	2
ARB_01705	N-terminus modified	ARB_01705		D4AZT5	SIG		Amine oxidase				9	4	10	8	3
ARB_01712	C-terminus extended	ARB_01712		D4AZU2	SIG		Uncharacterized protein				4	4	3	6	6
ARB_01713	N-terminus modified	ARB_01713		D4AZU3	SIG+GPI		1,3-beta-glucanosyltransferase (glycoside				458	424	283	399	294

							hydrolase family 72)								
ARB_01728	No changes	ARB_01728		D4AZV8	SIG+GPI		PLC-like phosphodiesterase				0	0	0	0	0
ARB_01751	No changes	ARB_01751		D4AZY1	SIG	pH4 & pH7	Alpha/Beta hydrolase fold-containing PAF acetylhydrolase				3	1	10	9	8
ARB_01786	No changes	ARB_01786		D4B015	SIG		Uncharacterized protein		up		10	22	1	1	1
ARB_01793	No changes	ARB_01793		D4B022	SIG+GPI		Uncharacterized protein				274	150	120	187	1515
ARB_01815	No changes	ARB_01815		D4B044	SIG		DUF3455 family protein			induced in vitro	1	8	69	51	81
ARB_01832	No changes	ARB_01832		D4B061	SIG		Uncharacterized protein				0	0	18	30	3
ARB_01844	No changes	ARB_01844		D4B073	SIG		Heat shock protein 70-like				43	43	95	130	64
ARB_01845	No changes	ARB_01845		D4B074	SIG+GPI		Uncharacterized protein				7	4	22	35	39
ARB_01857	SIG at N-terminus manually restored	ARB_01857		D4B086	SIG	pH7	Autophagy protein Atg27-like protein				123	127	112	194	143
ARB_01864	No changes	ARB_01864		D4B093	SIG	pH4 & pH7	Ser/Thr protein phosphatase family protein		down		17	13	112	127	178
ARB_01872	No changes	ARB_01872		D4B0A0	SIG		Alpha carbonic anhydrase				24	22	37	13	13
ARB_01932	N-terminus extended	ARB_01932		D4B0F8	SIG	pH4 & pH7	BYS1 domain-containing protein			induced in vitro	7	5	179	1332	263
ARB_02001	No changes	ARB_02001		D4B0M5	SIG	pH7	phospholipase A2				9	0	115	29	30
ARB_02015	No changes	ARB_02015		D4B0N9	SIG	pH4	Uncharacterized protein				6	8	11	16	16
ARB_02032	N-terminus extended	ARB_02032	CpS4	D4B0Q6	SIG		Serine carboxypeptidase (peptidase S10 family)				11	6	4	9	4

ARB_02077	No changes	ARB_02077		D4B0V1	SIG	pH4 & pH7	Exo-beta-1,3-glucanase				50	45	386	62	36
ARB_02081	Internal intron/exon prediction changes	ARB_02081		D4B0V4	SIG		polynucleotide adenylyltransferase		down		9	6	29	74	57
ARB_02084	No changes	ARB_02084		D4B0V6	SIG+ GPI		Uncharacterized protein			induced in vitro	1	0	96	123	1225
ARB_02097	Internal intron/exon prediction changes	ARB_02097		D4B0W9	SIG		Alpha-1,2-mannosidase (glycoside hydrolase family 92)				3	1	1	1	1
ARB_02099	No changes	ARB_02099		D4B0X1	SIG		Aspartic-type endopeptidase (peptidase A1 family)				16	9	6	8	9
ARB_02101	Internal intron/exon prediction changes	ARB_02101		D4B0X3	SIG	pH4 & pH7	Alpha-glucosidase (glycoside hydrolase, family 31)				34	26	15	21	8
ARB_02127	No changes	ARB_02127		D4B0Z9	SIG		Multicopper oxidase				500	469	8	8	112
ARB_02135	Internal intron/exon prediction changes	ARB_02135		D4B107	SIG		3-Isopropylmalate dehydrogenase				453	357	22	133	254
ARB_02148_02149	ORFs merged	ARB_02148 and ARB_02149		D4B119/D4B120	SIG		feruloyl esterase				3	3	3	4	4
ARB_02157	C-terminus modified	ARB_02157		D4B128	SIG		Ribonuclease H-like domain-containing protein		up		10	5	1	1	2
ARB_02186	No changes	ARB_02186		D4B157	SIG		Metallopeptidase				1	2	0	1	2
ARB_02187	N-terminus modified and extended	ARB_02187		D4B158	SIG		Chitinase (glycoside hydrolase, family 18)				1	0	1	3	3
ARB_02189	C-terminus modified	ARB_02189		D4B160	SIG		Uncharacterized protein		up		52	31	0	1	1
ARB_02206	N-terminus shortened	ARB_02206		D4B177	SIG		Sialidase		up		692	1026	10	5	5

ARB_02208	Internal intron/exon prediction changes	ARB_02208		D4B179	SIG+ GPI	pH4 & pH7	Bicupin, oxalate decarboxylase /oxidase		down	induced in vitro	13	3	841	239	179
ARB_02220	Internal intron/exon prediction changes	ARB_02220		D4B191	SIG+ GPI	pH4 & pH7	Peptisase S41 family protein				37	17	31	25	76
ARB_02223	No changes	ARB_02223	Sub5	D4B194	SIG		Subtilisin-like protease (peptidase S8 family)			induced in keratin and soy	5	3	38	134	10
ARB_02240	No changes	ARB_02240		D4B1B1	SIG+ GPI	pH4 & pH7	Uncharacterized protein		down		14	13	49	115	170
ARB_02251	No changes	ARB_02251		D4B1C2	SIG	pH4	Uncharacterized protein				2	5	3	6	4
ARB_02289	N-terminus extended	ARB_02289	ADM-B	D4B1G0	SIG		Metalloprotease ADAM-B (peptidase M12B family)				57	56	131	80	83
ARB_02327-1	ORF split in 2 ORFs	ARB_02327		D4B1J8	SIG	pH4 & pH7	Glucoamylase (glycoside hydrolase, family 15)	Sch c 1			5	6	312	163	20
ARB_02359	No changes	ARB_02359		D4B1N0	SIG		PHP domain-containing protein				0	0	3	1	1
ARB_02369	No changes	ARB_02369		D4B1N9	SIG	pH7	Carboxylesterase, type B				828	291	1727	562	11
ARB_02372	No changes	ARB_02372		D4B1P2	SIG	pH4 & pH7	FAD-dependent oxidoreductase				9	21	5	11	6
ARB_02390	No changes	ARB_02390	Gltcp	D4B1R0	SIG	pH7	Glutamate carboxypeptidase (peptidase M28 family)				151	139	83	88	29
ARB_02401	No changes	ARB_02401		D4B1S0	SIG		Uncharacterized protein				11	21	2	5	6
ARB_02406	No changes	ARB_02406	Mep1	D4B1S5	SIG	pH4	Extracellular metalloprotease/fungalysin (peptidase M36 family)				16	14	1172	27	14
ARB_02407	C-terminus modified	ARB_02407	McpB	D4B1S6	SIG	pH4 & pH7	Metallocarboxypeptidase (peptidase M14 family)				26	20	173	201	14

ARB_02433	No changes	ARB_02433		D4B1V2	SIG		EGF-like calcium-binding domain-containing protein				12	0	34	788	310
ARB_02441	N-terminus modified	ARB_02441		D4B1W0	SIG		BIG/ATPase V1 complex, subunit S1				178	184	128	273	270
ARB_02457	No changes	ARB_02457		D4B1X6	SIG		SGNH hydrolase-type esterase domain-containing protein				0	0	10	17	7
ARB_02458	N-terminus modified and shortened	ARB_02458		D4B1X7	SIG+GPI		Uncharacterized protein				11	26	986	884	3935
ARB_02459	No changes	ARB_02459		D4B1X8	SIG		Uncharacterized protein				4	0	0	0	0
ARB_02462	No changes	ARB_02462		D4B1Y1	SIG		FAD-dependent monooxygenase				15	14	26	25	9
ARB_02478	C-terminus modified and extended	ARB_02478		D4B1Z7	SIG	pH4 & pH7	UDP-N-acetylmuramate dehydrogenase				3	3	17	8	9
ARB_02487	SIG at N-terminus manually restored	ARB_02487		D4B206	SIG		SGNH hydrolase-type esterase domain				0	0	1	1	0
ARB_02569	No changes	ARB_02569		D4B286	SIG		Uncharacterized protein				1	0	2	2	1
ARB_02626	No changes	ARB_02626		D4B2L8	SIG		Protein disulfide-isomerase	Alt a 4			330	348	202	490	574
ARB_02697	No changes	ARB_02697		D4B2G9	SIG+GPI		GPI-anchored cell wall protein				2413	3205	1053	1075	1072
ARB_02701	Internal intron/exon prediction changes	ARB_02701		D4B2H3	SIG		Extracellular cellulase	Asp f 7	down		174	152	629	906	3424
ARB_02715_02716	ORFs merged	ARB_02715 and ARB_02716	1Dppl	D4B2N2/D4B2N3	SIG+GPI	pH7	Dipeptidase				10	12	167	181	13

ARB_02727	Internal intron/exon prediction changes	ARB_02727		D4B2P4	SIG		Polysaccharide deacetylase				24	14	14	25	15
ARB_02741	No changes	ARB_02741		D4B2Q8	SIG+GPI	pH4 & pH7	CFEM domain-containing protein				3503	3821	14805	8080	2149
ARB_02760_02761	ORFs merged	ARB_02760 and ARB_02761		D4B2S7/D4B2S8	SIG+GPI		Uncharacterized protein				15	9	12	27	55
ARB_02787	New exon near N-ter and C-ter modified	ARB_02787		D4B2V4	SIG		Oxidoreductase				49	35	110	38	47
ARB_02797	No changes	ARB_02797		D4B2W4	SIG	pH4 & pH7	1,3-beta-glucanosyltransferase (glycoside hydrolase family 72)	Tri t 1			457	477	246	317	490
ARB_02803	No changes	ARB_02803		D4B2X0	SIG+GPI		Uncharacterized protein				3064	3093	7273	6072	10321
ARB_02861	C-terminus modified and extended	ARB_02861		D4B327	SIG		SCP-like extracellular protein	V5/Tpx-1			246	218	97	149	356
ARB_02866	N-terminus and C-terminus extended	ARB_02866		D4B332	SIG		Glycosyl transferase, family 15				58	61	69	52	77
ARB_02919	No changes	ARB_02919	Pep2	D4B385	SIG	pH7	Aspartic-type endopeptidase (peptidase A1 family)				843	970	691	1136	550
ARB_02921	Internal intron/exon prediction changes	ARB_02921		D4B387	SIG	pH4 & pH7	Gamma-glutamyltranspeptidase				136	165	844	250	38
ARB_02922	No changes	ARB_02922		D4B388	SIG+GPI		FAS1 domain-containing protein		up		14	10	2	3	2
ARB_02924	No changes	ARB_02924		D4B390	SIG+GPI		Uncharacterized protein				6	10	8	5	2
ARB_02965	Internal intron/exon prediction changes	ARB_02965		D4B3C8	SIG	pH4 & pH7	Amidase family protein			induced in keratin and soy	0	0	159	93	1
ARB_02997	No changes	ARB_02997		D4B3G0	SIG+GPI		Peptisase S41 family protein		up	induced in vivo	182	221	3	3	2
ARB_03024	No changes	ARB_03024		D4B3I5	SIG+GPI	pH4 & pH7	Cupredoxin				13	34	115	48	37

ARB_03104	N-terminus shortened	ARB_03104		D4B3R5	SIG		EF-hand domain-containing protein				101	71	65	116	128
ARB_03106	No changes	ARB_03106		D4B3R7	SIG	pH4	O-glycosyl compounds hydrolase		down	induced in vitro	6	3	1191	984	149
ARB_03160	No changes	ARB_03160		D4B3X1	SIG		Uncharacterized protein				4	0	2	3	3
ARB_03208	No changes	ARB_03208		D4B419	SIG		Uncharacterized protein				4	4	2	1	3
ARB_03220	N-terminus modified and extended	ARB_03220		D4B431	SIG		Chaperone DnaJ-like protein				53	44	218	57	108
ARB_03232	No changes	ARB_03232		D4B443	SIG		Uncharacterized protein				148	117	208	168	160
ARB_03253	Internal intron/exon prediction changes	ARB_03253		D4B464	SIG		Glycoside hydrolase, family 47		up		152	132	16	27	37
ARB_03254	No changes	ARB_03254		D4B465	SIG+GPI		Lipase		up		49	15	1	1	1
ARB_03267	No changes	ARB_03267		D4B478	SIG		ATPase synthesis protein 25, mitochondrial				35	25	98	32	65
ARB_03272	N-terminus modified and extended	ARB_03272		D4B483	SIG		Lectin family protein				60	36	25	71	74
ARB_03382	C-terminus shortened	ARB_03382		D4B4J2	SIG+GPI		Cell wall glucanase (glycoside hydrolase, family 16)	Asp f 9/Asp f 16			346	311	479	91	203
ARB_03399	Internal intron/exon prediction changes	ARB_03399		D4B4K9	SIG		N-acetylglucosaminyl phosphatidylinositol deacetylase				26	21	32	39	25
ARB_03420	No changes	ARB_03420		D4B4N0	SIG		UDP-glucose:glycoprotein glucosyltransferase				25	20	16	21	27
ARB_03431	No changes	ARB_03431		D4B4P1	SIG	pH4	Sialidase				9	5	156	9	5

ARB_03436	N-terminus extended	ARB_03436		D4B4P6	SIG+ GPI		Uncharacterized protein				30	37	86	61	63
ARB_03438	C-terminus modified	ARB_03438		D4B4P8	SIG		LysM domain-containing protein				0	0	0	0	0
ARB_03442	C-terminus modified and extended	ARB_03442		D4B4Q2	SIG		LysM domain and chitin-binding domain-containg protein				2	3	1	0	1
ARB_03471	C-terminus modified	ARB_03471		D4B4T1	SIG		Carbohydrate-binding WSC domain protein				134	93	626	419	274
ARB_03491	SIG at N-terminus manually restored	ARB_03491		D4B4V1	SIG	pH4 & pH7	Histidine phosphatase superfamily protein				55	43	24	82	58
ARB_03492	No changes	ARB_03492		D4B4V2	SIG+ GPI		Leucine aminopeptidase (peptidase M28 family)				34	24	14	9	11
ARB_03496	No changes	ARB_03496		D4B4V6	SIG		Uncharacterized protein		up		4021	3952	12	9	18
ARB_03504	No changes	ARB_03504		D4B4W4	SIG		Uncharacterized protein				181	175	119	116	123
ARB_03514	N-terminus modified and extended	ARB_03514		D4B4X4	SIG	pH4 & pH7	Class III chitinase (glycoside hydrolase, family 18)				56	44	20	3	4
ARB_03537	N-terminus extended	ARB_03537		D4B4Z7	SIG		Uncharacterized protein				1	0	39	12	8
ARB_03568	No changes	ARB_03568	Lap1	D4B528	SIG	pH4 & pH7	Leucine aminopeptidase (peptidase M28 family)				21	35	3064	583	6
ARB_03594	N-terminus modified	ARB_03594		D4B568	SIG		Uncharacterized protein		down		0	0	12	22	20
ARB_03645-1	ORF split in 2 ORFs	ARB_03645		D4B5A5	SIG		Uncharacterized protein				34	55	34	13	9
ARB_03673	Internal intron/exon prediction changes	ARB_03673		D4B5D3	SIG	pH4	Uncharacterized protein				15	6	40	44	165

ARB_03674	N-terminus shortened	ARB_03674		D4B5D4	SIG	pH7	Superoxide dismutase				295	199	94	352	630
ARB_03696	No changes	ARB_03696		D4B5F6	SIG+GPI		Uncharacterized protein				14	12	3	23	61
ARB_03697	N-terminus extended by 1 Met	ARB_03697		D4B5F7	SIG+GPI		Uncharacterized protein				36	24	38	73	53
ARB_03699	C-terminus modified and extended	ARB_03699		D4B5F9	SIG+GPI	pH4 & pH7	Polysaccharide deacetylase				39	30	622	188	176
ARB_03715-1	ORF split in 2 ORFs	ARB_03715		D4B5H5	SIG		Class I glutamine amidotransferase-like protein				2	0	0	0	1
ARB_03719	No changes	ARB_03719		D4B5H9	SIG	pH4	Glycoside hydrolase, family 65				30	53	74	35	15
ARB_03765	C-terminus extended	ARB_03765		D4B5M5	SIG		Alpha/Beta hydrolase fold-containing protease				2	2	9	16	6
ARB_03766	No changes	ARB_03766		D4B5M6	SIG		Amine oxidase				166	108	6	12	101
ARB_03767	SIG at N-terminus manually restored	ARB_03767		D4B5M7	SIG		Amidase				51	23	9	5	28
ARB_03788_03789	ORFs merged	ARB_03788 and ARB_03789	Mcpal	D4B5M9/D4B5N0	SIG+GPI	pH4 & pH7	Metallocarboxypeptidase A-like (peptidase M14 family)				28	18	8	13	7
ARB_03790	No changes	ARB_03790	Sub9	D4B5N1	SIG	pH4 & pH7	Subtilisin-like protease (peptidase S8 family)				0	0	1	0	0
ARB_03792	No changes	ARB_03792		D4B5N3	SIG		Uncharacterized protein				12	12	6	8	18
ARB_03878	No changes	ARB_03878		D4B5X1	SIG		Alkaline phosphatase				39	49	433	121	142
ARB_03949	C-terminus modified	ARB_03949	NpIIA	D4B639	SIG+GPI	pH4	Deuterolysin (peptidase M35 family)				13	16	178	7	7
ARB_04006	N-terminus shortened	ARB_04006		D4AIB2	SIG		Cytochrome P450				0	0	1	2	22

ARB_04018	No changes	ARB_04018		D4AIC4	SIG		Aspartic-type endopeptidase (peptidase A1 family)				2	2	2	3	1
ARB_04046	No changes	ARB_04046	CpS1	D4AIF1	SIG+ GPI	pH4 & pH7	Serine carboxypeptidase (peptidase S10 family)				134	62	55	54	125
ARB_04074	No changes	ARB_04074		D4AIH9	SIG		Cysteine-rich secreted protein				4	4	2	1	20
ARB_04091	Internal intron/exon prediction changes	ARB_04091		D4AIJ6	SIG+ GPI		Glycoside hydrolase, family 18				78	30	1312	1038	175
ARB_04101	No changes	ARB_04101	SedD/Sed4	D4AIK6	SIG+ GPI	pH4	Tripeptyl peptidase/sedolisin (peptidase S53 family)				14	7	12	17	103
ARB_04134	No changes	ARB_04134		D4AIN8	SIG		DUF1183 domain-containing protein				34	26	83	140	40
ARB_04170	No changes	ARB_04170	OpsB	D4AIS3	SIG+ GPI	pH4	Aspartic-type endopeptidase (peptidase A1 family)		down		58	51	2113	579	889
ARB_04177	N-terminus extended	ARB_04177		D4AIS9	SIG	pH7	Glycerophosphoryl diester phosphodiesterase				9	10	54	22	21
ARB_04303_04304	ORFs merged	ARB_04303 and ARB_04304		D4AJ54/D4AJ55	SIG		Histidine acid phosphatase				11	18	6	16	9
ARB_04318	SIG at N-terminus manually restored	ARB_04318		D4AJ69	SIG		Alpha-mannosyltransferase		up		11	11	2	3	2
ARB_04336	C-terminus modified	ARB_04336	NpIIB	D4AJ87	SIG+ GPI		Neutral protease 2 homolog (peptidase M35 family)		up		1156	1120	13	13	9
ARB_04380	No changes	ARB_04380		D4AJD1	SIG		Alpha-1,3-mannosyltransferase				61	76	44	41	79
ARB_04463	N-terminus extended	ARB_04463		D4AJL3	SIG		Lipopolysaccharide-modifying protein				24	18	7	4	5

ARB_04464	N-terminus shortened	ARB_04464		D4AJL4	SIG+ GPI		Extracellular serine-threonine rich protein		down		257	202	18999	8714	4491
ARB_04467	No changes	ARB_04467		D4AJL7	SIG	pH4 & pH 7	Exo-beta-1,3-glucanase (glycoside hydrolase, family 5)				381	287	1818	428	87
ARB_04519	No changes	ARB_04519		D4AJR9	SIG	pH4	Endo-1,3(4)-beta-glucanase (glycoside hydrolase, family 16)				11	8	41	40	13
ARB_04522	Internal intron/exon prediction changes	ARB_04522		D4AJS2	SIG		Disulfide isomerase				93	98	42	94	87
ARB_04561	No changes	ARB_04561		D4AJW 1	SIG+ GPI		Cell wall serine-threonine-rich galactomanno protein		down		94	31	3214	1873	2728
ARB_04577	N-terminus shortened	ARB_04577		D4AJX7	SIG		Uncharacterized protein				0	0	0	0	0
ARB_04618	No changes	ARB_04618		D4AK17	SIG	pH7	PLC-like phosphodiesterase				27	18	41	8	3
ARB_04619	N-terminus shortened	ARB_04619		D4AK18	SIG	pH4 & pH7	DUF1524 family protein				25	0	40	13	8
ARB_04650	N-terminus extended	ARB_04650		D4AK49	SIG+ GPI	pH7	Uncharacterized protein				63	7	21	24	681
ARB_04677 _ARB_0467 8	ORFs manually merged	ARB_04677 and ARB_04678	SedC/Sed3	D4AK75	SIG		Tripeptyl peptidase/sedolisin (peptidase S53 family)				2	3	6	6	4
ARB_04696	C-terminus modified	ARB_04696		D4AK94	SIG	pH7	3-phytase like protein				42	49	43	41	18
ARB_04700	Internal intron/exon prediction changes	ARB_04700		D4AK98	SIG		TinC like protein				172	202	75	156	119
ARB_04732	No changes	ARB_04732		D4AM4 2	SIG		Peptidase M28 family protein			induced in keratin and soy	12	5	74	38	3

ARB_04735	No changes	ARB_04735		D4AM45	SIG		Uncharacterized protein				1	3	1	2	0
ARB_04737	N-terminus shortened	ARB_04737		D4AM47	SIG+GPI		Uncharacterized protein				0	0	0	0	0
ARB_04747	No changes	ARB_04747		D4AM57	SIG	pH4	SUN domain-containing protein				251	267	191	309	504
ARB_04768	No changes	ARB_04768		D4AM78	SIG	pH7	Aminoglycoside phosphotransferase				9	19	5	7	10
ARB_04769	C-terminus modified	ARB_04769		D4AM79	SIG		Deuterolysin (peptidase M35 family)				14	16	26	5	8
ARB_04773	No changes	ARB_04773		D4AM83	SIG		Uncharacterized protein				0	0	0	0	0
ARB_04807	N-terminus extended	ARB_04807		D4AKG4	SIG		Serine carboxypeptidase (peptidase S10 family)				8	4	7	5	8
ARB_04818	No changes	ARB_04818		D4AKH5	SIG+GPI		Uncharacterized protein			induced in Sabouraud	0	0	6	19	52
ARB_04825	Internal intron/exon prediction changes	ARB_04825		D4AKI2	SIG		Uncharacterized protein				7	3	11	14	10
ARB_04859	No changes	ARB_04859		D4AKL6	SIG	pH4 & pH7	Oxalate decarboxylase				19	10	710	65	42
ARB_04942	No changes	ARB_04942		D4AKU7	SIG		Carboxypeptidase A (peptidase M14 family)				126	135	99	101	62
ARB_04944	N-terminus shortened	ARB_04944	Sub1	D4AKU9	SIG+GPI		Subtilisin-like protease (peptidase S8 family)		up		422	370	30	55	62
ARB_04986	No changes	ARB_04986		D4AKZ0	SIG		Uncharacterized protein				6	0	12	24	10
ARB_04988	Internal intron/exon prediction changes	ARB_04988		D4AKZ2	SIG		Uncharacterized protein				15	10	24	17	27
ARB_05022	Internal intron/exon prediction changes	ARB_05022		D4AL26	SIG	pH4	Fucose-specific lectin				0	0	2	3	2
ARB_05076	No changes	ARB_05076		D4AL79	SIG		Alkaline phosphatase				22	17	7	10	11

ARB_05078	No changes	ARB_05078		D4AL81	SIG		Alpha carbonic anhydrase				1	0	0	0	1
ARB_05085	No changes	ARB_05085	Mep3	D4AL88	SIG	pH4 & pH7	Extracellular metalloprotease/fungalysin (peptidase M36 family)	Asp f 5		induced in keratin and soy	2	1	1370	35	7
ARB_05086	No changes	ARB_05086		D4AL89	SIG+ GPI		Uncharacterized protein			induced in soy	2	4	7	67	13
ARB_05128	No changes	ARB_05128		D4ALD1	SIG+ GPI		Uncharacterized protein				176	125	492	319	346
ARB_05144	No changes	ARB_05144		D4ALE7	SIG		Lysozyme-like protein				17	16	24	31	24
ARB_05145	Internal intron/exon prediction changes	ARB_05145		D4ALE8	SIG		NlpC/P60-like cell-wall endopeptidase (peptidase C40 family)				2	9	41	6	6
ARB_05152_05153_05154	ORFs merged	ARB_05154		D4ALF7	SIG		Chitinase (glycoside hydrolase, family 18)		down	induced in vitro	4	2	75	120	50
ARB_05155	N-terminus shortened	ARB_05155		D4ALF8	SIG+ GPI		Uncharacterized protein		down	induced in vitro	0	0	350	326	65
ARB_05157	Internal intron/exon prediction changes	ARB_05157		D4ALG0	SIG	pH7	LysM domain-containing protein				0	0	33	25	5
ARB_05164	No changes	ARB_05164		D4ALG7	SIG	pH7	Uncharacterized protein				310	64	507	98	7
ARB_05178	No changes	ARB_05178		D4ALI1	SIG+ GPI	pH4	Uncharacterized protein			induced in vitro	5	4	112	1100	2839
ARB_05215_05217	ORFs merged	ARB_05215 and ARB_05217 (ARB_05216 is antisens and disappears)		D4ALL7/D4ALL9	SIG+ GPI		Uncharacterized protein		up		3074	3500	42	107	216
ARB_05246	No changes	ARB_05246		D4ALP8	SIG		DNA J-like protein				37	32	16	31	49
ARB_05253	N-terminus modifies and extended	ARB_05253		D4ALQ5	SIG+ GPI	pH4	Glycoside hydrolase, family 16		down		241	262	2955	1051	1523

ARB_05266	N-terminus shortened	ARB_05266		D4ALR8	SIG		Heat shock protein 70 family protein				170	156	213	277	239
ARB_05272	N-terminus shortened	ARB_05272		D4ALS4	SIG		Isoamyl alcohol oxidase, putative				3	2	3	5	6
ARB_05304	N-terminus shortened	ARB_05304		D4ALV6	SIG	pH4 & pH7	Barwin-like endoglucanase	Asp f 13/Asp f 15			41	38	50	92	131
ARB_05307	No changes	ARB_05307	Sub6	D4ALV9	SIG	pH7	Subtilisin-like protease (peptidase S8 family)	Tri m 2/Tri r2	up	induced in vivo	5037	2632	1	2	3
ARB_05317	No changes	ARB_05317		D4ALW9	SIG		Probable metaloproteinase (peptidase M43 family)				80	60	1796	471	7
ARB_05361	SIG at N-terminus manually restored	ARB_05361		D4AM13	SIG		Uncharacterized protein				3	1	3	3	2
ARB_05372	No changes	ARB_05372		D4AMB9	SIG	pH4 & pH7	Aldose 1-epimerase				76	91	75	85	11
ARB_05397	N-terminus modified and extended	ARB_05397		D4AME4	SIG+GPI		Uncharacterized protein				1	0	0	1	0
ARB_05440	No changes	ARB_05440		D4AMI7	SIG		Uncharacterized protein				0	0	2	2	1
ARB_05442	No changes	ARB_05442		D4AMI9	SIG		Alpha/Beta hydrolase fold-containing protein				8	4	4	5	5
ARB_05496	N-terminus modified	ARB_05496		D4AMP3	SIG		Putative stress-responsive protein		up		640	945	17	112	48
ARB_05502	N-terminus extended	ARB_05502		D4AMP9	SIG+GPI		FAD binding domain protein				14	12	20	16	9
ARB_05535_05536	ORFs merged	ARB_05535 and ARB_05536		D4AMT2/D4AMT3	SIG+GPI	pH4 & pH7	Glutaminase				20	15	39	61	12
ARB_05566	No changes	ARB_05566		D4AMW3	SIG	pH4	Uncharacterized protein				12	6	8	10	13
ARB_05631	N-terminus shortened and C-ter extended	ARB_05631		D4AN27	SIG		Lipopolysaccharide-modifying protein				78	59	186	70	109

ARB_05642	SIG at N-terminus manually restored	ARB_05642		D4AN38	SIG		Cytochrome P450				1	0	2	5	7
ARB_05649	Internal intron/exon prediction changes	ARB_05649		D4AN45	SIG		Mannose-6-phosphate receptor binding domain protein				56	57	63	60	34
ARB_05654	C-terminus modified and extended	ARB_05654		D4AN50	SIG	pH4 & pH7	beta-D-glucoside glucohydrolase (glycoside hydrolase family 3)	Asp n 14			286	281	149	204	112
ARB_05667	No changes	ARB_05667		D4AN63	SIG+GPI		GPI anchored serine-rich protein		down		576	480	1394	1935	3153
ARB_05715	N-terminus shortened	ARB_05715		D4ANB0	SIG		Palmitoyl protein thioesterase				56	38	57	103	99
ARB_05717	No changes	ARB_05717		D4ANB2	SIG		Uncharacterized protein				10	12	5	7	10
ARB_05721	N-terminus shortened	ARB_05721	CpS6	D4ANB6	SIG	pH4	Serine carboxypeptidase (peptidase S10 family)			induced in vitro	7	5	73	69	35
ARB_05728	No changes	ARB_05728	Pep1	D4ANC3	SIG	pH4 & pH7	Aspartic-type endopeptidase (peptidase A1 family)	Asp f 10			1	0	0	0	0
ARB_05732-1	ORF split in 2 ORFs	ARB_05732		D4ANC7	SIG+GPI	pH4 & pH7?	Cupredoxin		down	induced in vitro	1	0	10425	5772	7328
ARB_05732-2	ORF split in 2 ORFs	ARB_05732		D4ANC7	SIG	pH4 & pH7?	Cysteine desulfurase				216	187	290	168	224
ARB_05749	Internal intron/exon prediction changes	ARB_05749		D4ANE4	SIG+GPI		Uncharacterized protein				17	18	29	13	22
ARB_05765	No changes	ARB_05765	SedB/Sed2	D4ANG0	SIG	pH4	Tripeptyl peptidase/sedolisin (peptidase S53 family)				3	4	3	4	2
ARB_05770	N-terminus modified and extended	ARB_05770		D4ANG5	SIG+GPI		1,3-beta-glucanosyltransferase (glycoside hydrolase family 72)				948	1299	462	369	412

ARB_05784	Internal intron/exon prediction changes	ARB_05784		D4ANH9	SIG		Cellobiose dehydrogenase				2	2	49	28	17
ARB_05809	N-terminus extended	ARB_05809		D4ANK4	SIG		Glucosidase subunit				116	99	15	67	79
ARB_05817	C-terminus modified	ARB_05817		D4ANL2	SIG+GPI		Deuterolysin (peptidase M35 family)				18	12	8	16	6
ARB_05828	Internal intron/exon prediction changes	ARB_05828		D4APX3	SIG	pH4	Cupredoxin				2	5	1	2	6
ARB_05864	No changes	ARB_05864		D4ANP7	SIG		Cell wall glucanase (glycoside hydrolase, family 16)				294	320	356	745	967
ARB_05911	No changes	ARB_05911		D4ANU4	SIG	pH4	Glycoside hydrolase, family 25				36	43	9	11	26
ARB_05919	No changes	ARB_05919		D4ANV2	SIG+GPI	pH4	Lysophospholipase				85	85	101	142	370
ARB_05933	Internal intron/exon prediction changes	ARB_05933		D4ANW6	SIG	pH4	Histidine acid phosphatase	Asp n 25			36	26	45	102	69
ARB_05938	No changes	ARB_05938		D4ANX1	SIG		Pantetheine-phosphate adenylyltransferase				57	71	35	71	51
ARB_05947	No changes	ARB_05947		D4ANY0	SIG		FAD-linked oxidase				4	6	21	5	34
ARB_05994	No changes	ARB_05994		D4AP27	SIG+GPI		Mannan endo-1,6-alpha-mannosidase (glycoside hydrolase family 76)				4	5	2	2	2
ARB_06014	No changes	ARB_06014		D4AP47	SIG		Uncharacterized protein				125	135	118	162	152
ARB_06019	Internal intron/exon prediction changes	ARB_06019	CpS2	D4AP52	SIG+GPI	pH4	Serine carboxypeptidase (peptidase S10 family)				4	9	124	248	33
ARB_06043	No changes	ARB_06043		D4AP76	SIG		Uncharacterized protein				57	56	69	81	64
ARB_06053	Internal intron/exon	ARB_06053		D4AP86	SIG	pH7	Pyruvate dehydrogenas				105	106	60	109	196

	prediction changes						e								
ARB_06057	No changes	ARB_06057		D4AP90	SIG		Uncharacterized protein		up	induced in vivo	62	80	0	3	2
ARB_06076	No changes, manually corrected	ARB_06076	Sub7	D4APA9	SIG+GPI	pH4 & pH7	Subtilisin-like protease (peptidase S8 family)				505	47	25	21	24
ARB_06107	No changes	ARB_06107		D4APD9	SIG		Serine-threonine rich protein				17	26	7	25	14
ARB_06108	No changes	ARB_06108		D4APE0	SIG+GPI	pH4	Uncharacterized protein				0	0	0	0	1
ARB_06110	Internal intron/exon prediction changes	ARB_06110	DppIV	D4APE2	SIG	pH4 & pH7	Dipeptidyl peptidase (peptidase S9B family)		down		42	22	793	825	219
ARB_06111	C-terminus modified	ARB_06111	Sub11	D4APE3	SIG	pH4 & pH7	Subtilisin-like protease (peptidase S8 family)				1	0	11	2	8
ARB_06168	No changes	ARB_06168		D4APK0	SIG+GPI		Uncharacterized protein				5	11	3	7	6
ARB_06191	No changes	ARB_06191		D4APM3	SIG		Uncharacterized protein				3	4	7	13	3
ARB_06224	No changes	ARB_06224		D4APQ6	SIG	pH4	Pyridine nucleotide-disulphide oxidoreductase				573	683	8	26	587
ARB_06227	No changes	ARB_06227		D4APQ9	SIG		Peptidyl-prolyl cis-trans isomerase				530	357	130	553	691
ARB_06229	No changes	ARB_06229		D4APR1	SIG		Beta-lactamase/transpeptidase-like protein				2	2	5	5	4
ARB_06308	No changes	ARB_06308		D4AQ01	SIG+GPI		Endo-1,3(4)-beta-glucanase				3	2	4	5	2
ARB_06334	No changes	ARB_06334		D4AQ27	SIG	pH7	Zinc metallopeptidase				7	8	73	45	18
ARB_06357	N-terminus extended	ARB_06357		D4AQ50	SIG		Carboxylesterase, type B				11	9	20	19	16

ARB_06359	No changes	ARB_06359		D4AQ52	SIG	pH4 & pH7	Glycosyl hydrolase, family 3				5	13	21	10	2
ARB_06361	No changes	ARB_06361	CpS3	D4AQ54	SIG	pH4 & pH7	Serine carboxypeptidase (peptidase S10 family)				98	116	25	15	9
ARB_06390	No changes	ARB_06390		D4AQ83	SIG		Cell wall protein	Asp f 4			760	750	2381	1308	2003
ARB_06414	Internal intron/exon prediction changes	ARB_06414	CpS5	D4AQA7	SIG	pH4 & pH7	Serine carboxypeptidase (peptidase S10 family)				460	326	316	236	57
ARB_06416	Internal intron/exon prediction changes	ARB_06416	Sub12	D4AQA9	SIG		Subtilisin-like protease (peptidase S8 family)				2	0	2	1	2
ARB_06439	No changes	ARB_06439		D4AQD2	SIG+GPI		Acid phosphatase				16	25	25	13	7
ARB_06463	No changes	ARB_06463		D4AQF6	SIG		Ribosomal protein-like				2093	1674	828	2733	3797
ARB_06467	Frameshift at position 4 manually corrected	ARB_06467	Sub10	D4AQG0	SIG+GPI		Subtilisin-like protease (peptidase S8 family)		up		791	789	12	13	13
ARB_06472	No changes	ARB_06472	Mep5	D4AQG5	SIG+GPI	pH4	Extracellular metalloprotease/fungalysin (peptidase M36 family)			induced in keratin	6	3	50	5	4
ARB_06477	No changes	ARB_06477		D4AQH0	SIG+GPI	pH4	Uncharacterized protein				317	208	4858	1120	895
ARB_06493	No changes	ARB_06493		D4AQI6	SIG		Glucosidase II beta subunit-like protein				58	60	22	55	43
ARB_06511	Internal intron/exon prediction changes	ARB_06511		D4AQK4	SIG		Prolyl oligopeptidase (Peptidase S9 family)				73	30	16	89	59
ARB_06528	C-terminus modified and shortened	ARB_06528		D4AQL9	SIG+GPI		Fungal lipase-like domain				61	44	54	83	36
ARB_06538	Internal intron/exon prediction changes	ARB_06538		D4AQM9	SIG+GPI		Extracellular matrix protein				669	911	193	281	700

ARB_06539	C-terminus modified and extended	ARB_06539		D4AQN0	SIG+GPI		Uncharacterized protein				0	0	0	1	0
ARB_06546	No changes	ARB_06546		D4AQN6	SIG		FAS1 domain-containing protein				224	284	92	144	63
ARB_06559	C-terminus extended	ARB_06559		D4AQP9	SIG+GPI		Serine/threonine-specific protein phosphatase				169	193	75	56	92
ARB_06576	No changes	ARB_06576		D4AQR6	SIG+GPI		Uncharacterized protein		down		14	6	363	430	435
ARB_06588_06589	ORFs merged	ARB_06588 and ARB_06589		D4AQS8/D4AQS9	SIG		Phosphoinositide phospholipase C				34	24	12	29	28
ARB_06629	Internal intron/exon prediction changes	ARB_06629		D4AQW9	SIG+GPI		Uncharacterized protein		down		14	17	549	294	447
ARB_06643	N-terminus shortened and C-ter modified	ARB_06643		D4ARA3	SIG		Glycosyl transferase		up		322	394	13	18	19
ARB_06651	No changes	ARB_06651	DppV	D4ARB1	SIG	pH4 & pH7	Dipeptidyl peptidase (peptidase S9B family)	Tri m 4/Tri r 4/Tri s 4/Tri t 4			90	62	761	1237	89
ARB_06718	No changes	ARB_06718		D4ARH5	SIG		WSC domain-containing protein		down		22	11	87	127	190
ARB_06732	No changes	ARB_06732		D4ARI9	SIG		Uncharacterized protein			induced in keratin and soy	3	0	171	531	13
ARB_06745	No changes	ARB_06745		D4ARK2	SIG		FUN14-domain containing protein				208	183	65	128	95
ARB_06753	No changes	ARB_06753		D4ARL0	SIG+GPI		Ecp2 effector-like protein				5	5	14	11	6
ARB_06825	N-terminus extended	ARB_06825		D4AQZ6	SIG		Uncharacterized protein				46	28	70	52	53
ARB_06834	C-terminus extended	ARB_06834		D4AR05	SIG+GPI		Uncharacterized protein				0	0	1	4	7
ARB_06838	No changes	ARB_06838		D4AR09	SIG		Endo-1,3(4)-beta-glucanase (glycosyl hydrolase,				9	12	6	30	107

							family 16)								
ARB_06893	No changes	ARB_06893		D4AR64	SIG		Uncharacterized protein				412	406	181	88	88
ARB_06907	N-terminus shortened	ARB_06907		D4AR77	SIG	pH4 & pH7	Prolyl oligopeptidase (peptidase S9 family)				18	18	13	18	15
ARB_06937	N-terminus shortened	ARB_06937		D4ARS3	SIG+GPI		Uncharacterized protein		down		16	38	2280	1305	655
ARB_06955	No changes	ARB_06955		D4ARU1	SIG		PAN-1 domain-containing protein				2	11	5	4	3
ARB_06966	Internal intron/exon prediction changes	ARB_06966		D4ARV2	SIG	pH4 & pH7	PLC-like phosphodiesterase		down		16	7	92	130	76
ARB_06975	No changes	ARB_06975		D4ARW0	SIG	pH7	Hydrophobin				7	26	162	9435	21445
ARB_07000	Internal intron/exon prediction changes	ARB_07000		D4ARY5	SIG		Uncharacterized protein		down	induced in Sabouraud	1	0	17	24	46
ARB_07026_07027	ORFs merged	ARB_07026 and ARB_07027	McpA	D4AS12	SIG	pH4 & pH7	Metallocarboxypeptidase (peptidase M14 family)				45	35	2133	282	5
ARB_07047	No changes	ARB_07047		D4AS32	SIG		Uncharacterized protein		up	induced in vivo	284	219	3	2	5
ARB_07056	N-terminus extended	ARB_07056		D4AS41	SIG	pH4 & pH7	FAD/FMN-containing isoamyl alcohol oxidase				64	36	561	213	22
ARB_07070	Internal intron/exon prediction changes	ARB_07070		D4AS55	SIG		Ribonuclease/ ribotoxin	Asp f 1	up		85	31	0	0	0
ARB_07085	No changes	ARB_07085		D4AS70	SIG	pH7	feruloyl esterase				8	11	1	2	2
ARB_07101	Internal intron/exon prediction changes	ARB_07101		D4AS86	SIG		Nucleotide-diphospho-sugar transferase (glycosyl transferase, family 2)				83	77	17	43	39

ARB_07161	N-terminus shortened	ARB_07161	CpS7	ARB_07161	SIG		Serine carboxypeptidase (peptidase S10 family)				17	19	3	9	6
ARB_07185_07186	ORFs merged	ARB_07185 and ARB_07186		D4ASH0/D4ASH1	SIG	pH4 & pH7	Carboxylesterase, type B				16	7	58	43	124
ARB_07195	Internal intron/exon prediction changes	ARB_07195		D4ASI0	SIG		Peptisase S41 family protein		up	induced in vivo	99	59	0	0	2
ARB_07342	N-terminus extended	ARB_07342		D4ASX8	SIG		Uncharacterized protein				47	36	101	62	42
ARB_07371	No changes	ARB_07371		D4AT07	SIG+GPI		Chitinase (glycoside hydrolase, family 18)		down	induced in vitro	7	10	1151	1300	607
ARB_07372	No changes	ARB_07372		D4AT08	SIG		Uncharacterized protein				35	44	26	13	22
ARB_07376	Internal intron/exon prediction changes	ARB_07376		D4AT12	SIG		Chitin binding domain-containg protein				15	23	17	16	10
ARB_07379	No changes	ARB_07379		D4AT15	SIG		Polysaccharide deacetylase				15	10	2	3	1
ARB_07381	C-terminus modified	ARB_07381		D4AT17	SIG		Uncharacterized protein				42	52	93	97	32
ARB_07385	No changes	ARB_07385		D4AT21	SIG		Uncharacterized protein				0	0	1	1	1
ARB_07390	No changes	ARB_07390		D4AT26	SIG		Glycoside hydrolase, family 24				3	2	9	12	18
ARB_07403	N-terminus shortened	ARB_07403		D4AT39	SIG		Aspartic-type endopeptidase (peptidase A1 family)				40	38	49	32	30
ARB_07415	C-terminus extended	ARB_07415		D4AT51	SIG		Defense response protein				35	24	3	6	214
ARB_07416	No changes	ARB_07416		D4AT52	SIG		Uncharacterized protein				59	58	9	34	28
ARB_07417	C-terminus shortened	ARB_07417		D4AT53	SIG+GPI		GPI anchored cell wall protein				12	23	121	479	59
ARB_07441	Internal intron/exon prediction changes	ARB_07441		D4AT77	SIG	pH7	Aconitase/isopropylmalate dehydratase				323	253	856	714	449

ARB_07446	No changes	ARB_07446		D4AT82	SIG		Uncharacterized protein				2	0	1	4	4
ARB_07466	C-terminus shortened	ARB_07466		D4ATA2	SIG	pH4	Uncharacterized protein		up		32	62	3	5	2
ARB_07487	Internal intron/exon prediction changes	ARB_07487		D4ATC3	SIG+GPI	pH4	1,3-beta-glucanosyltransferase (glycoside hydrolase family 72)				1465	1221	613	530	440
ARB_07491	N-terminus shortened	ARB_07491		D4ATC7	SIG		Cell wall glucanase (glycoside hydrolase family 17)				2	3	1	1	2
ARB_07495	No changes	ARB_07495		D4ATD1	SIG+GPI		Metalloproteinase (peptidase M43 family)		up		110	101	11	16	8
ARB_07525_07526	ORFs merged	ARB_07525 and ARB_07526		D4ATG1/D4ATG2	SIG		Nucleoside triphosphate hydrolase				68	59	37	38	56
ARB_07536	No changes	ARB_07536		D4ATH2	SIG	pH4	Aspartic-type endopeptidase (peptidase A1 family)				4	0	1	2	11
ARB_07582	Internal intron/exon prediction changes	ARB_07582		D4ATL8	SIG+GPI		Glycoside hydrolase, family 63				36	48	17	49	31
ARB_07590	No changes	ARB_07590		D4ATM6	SIG	pH4 & pH7	DUF4360 family protein				11	13	8	8	4
ARB_07623	Internal intron/exon prediction changes	ARB_07623		D4ATQ7	SIG+GPI		Amidophosphoribosyltransferase				64	59	1025	206	169
ARB_07629	Internal intron/exon prediction changes	ARB_07629		D4ATR3	SIG	pH4 & pH7	Alpha-1,2-mannosidase (glycoside hydrolase, family 92)				34	36	29	39	28
ARB_07637	No changes	ARB_07637		D4ATS1	SIG	pH4 & pH7	IgE-binding protein				136	171	37	222	52
ARB_07653	No changes	ARB_07653		D4ATT7	SIG+GPI		Mannan endo-1,6-alpha-mannosidase (glycoside hydrolase family 76)				201	143	495	368	187

ARB_07683	C-terminus modified	ARB_07683		D4AU53	SIG		(1->6)-beta-D-glucan biosynthetic process				103	86	54	114	89
ARB_07696	Internal intron/exon prediction changes	ARB_07696		D4AU66	SIG+GPI		GPI anchored serine-threonine rich protein				1629	1425	3463	2766	7210
ARB_07726	No changes	ARB_07726		D4AU96	SIG+GPI		Uncharacterized protein				2	1	1	2	1
ARB_07794	No changes	ARB_07794		D4ATY1	SIG		Cell wall mannoprotein 1			induced in Sabouraud	7	4	3	4	48
ARB_07824	C-terminus extended	ARB_07824		D4AU11	SIG+GPI		Uncharacterized protein				32	55	81	21	22
ARB_07852	No changes	ARB_07852		D4AUD6	SIG		Uncharacterized protein				4	0	3	2	2
ARB_07867	Internal intron/exon prediction changes	ARB_07867		D4AUF1	SIG	pH4 & pH7	WSC domain-containg galactose oxidase		down	induced in vitro	1	0	133	214	247
ARB_07870	Internal intron/exon prediction changes	ARB_07870		D4AUF4	SIG+GPI	pH4	WSC domain - containing haem peroxidase		down	induced in vitro	2	2	97	136	84
ARB_07879	C-terminus modified	ARB_07879		D4AUG2	SIG		Uncharacterized protein				3	1	1	2	1
ARB_07888	No changes	ARB_07888		D4AUH1	SIG	pH4	Glycosyl hydrolase, family 2				19	16	27	21	11
ARB_07893	No changes	ARB_07893		D4AUH6	SIG	pH4	Beta-hexosaminidase (glycoside hydrolase, family 20)				24	19	12	29	14
ARB_07952	No changes	ARB_07952		D4AUN5	SIG		Uncharacterized protein				13	20	0	2	7
ARB_07954	No changes	ARB_07954		D4AUN7	SIG		Glycoside hydrolase				2746	4708	164	866	2986
ARB_07956	No changes	ARB_07956		D4AUN9	SIG		Acetyl xylan esterase		up	induced in vivo	273	240	0	0	0
ARB_07958	N-terminus shortened	ARB_07958		D4AUP1	SIG		Uncharacterized protein			induced in keratin and soy	0	0	309	47	12

ARB_07990	N-terminus modified and extended	ARB_07990		D4AUS3	SIG+GPI		Multicopper oxidase, type 1				2	1	3	2	2
ARB_08043	Internal intron/exon prediction changes	ARB_08043		D4AUX6	SIG+GPI	pH4	PLC-like phosphodiesterase				55	38	19	39	50
ARB_08047	C-terminus modified	ARB_08047		D4AUY0	SIG		Ribonuclease/ ribotoxin				295	206	79	62	32
ARBNEW_12	New ORF				SIG		Uncharacterized protein conserved in dermatophytes		up		6	3	0	0	0
ARBNEW_124	New ORF				SIG+GPI		Pep2-like protease			induced in vitro	2	9	136	56	86
ARBNEW_137	New ORF				SIG		Uncharacterized protein conserved in dermatophytes				20	0	0	1	3
ARBNEW_138	New ORF				SIG	pH4 & pH7	Uncharacterized protein conserved in dermatophytes				0	0	4	3	2
ARBNEW_143	New ORF				SIG		Uncharacterized protein				1	0	3	6	3
ARBNEW_148	New ORF				SIG	pH7	Uncharacterized protein conserved in dermatophytes			induced in keratin and soy	3	0	372	37	6
ARBNEW_149	New ORF				SIG		Uncharacterized protein conserved in dermatophytes				3	4	1	1	2
ARBNEW_151	New ORF				SIG		Uncharacterized protein conserved in dermatophytes				16	19	41	38	20
ARBNEW_164	New ORF				SIG+GPI		Uncharacterized protein found also in *T. rubrum*		down		31	21	6855	2399	902
ARBNEW_166	New ORF				SIG		Uncharacterized protein conserved in dermatophytes				0	0	1	1	4
ARBNEW_171	New ORF				SIG	pH4 & pH7	Uncharacterized protein		up		4	12	0	0	0

ARBNEW_188	New ORF				SIG	pH7	Uncharacterized protein conserved in dermatophytes				47	37	9	15	13
ARBNEW_196	New ORF				SIG		Barwin-like endoglucanase				6	0	26	2	25
ARBNEW_201	New ORF				SIG	pH4 & pH7	Uncharacterized protein conserved in dermatophytes and Aspergilli				1	0	4	7	13
ARBNEW_206	New ORF				SIG		Uncharacterized protein conserved in dermatophytes				4	4	1	0	0
ARBNEW_231	New ORF				SIG+GPI		Uncharacterized protein conserved in filamentous fungi			repressed in keratin and soy	4219	1752	0	0	1376
ARBNEW_245	New ORF				SIG		PE-PGRS family protein				7	6	1	1	0
ARBNEW_246	New ORF				SIG		Uncharacterized protein conserved in dermatophytes		up		4	3	0	0	0
ARBNEW_248	New ORF				SIG		Uncharacterized protein conserved in dermatophytes				23	15	4	5	5
ARBNEW_255	New ORF				SIG		Uncharacterized protein conserved in dermatophytes				78	79	58	130	53
ARBNEW_266	New ORF				SIG		Uncharacterized protein conserved in dermatophytes				9	17	1	0	1
ARBNEW_271	New ORF				SIG+GPI		Uncharacterized protein conserved in dermatophytes			induced in vitro	3	8	159	147	265
ARBNEW_308	New ORF				SIG		LysM domain-containing protein				8	4	2	2	2
ARBNEW_309	New ORF				SIG	pH4 & pH7	Uncharacterized protein conserved in				34	49	18	9	3

							dermatophytes								
ARBNEW_320	New ORF				SIG	pH4 & pH7	Gamma-crystallin-related protein				35	7	87	234	156
ARBNEW_332	New ORF				SIG		Endoglucanase				3	2	0	1	0
ARBNEW_335	New ORF				SIG		S-phase kinase-associated protein 1-like			induced in soy and Sabouraud	4	13	1	134	37
ARBNEW_346	New ORF				SIG+ GPI		Oxoglutarate/iron-dependent dioxygenase				3	3	2	4	2
ARBNEW_348	New ORF				SIG		Long chronological lifespan protein 2-like protein		up		92	79	5	7	6
ARBNEW_359	New ORF				SIG		Flap endonuclease 1-like protein		up		17	15	0	0	0
ARBNEW_375	New ORF				SIG		Uncharacterized protein conserved in dermatophytes		up		15	11	0	0	0
ARBNEW_49	New ORF				SIG		Uncharacterized protein conserved in dermatophytes		up		10	30	0	0	0
ARBNEW_52	New ORF				SIG		LysM domain-containing protein		up		16	14	0	0	0
ARBNEW_61	New ORF				SIG		Uncharacterized protein conserved in dermatophytes				0	0	0	0	3
ARBNEW_63	New ORF				SIG		Endo-chitosanase		up		25	17	1	1	1
ARBNEW_77	New ORF				SIG		Uncharacterized protein				1	0	1	1	1
ARBNEW_81	New ORF				SIG	pH4 & pH7	NlpC/P60-like cell-wall endopeptidase (peptidase C40 family)			induced in Sabouraud	4	0	13	21	68

ARBNEW_86	New ORF				SIG+GPI		Uncharacterized protein conserved in dermatophytes			induced in soy and Sabouraud	2	0	8	108	119
ARBNEW_95	New ORF				SIG		Uncharacterized protein conserved in dermatophytes				6	5	0	0	11
ARBNEW_97	New ORF				SIG		Uncharacterized protein conserved in dermatophytes				0	0	0	0	0